AD

RSIC-410

NONDESTRUCTIVE MEASUREMENT OF RESIDUAL STRESSES IN METALS AND METAL STRUCTURES

by

Koichi Masubuchi

April 1965

Redstone Scientific Information Center

U S ARMY MISSILE COMMAND
REDSTONE ARSENAL, ALABAMA

N 65 - 33876

FACILITY FORM 602

(ACCESSION NUMBER)

(PAGES)

(NASA CR OR TMX OR AD NUMBER)

(THRU)

(CODE)

(CATEGORY)

CASE FILE
COPY

NONDESTRUCTIVE MEASUREMENT OF RESIDUAL

STRESSES IN METALS AND METAL STRUCTURES

by

Koichi Masubuchi

Battelle Memorial Institute

Columbus, Ohio

ABSTRACT

13387 6

This report presents a state-of-the-art survey of the nondestructive measurement and evaluation of residual stresses produced in metals and metal structures. The report is concerned primarily with residual stresses produced during the fabrication of structures made of high-strength aluminum alloys.

Discussions are presented in four sections which provide the following:

fundamental information on residual stresses that is needed to understand measurement techniques

review of methods of measuring residual stresses, including stress-relaxation techniques, X-ray diffraction technique, the ultrasonic technique, the hardness technique, and cracking techniques

measurement of residual stresses during fabrication of metal structures (methods of measuring residual stresses and typical experimental data are described)

selection and use of appropriate measurement techniques and evaluation of results.

On the basis of findings obtained during this survey, recommendations are given for future research on nondestructive measurement of residual stresses produced during fabrication of metal structures.

FOREWORD

The purpose of this survey was to review presently available information relative to the nondestructive measurement and evaluation of residual stresses produced in metals and metal structures, as requested by the Marshall Space Flight Center, Manufacturing Engineering Laboratory, NASA.

Information for this report was obtained from the literature and from a visit to Redstone Arsenal.

An attempt was made to use the most recent literature available to describe the techniques employed in measuring residual stresses; however, some old literature was necessarily used since it provided the basis for currently applicable techniques.

TABLE OF CONTENTS

TABLE OF CONTENTS (Concluded)

Appendix

STRESS CALCULATIONS

LIST OF ILLUSTRATIONS

Section I. INTRODUCTION

Residual stresses are those stresses that would exist in a body if all external loads were removed. Residual stresses in metal structures occur for many reasons during various manufacturing stages. They are known to be detrimental to the behavior of metals structures under certain conditions.

A state-of-the-art survey has been made of nondestructive measurement and evaluation of residual stresses in metals and metal structures. The survey is concerned primarily with residual stresses produced during the fabrication of structures made in high-strength aluminum alloys; however, some discussion is necessarily based on data relative to steel.

The first section describes fundamental information on residual stresses that is necessary for a complete understanding of measurement techniques.

The second section reviews presently available techniques for measuring residual stresses. Various methods based on the stress-relaxation techniques are reviewed. Discussions also are made on the X-ray diffraction technique, the ultrasonic technique, the hardness technique, and the cracking techniques.

The third section describes measurement of residual stresses produced during quenching, machining, forming, and welding. For each of these processes, methods of measuring residual stresses are discussed, along with typical data, especially those on high-strength aluminum alloys.

The fourth section describes information on (1) selection of measurement techniques appropriate for a particular job, (2) use of mathematical analysis in the experimental studies of residual stress, and (3) the evaluation of experimental data on the basis of the effects of residual stresses on the behavior of structures. On the basis of the quality of data and cost required, bonded strain gages are recommended as far as they are applicable. The X-ray diffraction technique may be used in some cases. The ultrasonic technique may become useful in the future.

On the basis of findings obtained during this survey, recommendations are given for future research on nondestructive measurement of residual stresses during fabrication of metal structures. Major areas where research is needed are:

development of nondestructive methods of measuring residual
stresses

measurement and control of residual stresses during fabri-
cation

effects of variations in procedures on the magnitude and dis-
tribution of residual stresses.

Section II. FUNDAMENTAL INFORMATION ON RESIDUAL STRESSES

This section provides fundamental information on stress, strain, and the mechanical properties of metals as they are important for the measurement of residual stresses. Also given is fundamental information on residual stresses that is needed to understand measurement techniques, as well as definitions of important technical terms.

1. Stress, Strain, and the Mechanical Properties of Metals

a. Stress and Strain

When a body is in equilibrium under the action forces, it is said to be in a condition of stress or in a stressed state.[1] Such stresses cause deformations or strains in the body.

(1) Stress. Stress intensity is usually measured in pounds per square inch.* In the simple case of a prismatical bar subjected to tension, as shown in Figure 1, the stress, σ, is

$$\sigma = \frac{P}{A}, \tag{1}$$

where

P = total tensile force, or tensile load

A = cross-sectional area.

In a general stress field, stresses are not distributed uniformly and stresses are not uniaxial. Figure 2 shows stress components acting on the three perpendicular planes passing through any point, 0, of a body. On each pair of parallel planes there are three components: a normal stress perpendicular to the plane and two components of shearing stress acting in the plane. Acting on the plane perpendicular to the x-axis, for example, are the normal stress, σ_x, and the shearing stresses, τ_{xy} and τ_{xz}, acting in the directions parallel to the y- and z-axes, respectively. Because of the equilibrium of the element, only six components are independent, as follows:

$$\sigma_x, \sigma_y, \sigma_z; \tau_{xy} = \tau_{yx}; \tau_{yz} = \tau_{zy}; \tau_{zx} = \tau_{xz}.$$

These six quantities are called the components of stress for that point.

---

*In the metric system, kg/mm^2 is commonly used to express the stress intensity:

$$1 \ kg/mm^2 = 1422 \ psi.$$

3
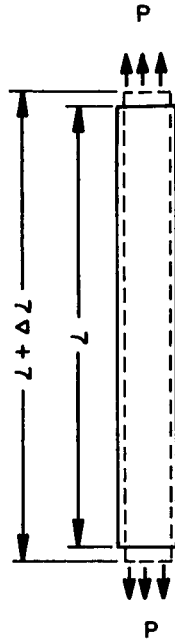
Figure 1. Prismatical Bar Subjected to Tension Load, P
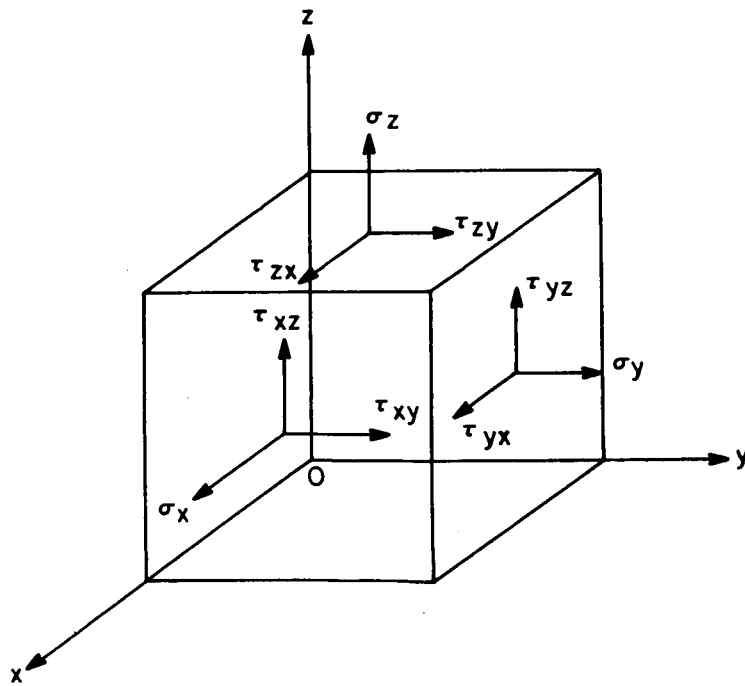
Figure 2. Stress Components

If the six components of stress are known, the stress on any inclined plane through the same point can be calculated (refer to Paragraph 1 of Appendix). It is always possible to find three perpendicular planes for which shearing stresses vanished. These planes are called the principal planes (coordinate axes perpendicular to these planes are called the principal axes), and stresses acting on these planes are called principal stresses.

(2) Strain. When forces are applied to a body, the body deforms slightly. In the simple case, as shown in Figure 1, the length of the bar increases from its original value L to L + ΔL. The strain, ϵ, is expressed as follows:

$$\epsilon = \frac{\Delta L}{L} .$$ (2)

In a general strain field, there are six independent strain components: normal strains, ϵ_x, ϵ_y, and ϵ_z, and shearing strains, γ_{xy}, γ_{yz}, and γ_{zx}.

(3) Stress-Strain Relationships, Hooke's Law. In most engineering stress analyses it is customary to assume that structural materials are purely elastic, homogeneous, and isotropic (material properties are the same in all directions). According to Hooke's law, the magnitudes of strains and stresses are proportional as follows:

$$\epsilon_x = \frac{1}{E} \left\{ \sigma_x - \nu (\sigma_y + \sigma_z) \right\}$$

$$\epsilon_y = \frac{1}{E} \left\{ \sigma_y - \nu (\sigma_z + \sigma_x) \right\}$$

$$\epsilon_z = \frac{1}{E} \left\{ \sigma_z - \nu (\sigma_x + \sigma_y) \right\}$$

$$\gamma_{xy} = \frac{1}{G} \tau_{xy}, \ \gamma_{yz} = \frac{1}{G} \tau_{yz}, \ \gamma_{zx} = \frac{1}{G} \tau_{zx},$$ (3)

where

E = Modulus of elasticity (in tension), or Young's modulus

ν = Poisson's ratio

G = modulus of rigidity, or shear modulus.

Stress-strain relationships in the plastic condition are much more complex.

b.   Mechanical Properties of Metals

Figure 3 shows schematically the stress-strain curve of
a metal, such as an aluminum alloy.   As the load or stress increases,
strain changes as shown by the curve OABCD.   The region OA is the
elastic region and its slope corresponds to Young's modulus.   The
stress at point B is the yield stress,* and when the load is increased,
the metal deforms plastically.   Point C represents the ultimate tensile
strength, and the metal fractures at point D.
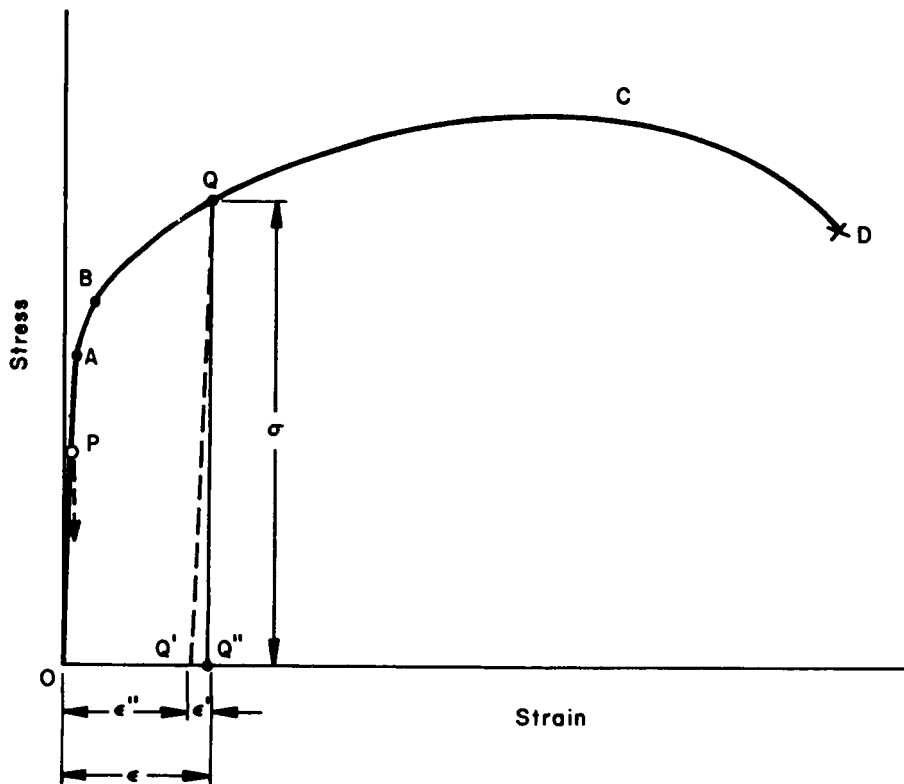
Figure 3.   Stress-Strain Curve of a Metal

---

*Some metals, including carbon steel, clearly exhibit yielding,
while others, including aluminum alloys, do not.   The stress at which
0.2 percent permanent extension has taken place is commonly used for
defining the yield stress in metals such as aluminum alloys.

Strain changes when the load is decreased or when the metal is unloaded. When stress is decreased from an arbitrary point, P, on the line OA, strain decreases as shown by the dotted arrow and no permanent set remains after the load is removed (returns to the origin, 0). When stress is decreased from an arbitrary point, **Q,** on the curve BC, strain changes as shown by the line QO'. OQ' (= ϵ'') represents the permanent set or the plastic strain. The line QQ' is parallel to the line AO. If the metal is loaded again, strain changes as shown by O'QCD, indicating an increase in the elastic limit from the stress which corresponds to A to that which corresponds to **Q.** The magnitude of stress σ at point Q can be determined by measuring the amount of elastic strain, Q'Q'' = ϵ', which takes place during unloading, as follows:

$$\sigma = E \epsilon' . \qquad\qquad (4)$$

An important characteristic of metals during unloading is that they behave in a purely elastic manner, even if they have undergone plastic deformation. This characteristic is the basis on which strain-relaxation techniques have been developed for measuring residual stresses in metals.

In most cases involving residual stress measurements, the history of the metal being investigated is not known. In many cases at least some portions of the specimen have undergone plastic deformation, and nonuniform plastic deformation is a major source of residual stresses in metals. Even so, it is possible to determine the magnitude of residual stress by measuring the amount of elastic strain that takes place during unloading. Table I shows typical tensile properties of 2024 aluminum alloy at various temperatures.[2]

2. Residual Stresses

Various technical terms have been used to refer to residual stresses,[3,4] such as

> internal stresses
> initial stresses
> inherent stresses
> reaction stresses
> locked-in stresses.

Residual stresses also occur when a body is subjected to nonuniform temperature change; these stresses are usually called thermal stresses.

Table I. Properties of 2024 Alloy at Various Temperatures
(Metals Handbook)[2]

Testing Temperature (°F)	Tensile Strength (psi)	Yield Strength (psi)	Elongation (percent)
Mechanical Properties*			
75	68,000	47,000	19
300	45,000	36,000	17
400	27,000	20,000	27
500	12,000	9,000	55
600	8,000	6,000	75
700	5,500	4,000	100
Coefficient of Linear Thermal Expansion, α			
Temperature (°F)		α, (micro inch/inch/°F)	
68 to 212		12.7	
68 to 392		13.3	
68 to 572		13.7	

*Data given above are for bare product (T4 temper). Young's modulus at room temperature is 10.8×10^6 psi. Poisson's ratio is 0.33.

a. Occurrence of Residual Stresses

Residual stresses in metals and metal structures occur for many reasons. Residual stresses may be produced as follows:

in many materials including plates, bars, and sections during rolling, casting, forging, etc.

during forming and shaping of metal parts by such processes as shearing, bending, machining, and grinding

during fabrication, such as during welding.

Heat treatments at various stages can also influence residual stresses. For example, quenching produces residual stresses while stress-relieving heat treatments reduce residual stresses.

Residual stresses are classified on the basis of the mechanisms which produce them, being those produced by structural mismatching and those produced by uneven distribution of elastic strains, including plastic and thermal strains.

b. Residual Stresses Produced by Mismatch

Figure 4 shows a simple case in which residual stresses are produced when bars of different length are forcibly connected. Tensile stresses are produced in the shorter bar, Q, and compressive stresses are produced in the longer bars P and P'. .

(a) Free State   (b) Stressed State
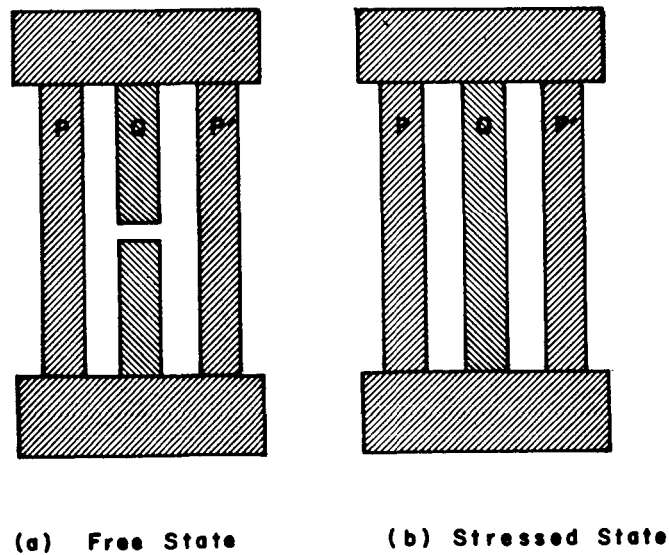
Figure 4. Residual Stresses Produced When Bars With Different Length are Forcibly Connected

Figure 5 shows how a heating-and-cooling cycle causes mismatch resulting in residual stresses. Illustrated is the case in which three 2024 alloy bars of equal length and sectional area are connected by two rigid blocks at the ends and the middle bar is heated to 500°F and then cooled to room temperature while the side bars are kept at the room temperature. The diagram shows the temperature versus stress relationship of the middle bar (details of the calculation made by the author are given in Paragraph 2 of the Appendix).* When the middle bar is heated, compressive stresses occur in it, since its expansion is restrained by the side bars which are kept at room temperature. As the temperature of the middle bar increases, the stress in it changes as shown by line AB. The yield stress in compression is reached when the temperature is approximately 230°F, as indicated by point B. Beyond point B, as the temperature rises, the stress in the middle bar is limited to the yield stress at each corresponding temperature, as shown by curve BC. When the temperature decreases below 500°F on cooling, the action in the middle bar is elastic again. The compressive stress in the middle bar drops rapidly, changes to tension, and soon reaches the yield stress in tension, as indicated by point D. Then, as the temperature decreases further, once more the stress in the middle bar is limited to the yield stress at each corresponding temperature, as shown by curve DE. Thus, a residual tensile stress equal to the yield stress at room temperature is set up in the middle bar. The residual stresses in the side bars are compressive stresses and equal to one-half of the tensile stress in the middle bar (because the two side bars are resisting the deformation of the one middle bar). Line B'E indicates that residual stress of the same magnitude, which is equal to the yield stress at room temperature, will be produced by heating the middle bar at any temperature exceeding 340°F.

c. Residual Stresses Produced by Unevenly Distributed Nonelastic Strains

When a material is heated uniformly, it expands uniformly and no thermal stress is produced. On the other hand, when a metal is heated unevenly, thermal stresses are produced. Residual stresses also are produced when unevenly distributed nonelastic strains such as

---

*Wilson and Hao[5] calculated the temperature versus stress relationship for low-carbon steel. It was assumed that $A_s = A_m$ (refer to Paragraph 2 of the Appendix).
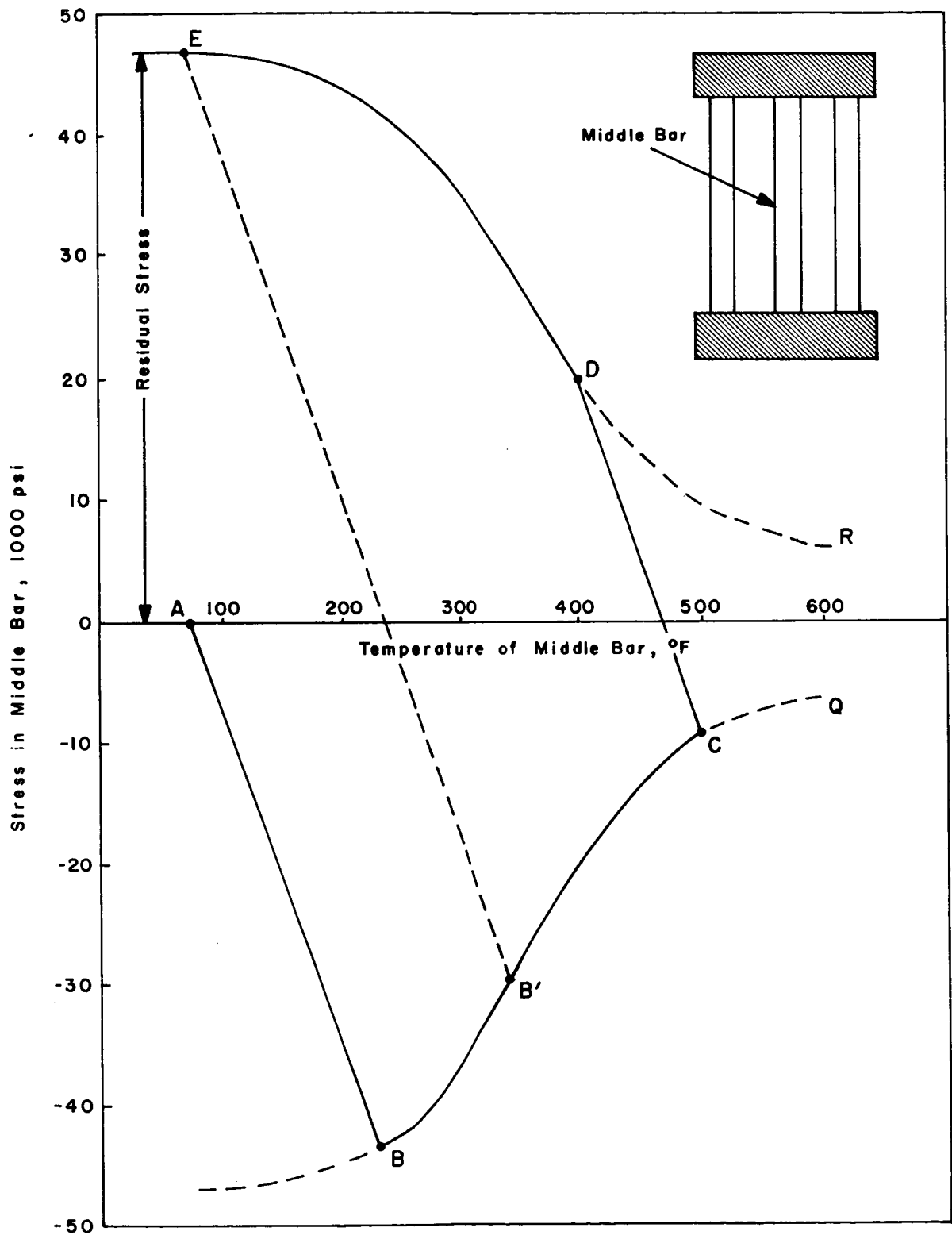
Figure 5. Temperature-Stress Curve for the Middle
Bar of a Three-Bar Frame

plastic strains exist. The following are fundamental relationships for a two-dimensional (plane stress, $\sigma_z = 0$) residual-stress field:[*][4]

Strains are composed of elastic strain and nonelastic strain:

$$\epsilon_x = \epsilon_x' + \epsilon_x''$$

$$\epsilon_y = \epsilon_y' + \epsilon_y''$$

$$\gamma_{xy} = \gamma_{xy}' + \gamma_{xy}'' , \tag{5}$$

where

ϵ_x, ϵ_y, γ_{xy} are components of the total strain

ϵ_x', ϵ_y', γ_{xy}' are components of the elastic strain

ϵ_x'', ϵ_y'', γ_{xy}'' are components of the nonelastic strain.

The nonelastic strain can be plastic strain, thermal strain, etc.[**]

A Hooke's law relationship exists between stress and elastic strain (refer to Equation (3)):

$$\epsilon_x' = \frac{1}{E} (\sigma_x - \nu \sigma_y)$$

$$\epsilon_y' = \frac{1}{E} (\sigma_y - \nu \sigma_x)$$

$$\gamma_{xy} = \frac{1}{G} \tau_{xy}. \tag{6}$$

---

[*]Stresses in a plate with uniform thickness are common cases of the plane-stress field. In this case, $\sigma_z = \tau_{xz} = \tau_{yz} = 0$. Equations are more complex for the three-dimensional stress field.

[**]In the case of thermal stress:

$$\epsilon_x'' = \epsilon_y'' = \alpha \cdot \Delta T \qquad \gamma_{xy}'' = 0 ,$$

where

α is the coefficient of linear thermal expansion, and
ΔT is the change of temperature from the initial temperature.

The stress must satisfy the equilibrium condition:

$$\frac{\partial \sigma_x}{\partial x} + \frac{\partial \tau_{xy}}{\partial y} = 0$$

$$\frac{\partial \tau_{xy}}{\partial x} + \frac{\partial \sigma_y}{\partial y} = 0. \tag{7}$$

The total strain must satisfy the condition of compatibility:[1]

$$\left(\frac{\partial^2 \epsilon'_x}{\partial y^2} + \frac{\partial^2 \epsilon'_y}{\partial x^2} - \frac{\partial^2 \gamma'_{xy}}{\partial x \cdot \partial y}\right) + \left(\frac{\partial^2 \epsilon''_x}{\partial y^2} + \frac{\partial \epsilon''_y}{\partial x^2} - \frac{\partial^2 \gamma''_{xy}}{\partial x \cdot \partial y}\right) = 0. \tag{8}$$

The above equations indicate that residual stresses exist when the value of R, which is determined by the nonelastic strain as follows, is not zero:*

$$R = -\left(\frac{\partial^2 \epsilon''_x}{\partial y^2} + \frac{\partial^2 \epsilon''_x}{\partial x^2} - \frac{\partial^2 \gamma''_{xy}}{\partial x \cdot \partial y}\right). \tag{9}$$

R can be considered as the cause of residual stresses.[6] Moriguchi[7] called R "incompatibility."

Many investigators have made mathematical analyses of residual stresses.[3,4,6,7,8] Several equations have been proposed to calculate stress components σ_x, σ_y, and τ_{xy} for given values of nonelastic strain ϵ''_x, ϵ''_y, and γ''_{xy}.[4,7] Important findings obtained from these mathematical analyses with regard to the measurement of residual stresses are:

Residual stresses in a body cannot be determined by measuring the stress change that takes place when external load is applied to the body. (Because of this, the body is cut to determine residual stresses.)

---

*R = 0, consequently residual stress will not occur when the nonelastic-strain components are linear functions of the position:

$$\epsilon''_x = a + bx + dy, \quad \epsilon''_y = e + fx + gy, \quad \gamma''_{xy} = k + \ell x + my.$$

Residual stresses σ_x, σ_y, and τ_{xy} can be calculated from Equation (6) when elastic-strain components ϵ_x', ϵ_y', and γ_{xy}' are determined. However, components of nonelastic strain ϵ_x'', ϵ_y'', and γ_{xy}'', which have caused residual stresses, cannot be determined theoretically.

d. Equilibrium Condition of Residual Stresses

Since residual stresses exist without external forces, the resultant force and the resultant moment produced by the residual stresses must vanish:

$$\int \sigma \cdot dA = 0 \text{ on any plane section,} \qquad (10)$$

and

$$\int dM = 0. \qquad (11)$$

It is very important to check whether residual-stress data determined in any experiment satisfy the above conditions.

e. Macroscopic and Microscopic Residual Stresses

Areas in which residual stresses exist vary greatly from a large portion of a metal structure down to areas on the atomic scale. Figure 6 shows macroscopic residual stresses on various scales. For example, when a structure is heated by solar radiation from one side, thermal distortions and thermal stresses are produced in the structure, as shown in Figure 6(a). Figure 6(b) shows residual stresses by welding residual stresses and distributed in areas near the weld. Figure 6(c) shows residual stresses produced by grinding; residual stresses are highly localized in a thin layer near the surface.

Residual stresses also occur on a microscopic scale.[9] For example, residual stresses are produced in areas near martensitic structures in steel since the martensite transformation that takes place at relatively low temperatures results in the expansion of the metal. Residual stresses on the atomic scale exist in areas near dislocations.

This report is concerned primarily with microscopic residual stresses.
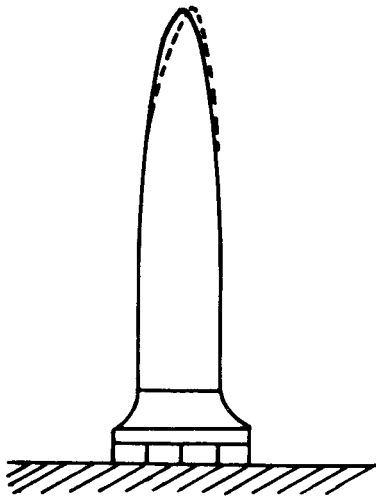
(a) Thermal Distortion in a
Structure Due to Heating
by Solar Radiation
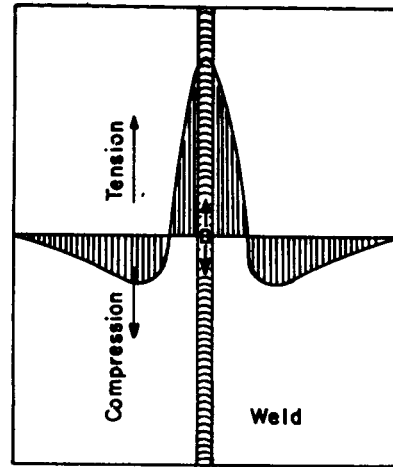
(b) Residual Stresses Due to
Welding
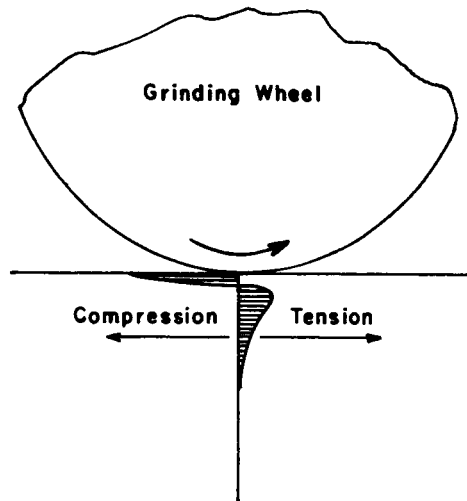
(c) Residual Stresses Due to
Grinding

Figure 6. Macroscopic Residual Stresses on Various Scales

15

Section III. REVIEW OF METHODS OF MEASURING RESIDUAL STRESSES

This section reviews various methods of measuring residual stresses in metals and metal structures.[10, 11, 12, 13] These methods can be classified into the following four groups according to the principles on which these methods are based:

methods in which residual stresses are determined by measuring elastic-strain release that takes place when residual stresses are relaxed by cutting the specimen into pieces or by removing a piece from the specimen: the stress-relaxation techniques

methods in which elastic strains are determined by measuring the lattice parameter of the specimen

methods in which residual stresses are determined by measuring stress-sensitive properties such as ultrasonic attenuation

methods in which residual stresses are determined by observing cracks produced in the specimen by residual stresses.

Stress-relaxation techniques, which have been widely used for measuring residual stresses, will be covered in three parts as follows:

principles of stress-relaxation techniques for measuring residual stresses

methods for measuring strains

various methods of measuring residual stresses based on stress-relaxation techniques.

Discussions will then be conducted on methods of measuring residual stresses other than stress-relaxation techniques.

1. Principles of Stress-Relaxation Techniques for Measuring Residual Stresses

Stress-relaxation techniques are based on the fact that strains that develop during the stress relaxation are elastic even when the material has undergone plastic deformation, as shown in Figure 3.

a. Complete Stress-Relaxation Technique Applied to a Plate

Residual stresses in a plate can be determined by measuring the strain change that takes place in a small piece when it is removed from the plate. Suppose that a small piece of metal surrounding the point of interest is removed with a trepan saw, as shown in Figure 7,
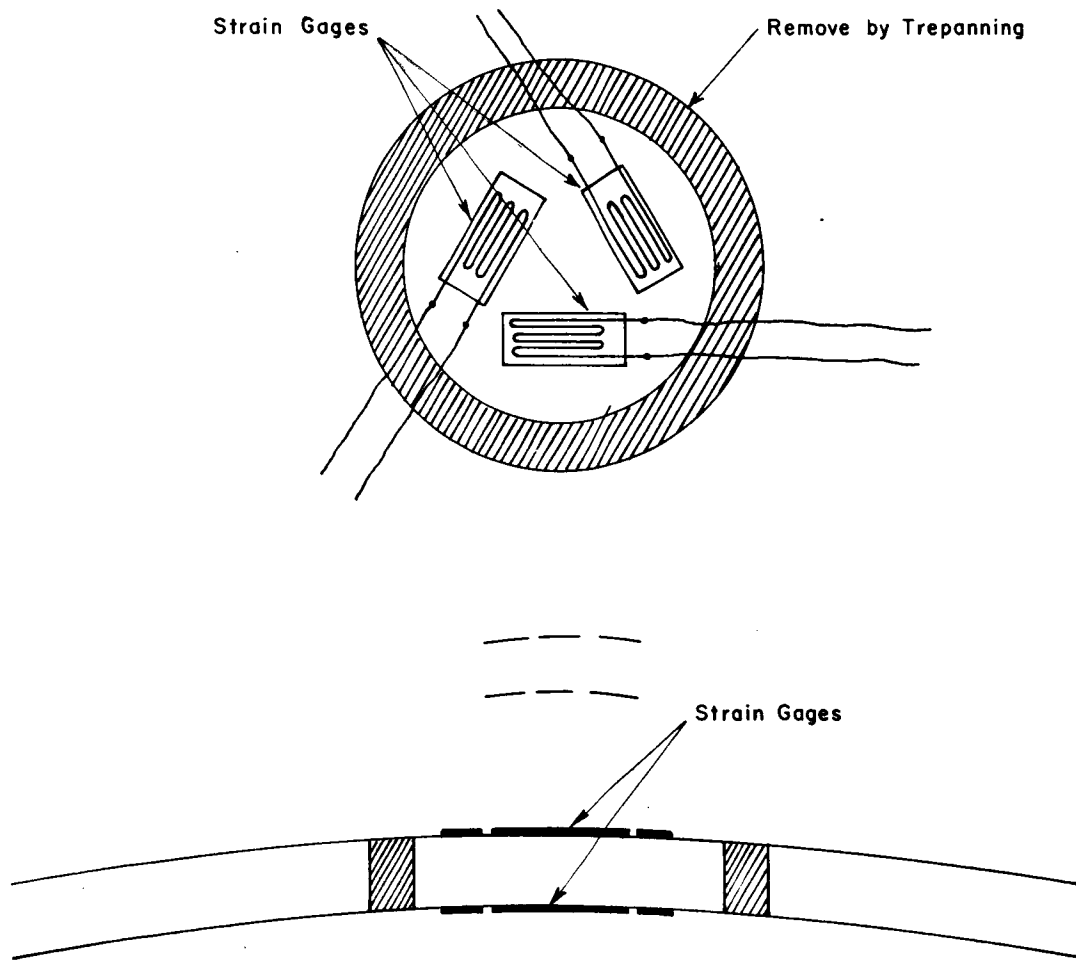
Figure 7. Complete Stress-Relaxation Technique
Applied to a Plate

and the strains due to the stress-relaxation process, $\overline{\epsilon}_x$, $\overline{\epsilon}_y$, and $\overline{\gamma}_{xy}$, are measured by electric strain gages. If the piece is small enough, it can be assumed that residual stresses no longer exist in the piece after removal; then, the following holds good:

$$\overline{\epsilon}_x = -\epsilon'_x, \quad \overline{\epsilon}_y = -\epsilon'_y, \quad \overline{\gamma}_{xy} \quad -\gamma'_{xy}, \tag{12}$$

where, ϵ'_x, ϵ'_y, and γ'_{xy} are elastic-strain components of the residual stress. The minus signs in Equation (12) indicate that, when tensile residual stress exists, shrinkage (not elongation) takes place during stress-relaxation. Then residual stresses are

$$\sigma_x + - \frac{E}{1-\nu^2} (\overline{\epsilon}_x + \nu \overline{\epsilon}_y)$$

$$\sigma_y + - \frac{E}{1-\nu^2} (\overline{\epsilon}_y + \nu \overline{\epsilon}_x)$$

$$\tau_{xy} = - G \overline{\gamma}_{xy} . \tag{13}$$

It is advisable to make strain measurements on both surfaces of the plate, because there may be residual stresses caused by bending. The mean value of strains measured on both surfaces represents the plane-stress component, while the difference between the strains on both surfaces represents the stress component caused by bending.

b. Determination of Residual Stress by Partial Stress-Relaxation Technique

When a small circular hole is drilled in a plate containing residual stresses, residual stresses in areas outside the hole are relaxed partially. It is possible to determine residual stresses that existed in the drilled area by measuring stress relaxation in areas outside the drilled hole. The hole method of measuring residual stress was first proposed and used by Mathar[14] and was later developed by Soete,[15] Suppiger, et al.[16]

For an illustration of how the technique is used, suppose that the components of residual stress at point O are σ_{xo}, σ_{yo}, and τ_{xyo}. Then the components of residual stress along the periphery of a small circle surrounding point O are given by Equation (14). See Figure 8(a) and Paragraph 3 of Appendix.

$$\sigma_{ro} = \frac{1}{2}(\sigma_{xo} + \sigma_{yo}) + \frac{1}{2}(\sigma_{xo} - \sigma_{yo})\cos 2\theta + 2\tau_{xyo}\sin 2\theta$$

$$\sigma_{\theta o} = \frac{1}{2}(\sigma_{xo} + \sigma_{yo}) - \frac{1}{2}(\sigma_{xo} - \sigma_{yo})\cos 2\theta - 2\tau_{xyo}\sin 2\theta$$

$$\tau_{r\theta o} = \tau_{xyo}\cos 2\theta - \frac{1}{2}(\sigma_{xo} - \sigma_{yo})\sin 2\theta \ , \tag{14}$$

where

σ_{ro} = the residual component

$\sigma_{\theta o}$ = the tangential component

$\tau_{r\theta o}$ = the shearing component of residual stress along the periphery at an angle θ.

In Equation (14), it is assumed that residual stresses are uniform in the area inside the small circle.

The next step is to calculate the strain change that will take place in areas outside the small circle, radius a, when the material inside the circle is removed, e. g. , by drilling. The important fact about the strain change is that the circle will become stress free; in other words, σ_{ro} and $\tau_{r\theta o}$ will vanish. Therefore, the strain change during the stress-relaxation process is the same as the strain caused in a plate with a hole (but no residual stress) by applying stresses $-\sigma_{ro}$ and $-\tau_{r\theta o}$ to the edge of the hole.

To simplify discussion, assume that $\sigma_{xo} = \sigma_{yo} = \sigma_o$ and $\tau_{xyo} = 0$; or residual stresses are biaxially tensile. Then, $\sigma_{ro} = \sigma_o$ and $\tau_{r\theta o} = 0$. The strain release which takes place at point P (r, θ) when a hole (radius a) is drilled around point O is given in Equation (15) and shown in Figure 8(b):

$$\overline{\epsilon}_r = -\overline{\epsilon}_\theta = -\frac{1 + \nu}{E}\sigma_o\frac{a^2}{\gamma^2}$$

$$\overline{\gamma}_{r\theta} = 0 \ , \tag{15}$$

where $\overline{\epsilon}_r$, $\overline{\epsilon}_\theta$, and $\overline{\gamma}_{r\theta}$ are components of the strain release.

When residual tensile stresses exist in areas around point O, the strain change in the radial direction $\overline{\epsilon}_r$ will be shrinking from the stretched state. Equation (15) indicates that if values of a and r are

known and $\bar{\epsilon}_r$ or $\bar{\epsilon}_\theta$ is measured, it is possible to determine the amount of the residual stress, σ_O.

In the case of a general stress field in which three components, σ_{xo}, σ_{yo}, and τ_{xyo} exist, the strain release that takes place around the drilled hole is more complex than that given in Equation (15). A common way to determine stresses is to place strain gages in a star form, at 120 degrees from each other, as shown in Figure 8(c). The magnitudes and directions of the principal stresses are determined as follows:[16, 17]

$$\sigma_1 = -E \left\{ \mu_1(\lambda) \cdot a + \mu_2(\lambda)\beta \right\}$$

$$\sigma_2 = -E \left\{ \mu_1(\lambda) a - \mu_2(\lambda)\beta \right\}$$

$$\tan 2\phi = \frac{\delta}{\bar{\epsilon}_{r1} - a}, \qquad\qquad (16)$$

where

σ_1 and σ_2 = the magnitudes of principal stresses

ϕ = the angle between the No. 1 gage and the direction of the σ_1-principal stress

$\lambda = \dfrac{r}{a}$ = the ratio of the distance of the measuring points from the center of the hole, r, and the radius of hole, a.

$$\mu_1(\lambda) = \frac{\lambda^2}{1 + \nu}$$

$$\mu_2(\lambda) = \frac{\lambda^4}{4\lambda^2 - 3(1 + \nu)}$$

$$a = \frac{1}{3}(\bar{\epsilon}_{r1} + \bar{\epsilon}_{r2} + \bar{\epsilon}_{r3})$$

$$\beta = \sqrt{(\bar{\epsilon}_{r1} - a)^2 + \delta^2}$$

$$\delta = \frac{1}{\sqrt{3}}(\bar{\epsilon}_{r2} - \bar{\epsilon}_{r3}), \qquad\qquad (16')$$

where $\bar{\epsilon}_{r1}$, $\bar{\epsilon}_{r2}$, and $\bar{\epsilon}_{r3}$ = radial strains measured on No. 1, No. 2, and No. 3 strain gages, respectively.
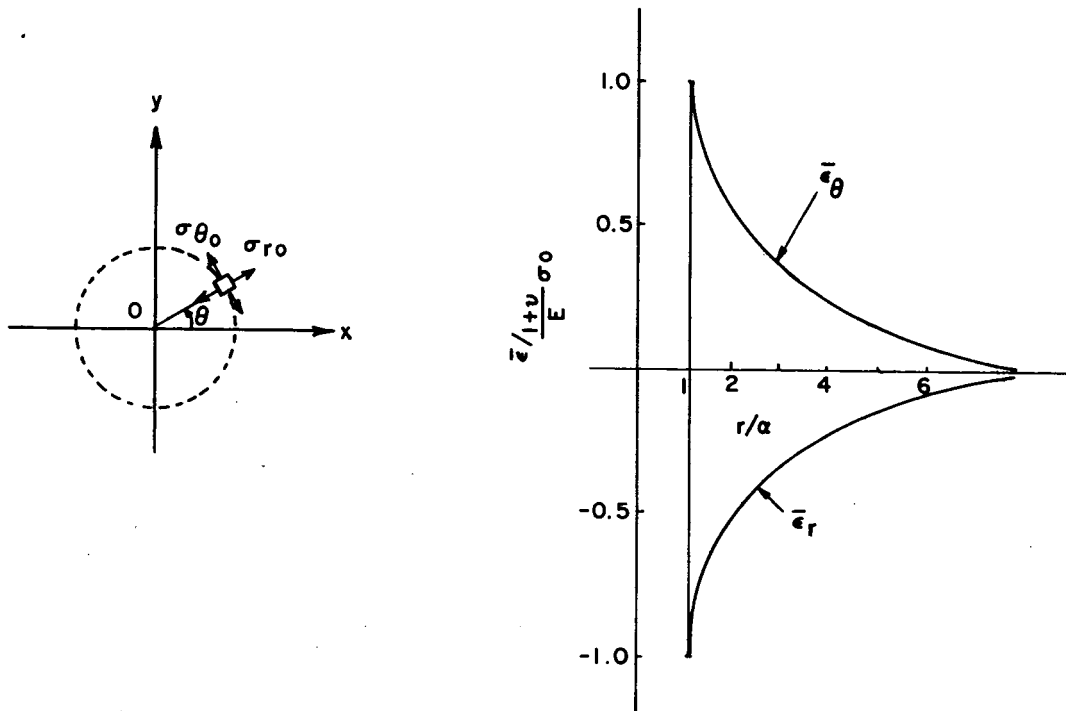
(a) Radial and Tangential
    Residual Stress, σ_{ro} and
    $\sigma_{\theta o}$, Along the Periphery
    of a Small Circle Surrounding
    Point O

(b) Distribution of $\bar{\epsilon}_r$ and
    $\bar{\epsilon}_\theta$ for $\sigma_{xo} = \sigma_{yo} = \sigma_o$,
    $\tau_{xyo} = 0$
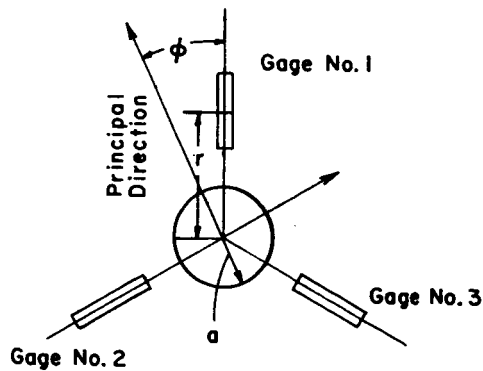
(c) 120-Degree Star Arrangement
    of Strain Gages

Figure 8. The Mathar Method of Measuring Residual Stresses

c.   Determination of Residual Stresses in Solids

A complete stress-relaxation technique such as shown in Figure 7 is not feasible in the determination of residual stresses in a three-dimensional body because a small piece must be taken from the interior of the body, while strain measurements can be made only on the surface of the body. Consequently, all techniques for measuring residual stresses in three-dimensional solids are partial stress-relaxation techniques requiring complex experimental procedures such as follows:

strain changes are measured when portions of the specimen are removed successively.

narrow blocks in different directions are taken from the specimen, and residual stresses left in the blocks are measured.

Residual stresses that existed in the specimen are then calculated. A number of methods have been proposed and used to determine residual stresses in solids of various shapes such as cylindrical bars, pipes, and heavy weldments. Most methods, however, require complete destruction of the specimen and they are also time consuming and costly. The following describes, as a simple example, principles of the Bauer-Heyn[18,19] technique for determining residual stresses in a cylinder, especially in a cylinder containing longitudinal tensile stresses in the outer portion and compressive stresses in the core.

Figure 9 shows, schematically, the basic principles of the Bauer-Heyn method.[11]   The tensile stresses in the outer portion of the rod are represented by a system of stretched springs balanced by compressed springs in the inner portion, which represent the longitudinal compressive stresses, as shown in Figure 9(a). If the outer springs are removed, the core will expand, as shown in Figure 9(b).

If A_O is the original cross-sectional area of the bar, A_1 is the area of the core (area of the skin is $dA_1 = A_O - A$), and the average residual stress which existed in the skin is $\overline{\sigma}_1$, then the force in the removed outer skin, F_{skin}, is

$$F_{skin} = \overline{\sigma}_1 \ dA_1.$$

Now the force in the core which is released, F_{core}, is

$$F_{core} = A_1 E \cdot de_1 ,$$

where de_1 is the strain release (expansion per unit length) of the core. The two forces must be equal; therefore, the residual stress which existed in the skin, $\bar{\sigma}_1$, can be determined by

$$\bar{\sigma}_1 = \frac{A_1 \cdot E \cdot de_1}{dA_1} \; .$$

(17)

(a) Original State

(b) Core Expanded by the Removal of Outer Skin
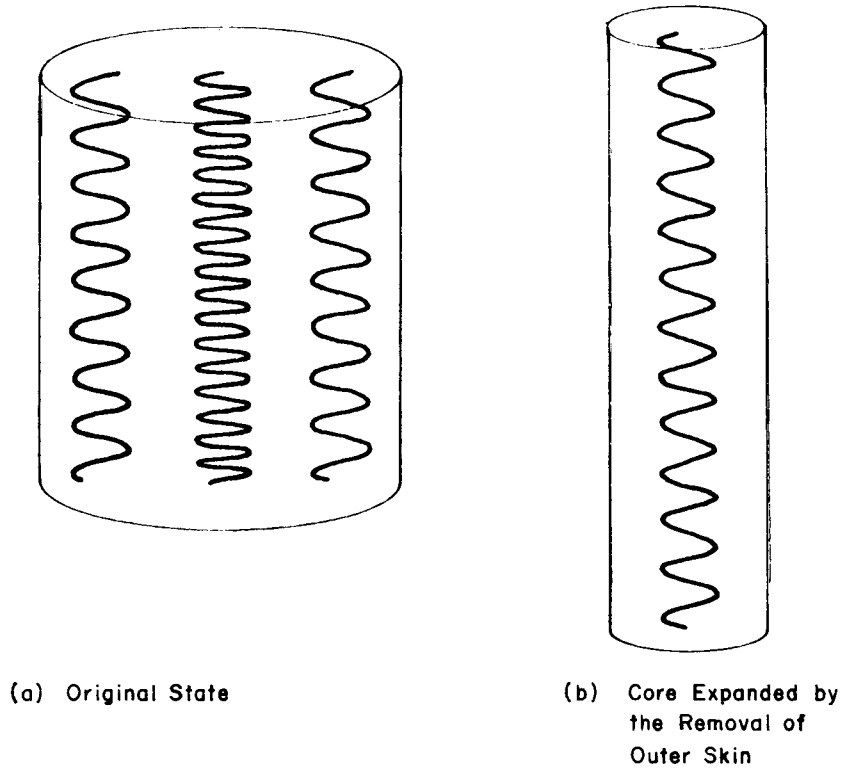
Figure 9. Spring Analogy of Bauer-Heyn's Method of Determining Longitudinal Residual Stress in a Cylinder

Equation (17) satisfies the condition when the residual stress pattern is of the case and core type exemplified in Figure 10(a). In order to determine residual-stress patterns as shown in Figure 10(b), it is necessary to remove thin layers from the cylinder in a sufficient number of steps and to measure the length of the remaining portion. The stress which existed in the n-th layer is given by

$$\sigma_n = \frac{A_n E \cdot de_n}{dA_n} - E \left(de_1 + de_2 + de_3 + \cdots\cdots + de_{n-1} \right), \quad (18)$$

where

A_n = the sectional area after the removal of the n-th layer

dA_n = the area of the n-th layer

de_i = the strain change due to the removal of the i-th layer $(i = 1, 2, 3, \cdots\cdots, n)$.

Rod Diameter

(a) Constant-Stress Case and Core Type

Rod Diameter

(b) Variable Stress Type
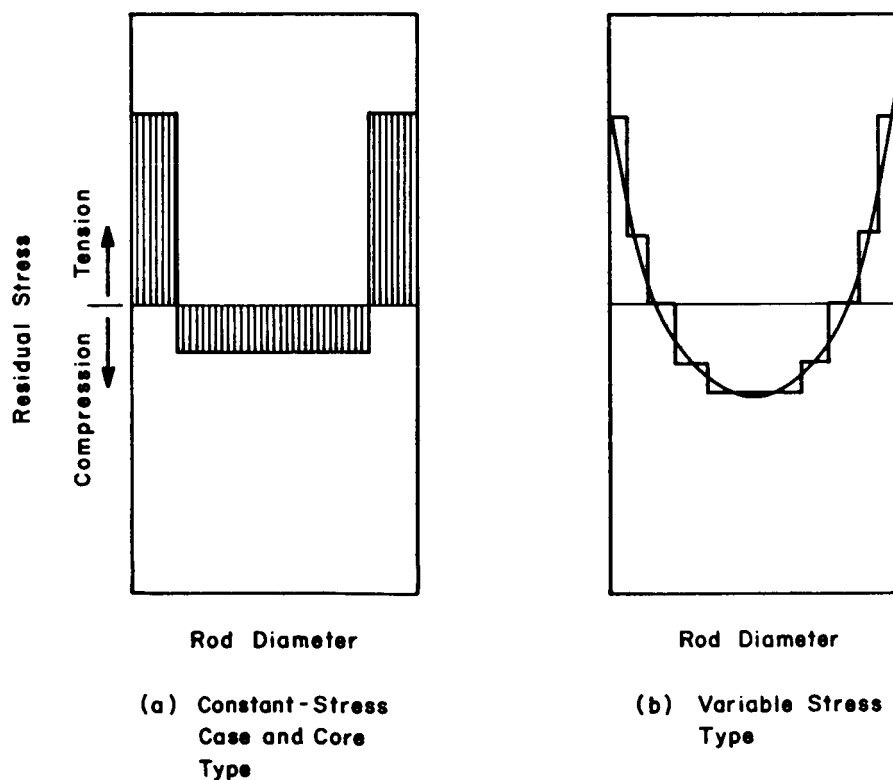
Figure 10. Longitudinal Residual Stresses in Cylinders

2. Methods for Measuring Strains

Various methods for measuring strain have been used for determining residual stresses, such as bonded strain-gage techniques, extensometers, grid systems, brittle coatings, and photoelastic coatings.

Basically, techniques used for residual-stress measurements are the same as those used for ordinary stress measurements, or for measurement of stresses caused by external loading. Information on stress-measuring techniques in general are available from various sources including the Handbook of Experimental Stress Analysis edited by Hetényi,[10] and recent reviews by Crites.[20, 21, 22, 23] This section describes briefly the characteristics of various stress-measuring techniques as they are used for measuring residual stresses.

a. Bonded Strain-Gage Technique[22, 23, 24]
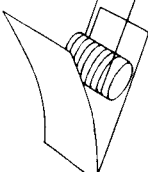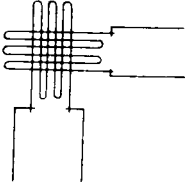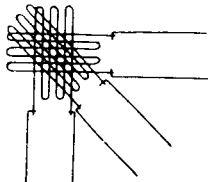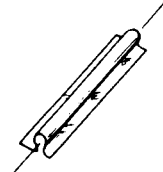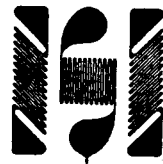
In the resistance-type bonded strain-gage techniques, gages are bonded on the test specimen. As the specimen is strained, the resistance of the gages changes, and the magnitude of strain is determined by measuring the resistance change. Most bonded electrical-resistance strain gages are made from either metallic wire or foil materials. There are also the recently developed semiconductor gages. A variety of sizes, shapes, and configurations are available including single-element gages and rosettes with two, three, or four elements. Table II illustrates various types of strain gages.

(1) Wire Gages, Foil Gages, and Semiconductor Gages. Wire gages were the first to become commercially available. Wire materials commonly used include constantan, nichrome V, and iso-elastic. Wire gages are made in three general forms: flat-wound, helix-wound, and single-filament. Flat-wound and helix-wound gages are widely used. Flat-wound gages are manufactured in sizes from approximately 6 inches to $\frac{1}{2}$ inch, and are backed with paper or phenolic material. Helix-wound gages are made in sizes from $\frac{1}{2}$ inch down to $\frac{1}{16}$ inch. Single-filament gages, available in several sizes up to approximately 8 inches, are suited for high-temperature applications.

Foil gages are a more recent development. They are manufactured in a grid configuration from metallic foil between 0.001-inch and 0.0001-inch thick, and are usually backed by paper, epoxy, or phenolic materials. When compared with wire gages, foil gages have excellent features, as follows:

Table II. Various Types of Bonded Strain Gages (Crites)[22]

					Type
WIRE GAGES	FLAT-WOUND	HELIX-WOUND	FREE-FILAMENT		Single-strand
					Flat-wound
					Helix-wound
					Free-filament
MONOFILAMENT	90°-ROSETTE	45°-ROSETTE	WELDABLE, SINGLE-WIRE		Monofilament
					90°-Rosette
					60°-Rosette
					45°-Rosette
					Weldable
FOIL GAGES	RECTANGULAR-GRID	RECTANGULAR-GRID, HIGH-TEMP	90°-ROSETTE		Rectangular-grid
					Rectangular-grid
					Weldable
					90°-Rosette
120°-ROSETTE	45°-ROSETTE	DUAL-ELEMENT	HIGH ELONGATION		120°-Rosette
					45°-Rosette
					Dual-element
					High elongation
SEMICONDUCTOR GAGES		SINGLE-ELEMENT	HIGH ELONGATION U-SHAPED		Single-element
					U-shaped
					Dual-element

/

	Gage Length Range (in.)	Gage Backing
	$1\text{-}^5/_8$ to 8	Paper, bakelite
	$^1/_2$ to 6	Paper, epoxy, polyester, bakelite
	$^1/_{16}$ to $^1/_2$	Paper, bakelite
	$^1/_8$ to $^5/_{16}$	None
	$^1/_4$ to 1	Ceramic coating
	$^1/_4$ to $^7/_{16}$	Paper
	$^3/_8$ to $^3/_4$	Paper, bakelite
	$^1/_4$ to $^3/_4$	Paper, bakelite
	$^9/_{16}$ to $1\text{-}^5/_{16}$	Stainless steel
(std.)	$^1/_{64}$ to 6	Paper, epoxy
(high-temp)	$^1/_{16}$ to 1	Bakelite, strippable
	$^1/_4$, $^1/_2$	Stainless
	$^1/_8$ to $^1/_2$	Epoxy, bakelite
	$^1/_8$ to $^1/_4$	Epoxy
	$^1/_{16}$ to $^1/_2$	Bakelite, epoxy
	$^1/_2$	Bakelite, strippable
	$^1/_{64}$ to 1	Epoxy
	0.05 to -0.5	Epoxy, mica, etc.
	0.16	High temperature, none
	0.16	Selected

2

Applications
Narrow widths, wrap around
General purpose, static, dynamic
Limited space, static dynamic
High temperature
High temperature
Biaxial strain, principal, strains known
Biaxial strain, principal, strains unknown
Biaxial strain, principal, strains unknown
Elevated-temperature, quick installation
General purpose, dynamic
Elevated temperature
Elevated temperature, easy installation
Biaxial strains, principal strains known
Biaxial strains, principal strains
Biaxial strains, principal strains
High-low temperature compensation
Tensile tests or high elongation conditions
High sensitivity, transducers
High sensitivity, transducers
Temperature compensation, high sensitivity

3

they can be manufactured to smaller sizes with greater accuracy

they can carry heavier currents because their generally greater surface area and thin backing provides better heat dissipation

they can be formed around sharper radii because they are thinner.

Semiconductor gages are made of thin crystals of germanium or silicon and are usually less than $1/2$-inch long. Semiconductor gages are very sensitive strain indicators; however, they also are sensitive to temperature changes and are somewhat expensive. Semiconductor gages will undoubtedly become more popular as manufacturing techniques improve and as they become more widely known.

(2) Temperature Effects and Temperature Compensation. A key consideration in gage selection is the temperature range in which the gage must function. Although the largest selection is available in the room-temperature range, many gages are available for use at extremely low and high temperatures, as follows:

paper-backed gages for temperatures ranging from cryogenic to about 175°F

epoxy-backed gages from -400°F to 250°F

phenolic- or bakelite-backed gages from cryogenic temperature to 350°F

phenolic-backed or epoxy-backed gages reinforced with glass fiber for temperatures from cryogenic to 450°F.

With each gage, appropriate cements must be used. For applications above 500°F, no backing materials are employed except with weldable-ype gages.

Changes in temperature tend to cause an apparent strain; therefore, some type of temperature compensation is needed. Frequently, a "dummy gage," which is not subjected to the strain, is exposed to the same temperature as the actual gage to provide a basis for comparison. A temperature-compensated gage can also be used.

(3) Gage Bonding. Gages must be bonded securely to the specimen. Various types of organic cements are used widely for applications up to 500°F. Ceramic cements are used for high-temperature applications. Gages are sometimes spot welded to the specimen. Figure 11 shows temperature ranges for commonly used strain-gage cements.
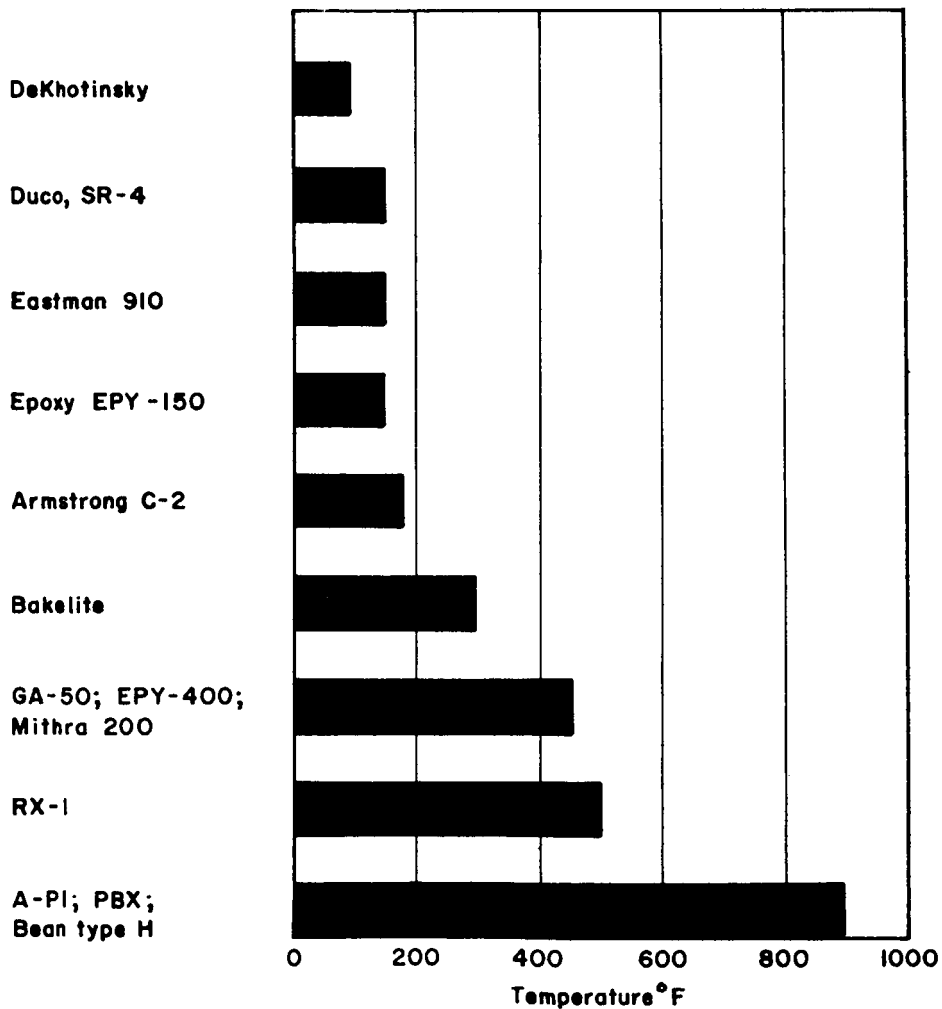
Figure 11. Temperature Ranges for Strain-Gage Cements

Organic cements in current use are nitrocellulose, phenolic, epoxy, cyanoacrylate, and shellac. Nitrocellulose cements, which were the first cements employed for strain-gage applications, are used exclusively for paper-backed gages and can not be employed with bakelite- and epoxy-backed gages. Nitrocellulose cements commercially available include SR-4 (Baldwin), Post-Yield (Baldwin), and household Duco (Du Pont). Phenolic cements have long given satisfactory results. However, they require a high cementing temperature (between 200 and 300°F) and a high clamping pressure (not less than 50 to 75 psi).

Epoxy cements, which are used for bonding epoxy- and phenolic-backed gages to the specimen, are noted for their strength of bond and for their ability to penetrate surface films to secure good adhesion. There are two general types of epoxy cements: room-temperature curing cements and heat-curing cements. EPY-100 (Baldwin) cures in 12 to 15 hours at 75°F. Commercially available heat-curing cements include Armstrong C-2, EPY-400 (Baldwin), Mithra 200 (Mithra Engineering), and GA-50 (Budd).

One of the newest cements adapted for strain-gage application is a modified cyanoacrylate cement called Eastman 910. Because of its rapid setting characteristics (it can be ready within a minute or so), the cement is widely used, however; the cement tends to be brittle and is limited to elongation in the order of 2 percent at room temperature.

Shellac cements (de Khotinsky, hard) can be employed with most strain gages, but bonds tend to creep. Therefore, shellac cements are not suitable for residual-stress determinations in which measurements must be made before and after machining.

Three types of ceramic cements are available: silicate cements, phosphate cements, and fusible materials. X-Y and RX-1 (both Baldwin) are silicate cements. The most widely employed ceramic cements are phosphate cements, which can be used up to 1000°F statically and even higher dynamically. Commercially available phosphate cements include Allen Pl, Allen PBY, and Bean Type H. Fusible materials are now available for bonding gages. A bonding process developed by the Norton Company involves spraying molten aluminum oxide (Rokide A) and other refractory materials by means of a special gun.

Spot welding strain gages to a structure is an increasingly popular technique. The method provides quick installation for high-temperature analysis. A number of weldable gages are on the market or in late stages of development.

(4) Gage Protection. In most residual-stress measurements, gages must be protected from metal chips produced during machining as well as from the oil or water necessary to cool the specimen. A number of systems have been devised for protecting gages under various conditions.

Some coating can be applied cold, while others require heat. Cold-applied coatings include petroleum jelly, Di-Jell, and silicone greases. Protective coating applied with heat include microcrystalline waxes and epoxy coatings. A combination of coatings is used when more extensive protection is needed.

A combination coating developed at Battelle has been proved in field service on various pipe lines for a number of years.[22] It consists of multiple coatings of Glyptal enamel, Neoprene, and Petrosene wax, as shown in Figure 12. Gages are first thoroughly dried and the lead wires soldered. A coating of Glyptal enamel is applied to gage, gage leads, and surrounding areas of the test specimen. The enamel is dried at 120 to 180°F for approximately 1 hour. Four successive coats of neoprene cement are then applied. Each coat is extended just beyond the periphery of the preceding coat. Also, each coat is dried about $1/2$ hour at 120°F. The final coat of Petrosene is applied over the whole area while the test specimen is still hot. When additional mechanical protection is required, a small metal shield is placed over the gage.

(5) Strain Indicators. To obtain accurate measurements of strain in structures with the use of electric-resistance strain gages requires careful selection of highly sensitive measuring instruments and circuitry.[22] A quick evaluation of the degree of sensitivity that is required in straingage equipment can be obtained by referring to the basic equation which relates changes in resistance to changes in strain

$$\Delta R = (GF) \times R \times \frac{\Delta L}{L} , \qquad (19)$$

where

    R = gage resistance (ohms)

    L = length of conductor

    GF = gage factor, experimentally determined by the gage manufacturer.
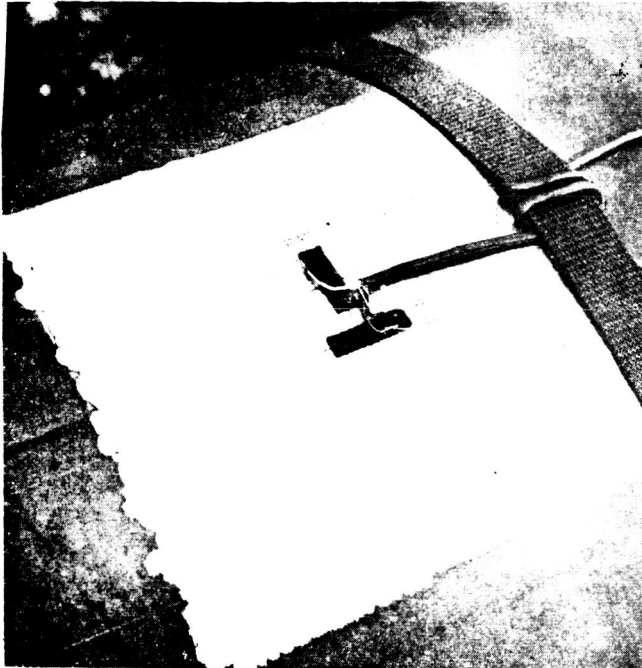
Unprotected strain gage cemented to structure.
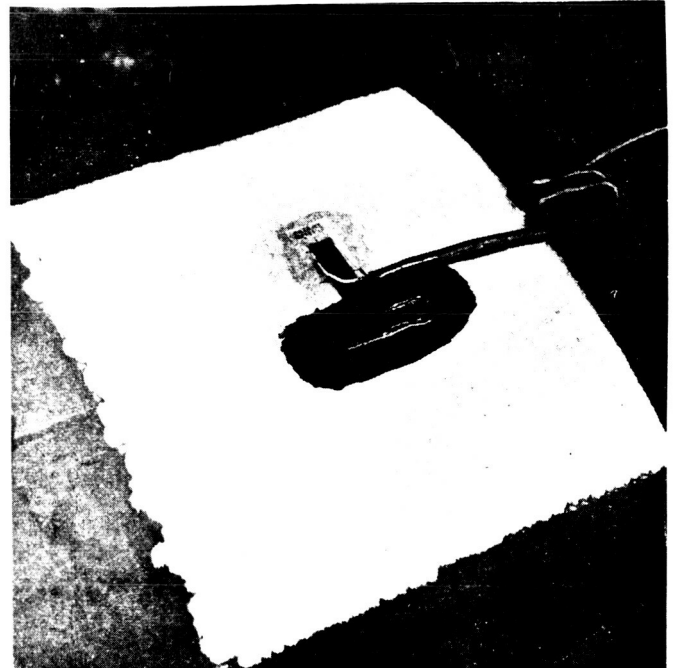
Coat of Glyptal applied to gage, leads and surrounding area.

Four successive coats of Neoprene over Glyptal.
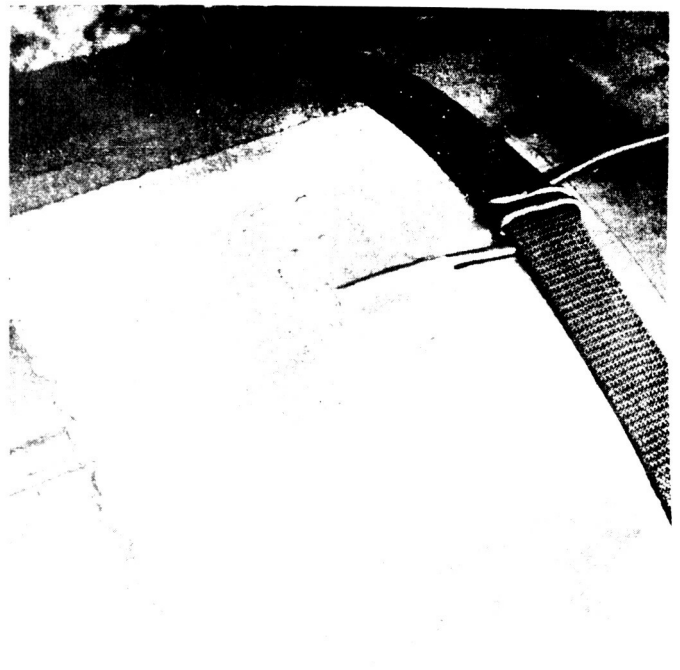
Final coat of Petrosene microcrystalline wax.

Figure 12. Strain-Gage Coating Technique Developed at Battelle (Crites)[22]

For example, for measurement of a 1000- psi stress in an alumi-num member, equipment and circuitry sensitive enough to detect a change in resistance of 0.024 ohm would be required. This is deter-mined by noting that Young's modulus for aluminum is approximately 10×10^6 psi; hence, the strain is 0.0001 in./in. If the gage factor is 2.0, and the gage resistance is 120 ohm, the sensitivity required is

$$\Delta R = 2 \times 120 \times 0.0001 = 0.024 \text{ ohm.}$$

To detect such small resistance changes, specially designed instruments, which are frequently called static-strain indicators, are used. These instruments have a built-in current source, balancing galvanometer, gage-factor adjustment, balancing resistors, and gage connections. Switching devices are used for taking measurements from a series of gages on a specimen or structure. Recorders for dynamic measurement also are available.

b. Techniques Using Extensometers

Extensometers are strain-measuring devices. Mechanical-electrical, and optical extensometers are commonly used.[10] Most commercially available extensometers are primarily for developing stress-strain curves during the material testing. Some of them, however, can be used for residual-stress measurements.

Figure 13(a) shows a mechanical extensometer which has been developed by Gunnert[25] primarily for measuring residual stresses in weldments. The legs, 1 and 2, are supported against each other by two points, 3. The adjusting screw, 4, is threaded into leg 1 and the nut, 5, is fixed to leg 2. The flat end of the adjusting screw lies against the gage pin, 7, of the special indicator, 6, invented by Abramson. The indicator is fixed to leg 2 by holder 8. The parts 9, 10, and 11 form a protective cover. The adjusting screw, 4, is accessible through a hole, 12. A holder, 13, with balls, 14, is fixed to the lower part of legs 1 and 2. These balls are Brinell balls and are 0.079 inch in diameter.

In carrying out strain measurements, the Gunnert extensometer is placed with its balls in conical depressions 0.354-inch apart on the test specimen, as illustrated in Figure 13(b). The shape of the depres-sions is shown in Figure 13(c). For measuring residual stresses, eight depressions are made along the periphery of a circle 0.177 inch in radius. After the distances between four sets of depressions are measured, the measuring area is freed from the surrounding material by means of a core drill which produces a groove around the measuring
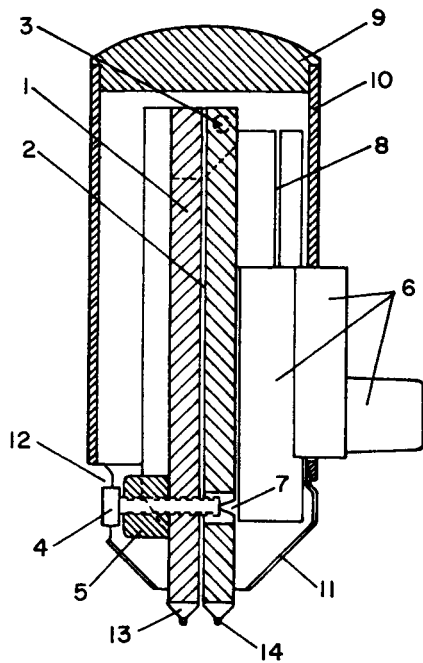
(a) Extensometer
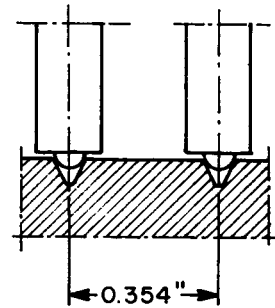
(b) Extensometer Balls in the Gage Holes
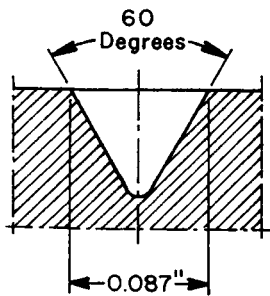
(c) Shape of Gage Holes
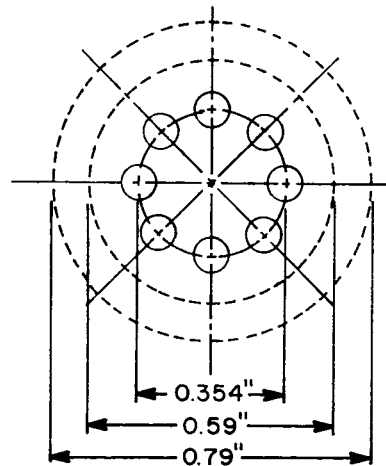
(d) Measuring Surface

Figure 13.   Gunnert's Method for Measuring
Residual Stress

area, as shown by the broken lines in Figure 13(d). The distance between the four sets of depressions are measured to determine elastic strains released during the stress relaxation.*

c. Grid Systems[20]

Probably the simplest method for determining distortion or plastic deformation in a model or a part is by marking it with a system of grid lines. The lines are applied by several means, depending upon the material and the geometry: they can be scratched by hand, machine scribed, drawn with ink, imposed on photosensitive coatings by a photographic process, or stamped with an inked rubber stamp.

The sensitivity of measurement is dependent upon the size and accuracy of the scratches or lines and the kind of measuring instrument used. With an optical micrometer, measurements can be made to about 50 to 100 microinches per inch. However, the measurements require pain-taking efforts.

d. Brittle-Coating Technique[10, 21]

The use of brittle coatings or brittle lacquers as strain indicators is based on the observation that such coatings through their rupture, can reveal the magnitude of strain in the underlying material of the test piece. These coatings work on the principle that, under strain, cracks will appear normal to the direction of maximum principal stress.

There are two general classes of brittle coatings: resin-based coatings and glass-based coatings. Resin-based coatings are designed for room-temperature use, while glass-based coatings can be used at high temperatures up to about 600° F. Best results are obtained when coatings are sprayed on specimens. A kit is available which includes a spray gun, a calibration device, and other necessary equipment.

e. Photoelastic-Coating Technique

Under the action of stresses, transparent materials become doubly refracting (birefringent) and if a beam of a polarized light is passed through a model (under stress) made of such a material, a

---

*Theoretically, measurements of distances between three sets of depressions are enough for determining residual stresses. The fourth set is used for improving the accuracy of measurement.

colored picture is obtained from which the stress distribution can be determined. This technique is called the photoelasticity.*[10, 26, 27]

The photoelastic-coating technique is a method of stress analysis in which the actual structure to be stress analyzed is coated with a photoelastic plastic.[28, 29, 30, 31] When strains occur in the specimen, the strains are transmitted to the plastic coating, which then becomes birefringent. The birefringence can be observed and measured, using a reflection polariscope, as shown schematically in Figure 14. Figure 15 shows an example of fringe pattern. The principles of analyzing fringe patterns, which are basically the same as those obtained in ordinary photoelasticity, are found in instructions provided by the manufacturer.

Ring for simultaneous rotation of the analyzer-polarizer assembly

Eyepiece

Analyzer

Babinet Compensator

Light Source

Polarizer

Lens

Coatings

Specimen
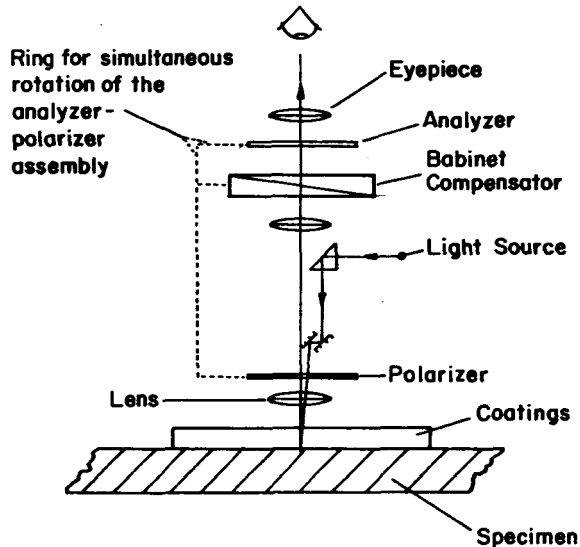
Figure 14. Schematic of Optical System
of Reflection Polariscope

---

*The usual photoelastic technique which employs models made with special plastic materials are seldom used for studying residual stresses in metals and metal structures primarily because distributions of residual stresses produced in metals are different from those produced in the plastic materials.

Figure 15.   Photostress Coating Technique
for Measuring Stresses

(Crites)[20]

The photoelastic coating can be applied by brushing a liquid plastic
on the surface of the specimen and polymerizing it by applying heat.
Alternatively, a prefabricated flat or countered sheet of plastic can be
bonded to the part at room temperature.   The maximum strain measured
ranges between 3 and 50 percent, depending on the type of plastic used;
the strain sensitivity usually decreases with the increased in the max-
imum measurable strain.

3.   **Various Methods of Measuring Residual Stresses Based on Stress-Relaxation Techniques**

Summarized in the following pages are 15 methods of measur-
ing residual stresses based on stress-relaxation techniques:[32, 33, 34]

Methods 1 through 8:   applicable primarily to plates

Methods 9 through 12:   applicable primarily to solid
cylinders and tubes

Methods 13 through 15:   applicable primarily to three-
dimensional solids.

The methods are named on the basis of the principle involved, the strain-measuring techniques used, or the name of the persons who have developed or described them. For each of these methods the description includes experimental procedures, range of application, advantages, and disadvantages.

a. Method 1. Electric-Resistance Strain Gage Sectioning or Trepanning[35, 36]

(1) Procedures. Electric-resistance strain gages are mounted on the surface (both surfaces if possible) of the test structure or specimen, and then a small piece (or pieces) of metal containing the gages is taken from the structure and measurement is made of strain changes that occur due to the removal, as shown in Figure 7.

(2) Application. Relatively all-around use, with the measuring surface placed in any position.

(3) Advantages. Reliable method. Simple principle. High measuring accuracy.

(4) Disadvantages. Destructive. Gives average stresses over the area of the piece removed from the specimen; not suitable for measuring locally concentrated stresses. Machining is sometimes expensive and time consuming.

b. Method 2. The Gunnert Technique for Plates[25]

(1) Procedures. Details of the Gunnert technique are described previously in connection with Figure 13.

(2) Application. Suitable for laboratory and field work. Can be used on horizontal, inclined, or vertical measuring surfaces.

(3) Advantages. Rapid. The main stresses at a measuring point can be determined both as regards direction and magnitude in about 1 hour. Easily repaired damage of the measured object. Permits the measurement of stress peaks to some extent owing to the small measuring distances. Robust apparatus which permits measurements in unfavorable weather.

(4) Disadvantages. The method entails considerable manual training in order to ensure correct manipulation.

c.   Method 3. Vinckier's Method[32, 37]

(1) Procedures. Hardened steel balls are punched into
a measuring surface. The distance between them is measured before
and after the material (with the balls in position) has been removed
from the object. From the differences in the measurements of the
distance between the balls which have occurred, the original residual
stresses can be calculated.

(2) Application. Suitable for laboratory and field work.
Can also be used for inclined, vertical, and overhead surfaces.

(3) Advantages. Rapid method. Easily repaired damage
of the test piece. High measuring accuracy.

(4) Disadvantages. The relatively long distance between
the measuring balls ($3/4$ inch) do not permit the measurement of stress
peaks or accurate measurements in regions with pronounced differences
in the stress distribution.

d.   Method 4. Dividing-Grid System[32]

(1) Procedures. The surface of the object measured is
provided with a system of suitably located measuring points, placed
at the corners of a square network, for example. The distance between
the points is determined and the distance between their diagonals is also
measured, generally with a mechanical measuring instrument. The
points may consist of depressions or punched-in balls. The whole
object is then divided into square elements, each containing four
measuring points. The distances previously measured are measured
again. The stresses can be calculated from the difference between the
two measurements.

(2) Application. Laboratory method, since a division of
the object tested is not usually permissible.

(3) Advantages. Simple principle and measurement.
Allows the determination of closely adjoining areas over large surfaces.

(4) Disadvantages. Involves total destruction of the object.

e.   Method 5. Drilling-Strain Gage (Mathar-Soete)[14, 15, 16]

(1) Procedures. Residual stresses are relieved by drill-
ing a hole, for example $1/4$ inch in diameter. Strain changes that take

place in areas around the hole due to drilling are measured, and the residual stresses that existed in the drilled area are calculated (Figure 8).

(2) _Application._ The method can be used for laboratory and field work and on horizontal, vertical, and overhead surfaces.

(3) _Advantages._ A simple principle. Causes little damage to the test piece, convenient to use on welds and adjoining material.

(4) _Disadvantages._ Drilling causes plastic strains at the periphery of the hole, which may displace the measured results. The method must be used with critical care.

f. Method 6. Drilling-Brittle Coating (Gadd)[11,38]

(1) _Procedures._ The measuring point and its surrounding areas are coated with a brittle lacquer. A hole (diameter d, e.g. $1/8$ inch) is drilled at the measuring point to a depth of between $1/2$ d and d. Cracks are produced in the lacquer due to relaxation of residual stresses caused by the drilling. As shown in Figure 16, radial cracks occur if residual stresses are tensile, and circular cracks occur if residual stresses are compressive. From the direction and distribution of the cracks, it is possible to determine the direction of main stresses since the latter are perpendicular to the direction of the cracks.

(2) _Application._ Preferably a laboratory method, but it can also be used for field measurements if the atmosphere is dry. The measuring surface can be chosen as desired.

(3) _Advantages._ Little damage to the test piece. Rapid determination of the directions of the principal stresses and an indication of their magnitude.

(4) _Disadvantages._ Only qualitative.

g. Method 7. Photoelastic Coating[30,32,39]

(1) _Procedures._ A photoelastic coating is placed on the specimen. A hole is drilled at the measuring point through the photoelastic coating and a portion of the specimen to a certain depth, e.g., equal to the diameter. If residual stresses exist, birefringence occurs in areas near the drilled hole. By analysis, the birefringence strain release that took place due to drilling is determined and then the residual stresses that existed in the drilled areas are calculated.
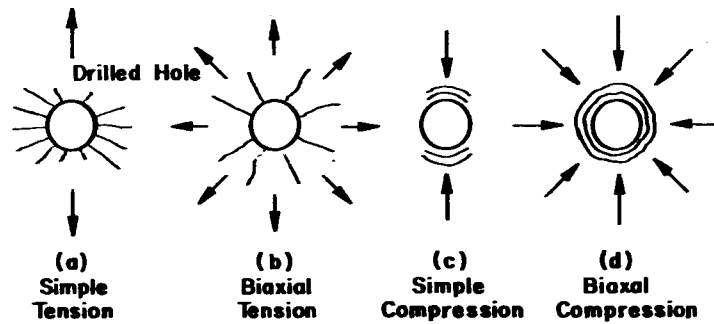
Figure 16. Typical Crack Pattern Obtained Under Various
Surface-Stress Conditions, Showing Combination of the
Mathar Hole Method and Brittle Coating

(2) Application. Primarily a laboratory method, but it
can also be used for field measurements under certain circumstances.

(3) Advantages. Permits the measurement of local
stress peaks. Little damage to the material.

(4) Disadvantages. Sensitive to plastic strains which
sometimes occur at the edge of the drilled hole.

h. Method 8. Successive Removal of Metal Layers
(Stäblein)[11, 32, 40]

(1) Procedures. Let it be assumed that residual stresses
are present in a bar-shaped body. When material is removed on one
side of the body by milling, for example, the bar will bend toward the
milled side if they are tensile stresses, as shown in Figure 17. By
this means, the opposite side of the bar will either be lengthened or
shortened. If measuring devices such as strain gages are applied to
this side, it is possible to study to what extent the surface has changed
in length for each layer of the material removed on the opposite side
and, from the values read off, the residual stresses in the different
layers can be calculated. Instead of measuring the surface changes
in length, the bending of the bar can be measured.

(2) Application. Measurement of the uniaxial residual
stresses along plates, shafts, surface-treated, heat-treated, or surface
bar-shaped objects.

(a) Before the Removal of the Metal Layer

(b) After the removal of the Metal Layer
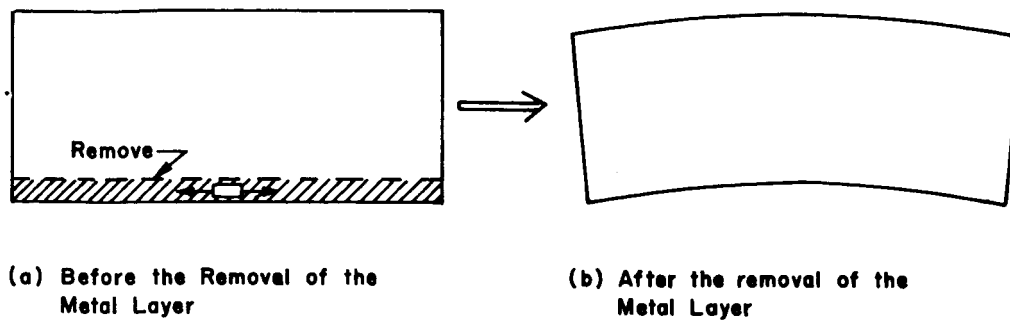
Figure 17. Residual Stress Measurement by
Successive Removal of Metal Layers

(3) Advantages. Reliable method for measuring the mean stresses over a relatively large surface.

(4) Disadvantages. Does not permit measurement of stress peaks. Involves total destruction of the object measured. Only uniaxial stresses are measured. Risk of residual stresses set up mechanically owing to the milling.

i.   Method 9.   Bauer-Heyn's Method[11, 18, 19]

(1) Procedures. Metal in a thin outside layer of a cylindrical specimen is removed in a sufficient number of steps, and the length of the remaining portion is measured, as shown in Figures 9 and 10. Residual stresses are then calculated.

(2) Application. Cylindrical bodies with rotationally symmetrical stresses.

(3) Advantages. Rather simple.

(4) Disadvantages. Longitudinal stresses only are considered. Applicable to limited cases.

j.   Method 10.   Mesnager-Sachs' Boring-Out Method[11, 41, 42]

(1) Procedures. On the outside of a cylindrical body, measuring devices are applied to the measured object in the longitudinal and tangential directions, in the form of strain gages for example, or in the longitudinal direction and across the diameter in the form of

mechanical measuring devices. A central hole is drilled in the body .
and the changes in the deflections of the measuring devices are noted
as the diameter of the hole is increased in steps by repeated drilling.

(2) Application. Circular cylindrical bodies with rotation-
ally symmetrical distribution stresses.

(3) Advantages. Permits the measurement of the uni-
and biaxial residual stress distribution in the whole of the test piece.

(4) Disadvantages. Assumes that the stresses are con-
stant along the cylinder and that the stress distribution is rotationally
symmetrical. Involves total destruction. Risk of mechanically caused
residual stresses due to working. Not very suitable for measuring
residual stresses in welds.

 k. Method 11. Deflection Measurements by Splitting Strips
   or Bars[11]

(1) Procedures. A strip or a bar is split down its central
longitudinal plane and, as a result, the two halves curl back. The deflec-
tion of the bars, or the amount of split, is measured and residual
stresses are calculated.

(2) Application. For laboratory and field measurements.

(3) Advantages. Simple.

(4) Disadvantages. Only an approximate method and
applicable only to cases in which the stresses are thought to vary
linearly through the thickness of a plate or shell but are constant along
the length, across the width of the plate, or around the circumference
of the shell.

 l. Method 12. Slitting a Tube (Sachs-Espey)[11, 43]

(1) Procedures. A slit is made in a tube, and the deflec-
tion of the tongue is measured. The removal of metal from the tube
may be made by pickling or machining. Residual stresses are cal-
culated from the deflection.

(2) Application. For laboratory and field measurements.

(3) Advantages. Relatively simple.

(4) Disadvantages. Not very accurate.

m. Method 13. Successive Drilling (Soete-Vancrombrugge)[32, 44]

(1) Procedures. Strain gages are applied in a star around
the measuring point, similarly to the Mathar-Soete method (Method 5).
As in that method, a hole is drilled at the center of the star, but in steps
of about 1 mm in depth at a time. For each step the changes in measure-
ments are read off on strain gages. From the values obtained for dif-
ferent drilling depths it is possible, with the help of empirical values,
to calculate the original residual stresses at the different levels.

(2) Application. The method can be used both for labora-
tory and field work.

(3) Advantages. If the directions of the main stresses
are not known, they can be determined. Damage to the object measured
is easily repaired. Can be employed for all inclinations of the plate.

(4) Disadvantages. Drilling causes plastic strains at the
periphery of the hole which may displace the measured results. The
method must be used with critical care.

n. Method 14. The Gunnert Drilling Method[45, 46]

(1) Procedures. Four 3-mm (0.12 inch) parallel holes
located at the periphery of a circle with a 4.5-mm (0.18 inch) radius
are drilled through the plate at the measuring point, as shown in
Figure 18. The diametrical distance between these holes at different
levels below the surface of the plate is measured by means of a spe-
cially designed mechanical gage. The perpendicular distance between
the plate surface and measuring points at different levels below the
surface is also measured. A groove is then drilled around the measur-
ing points in steps of about 0.08 inch in depth. The perpendicular dis-
tance is read off for each step. After the groove has been drilled to
the desired depth, the four holes will be located in a plug with a dia-
meter of 16 mm (0.63 inch), and this plug is free from the surroundings
and is thus also free from residual stresses. A further measurement
of the diametrical distance at all levels previously measured, together
with the perpendicular measurements, provide information for calculat-
ing the original residual stresses.

(a) Plan　　　　　　　　　　　　　(b) Side View
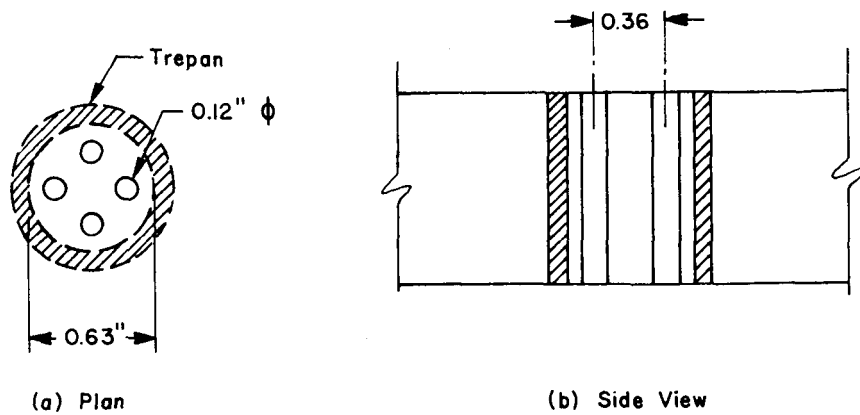
Figure 18.　The Gunnert Drilling Method

(2)　Application.　Can be used both for laboratory and field work.　The surface of the plate must be substantially horizontal.

(3)　Advantages.　Robust and simple apparatus.　Semi-nondestructive; damage to the object tested can be easily repaired.

(4)　Disadvantages.　Relatively large margin of error for the stresses measured in a perpendicular direction.　The underside of the plate must be accessible for the attachment of a fixture.　The method entails manual training.

o.　Method 15.　The Rosenthal-Norton Sectioning Technique[47]

(1)　Procedures.　Two narrow blocks having the full thickness of the plate are cut with their long axes directed along the axis of weld and transverse to the weld, as shown in Figure 19.　The blocks should be made narrow with respect to the thickness; then it may be assumed that the operation has relieved practically all of the residual stresses acting in the direction perpendicular to the long axis, while relieving only a part of the stress in the direction parallel to the long axis.　At the same time, the blocks should be made long enough with respect to thickness (twice the thickness or more, if possible).　Subsequently, the stress that has been relieved in the central portion of the block is very nearly a linear function of the thickness.　In other words, if the value of this stress is known on the top and bottom faces of the plate, then values of the stress relieved throughout the thickness can be computed.　The next step is to determine residual stresses still left in the blocks.　This can be done by mounting strain gages on the walls of the blocks and then measuring strain relaxation that results from slicing them into small pieces.

46
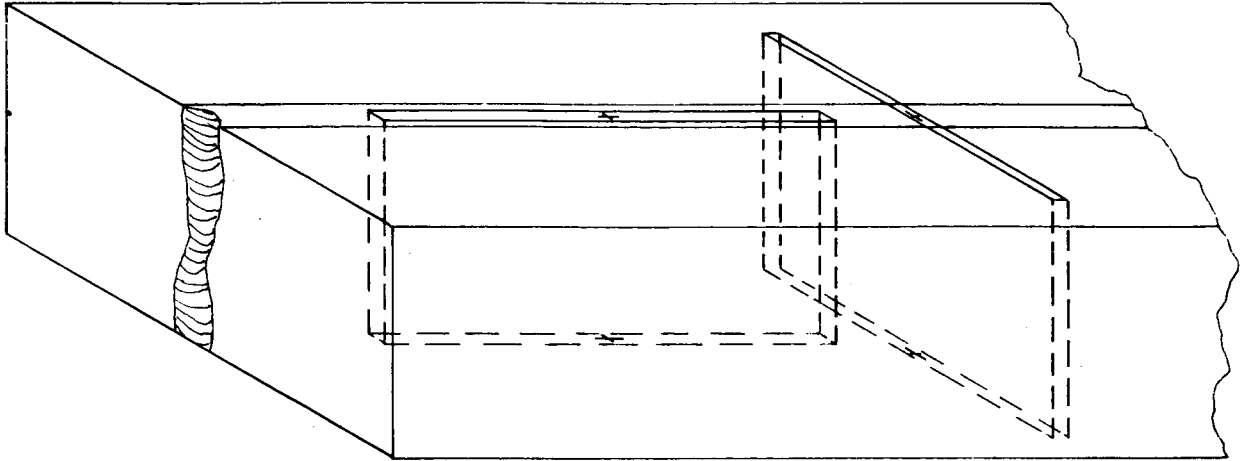
(a) Sectioning the Weldment to prepare Longitudinal and Transverse Blocks.
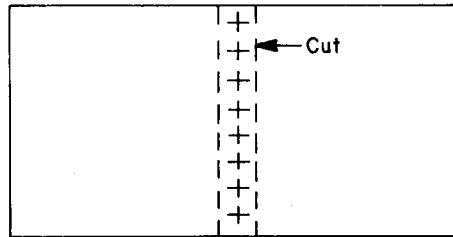
(b) Further Sectioning of Block.

Figure 19. Rosenthal-Norton Sectioning Method

Two blocks, one longitudinal and one transverse, must be cut in order to determine three-dimensional stress distribution. Since two blocks cannot be cut from the same spot, the layout must be so arranged so as to make use of the symmetry of the specimen, or using the method of interpolation.

(2) Application. For laboratory measurements.

(3) Advantages. When the measurements are carried out carefully, there should be little error.

(4) __Disadvantages.__ A troublesome, time-consuming, and completely destructive method.

4. Measurement of Residual Stresses by X-Ray Diffraction Techniques

Elastic strains in metals that have crystalline structures can be determined by measuring the lattice parameter by X-ray diffraction techniques.[48, 49, 50, 51, 52, 53, 54, 55] Since the lattice parameter of a metal in the unstressed state is known or can be determined separately, elastic strains in the metal can be determined nondestructively without machining or drilling. X-ray diffraction techniques are applicable only to crystalline materials having randomly oriented small grains, but most metals fall into this category.

a. Basic Principles

When external or internal forces are applied to a structure made up of metallic crystals, the crystalline lattice is distorted, thus changing the interatomic distances. When the deformation exceeds the elastic limit, plastic deformation takes place as a result of slipping between the lattice planes. In any event, the change in the interatomic spacing is directly proportional to the stress.

X-ray diffraction techniques of measuring stresses in metals are based on the fact that the wavelengths of X-rays are of the same general order of magnitude as the atomic spacings in metallic crystals, which are approximately 1 angstrom unit or 4×10^{-9} inch. The short wavelength of X-rays makes it possible for the rays to penetrate the crystalline lattice to some extent and be reflected back from the atomic planes which they have penetrated.

Suppose that a monochromatic plane wave is introduced to the atomic planes in the direction AB, as shown in Figure 20. The reflected beams from successive parallel planes of atoms are reinforced in one direction BC: the diffraction direction. Bragg's law defines the condition for diffraction as follows:*[55]

---

*ABC and DFH, in Figure 20, represent paths traveled by points in the wave front which excite atoms at B and F in adjacent planes. Reinforcement in the direction BC (or FH) requires that the path difference (EF + FG) be equal to an integral number of wavelengths, i. e.,

$$EF = FG = \frac{1}{2} = n\lambda, \text{ where n is an integer.}$$
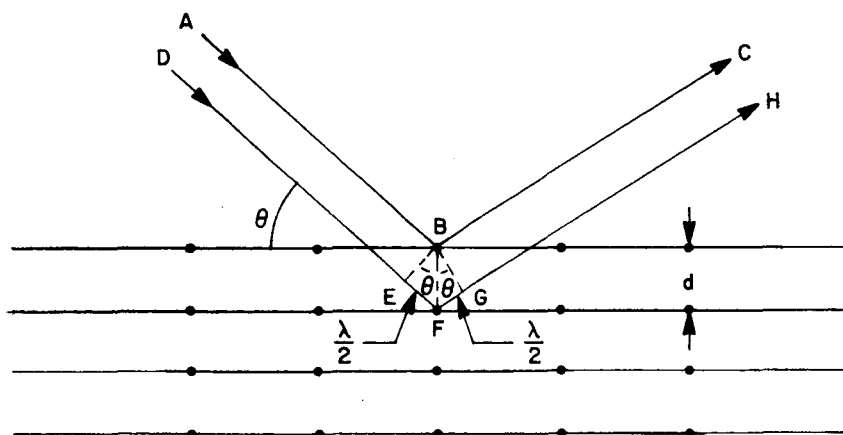
Figure 20. Diffraction Resulting from Reflections from
Adjacent Atomic Planes of a Monochromatic
Plane Wave

$$n\lambda = 2d \sin \theta \, , \qquad\qquad (20)$$

where

λ = the wavelength of incident beam

θ = the angle between incident or reflected beams and surface
of reflecting planes

d = the interplaner spacing

n = the order of reflection (n = 1, 2, 3, ...).

Equation (20) shows that, if the wavelength of the X-ray is known,
the interplaner spacing, d, can be determined by measuring the angle θ.

    (1) Precision in Measurements. Equation (20) shows
that precision in measuring the interplaner spacings depends on the
precision in measuring angle θ. To evaluate the effect of errors,
the Bragg equation is differentiated with respect to θ:

$$\frac{\Delta d}{d} = -\cot \theta \cdot \Delta \theta \, . \qquad\qquad (21)$$

Thus, more precise values of d, corresponding to a small product of
$\cot \theta \cdot \Delta \theta$, are obtained at large angles of θ because $\cot \theta$ decreases as θ

approaches 90 degrees. Figure 21 shows the precision required in measuring θ to obtain a precision in the interplaner distance d of 0.01 percent and 0.005 percent. Since it is difficult to measure Δθ to better than 0.005 degree, diffraction angles of 60 degrees and preferably over 70 degrees are used to select X-ray radiation wavelengths for the particular material to be investigated.
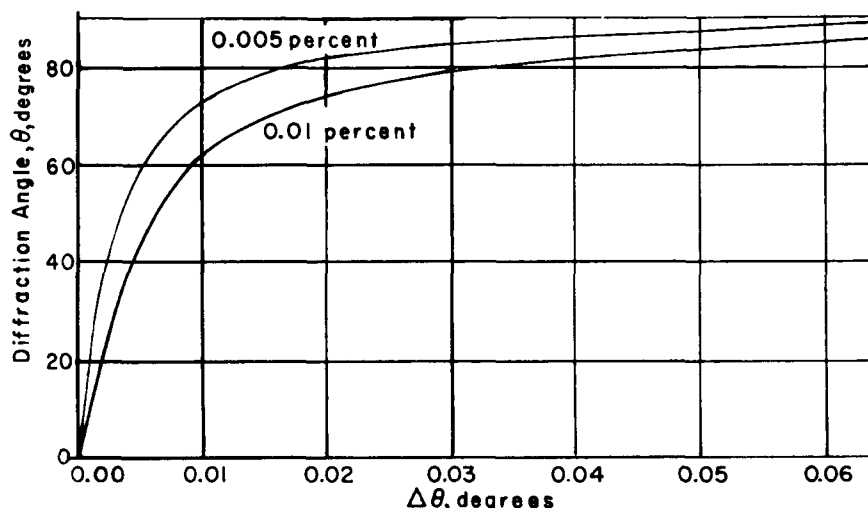
Figure 21. Precision of Measurement of Δθ, as a Function of Diffracting Angle θ, to Obtain a Precision in Interplaner Distance of 0.01 and 0.005 Percent

(Vaughan and Crites)[55]

Table 3 gives the diffraction angle, θ, the diffraction plane, (hkℓ), and the radiation employed for stress analysis of a number of metals.* In aluminum, for example, X-rays produced by a copper target can be used (the diffraction angle is 81 degrees). Sometimes, however, these optimum conditions cannot be employed because of adverse X-ray scattering by the sample. When this condition occurs, other diffraction planes must be chosen, at some sacrifice in the precision of analysis.

---

*The miller index, hkℓ, is the crystallographers' method of defining the various sets of planes in reference to the three coordinate axes of crystals.[56]

Table III. Properties of Metals for X-Ray Analysis (Vaughan and Crites)[55]

Metal of Test Specimen	Crystallographic Plane (hkℓ)	Target to Produce Radiation (in X-ray tube)	Wavelength, λ, Angstrom Units		Diffraction Angle* (degrees)
			$K\alpha_1$	$K\alpha_2$	
Ferritic iron	310	Cobalt	1.78890	1.79274	80.6
	211	Chromium	2.28962	2.29352	78.0
Austenitic steels	311	Manganese	2.10174	2.10570	78.0
	420	Copper	1.54070	1.54434	76.0
Aluminum	511	Copper	1.54050	1.54434	81.0
Copper	400	Cobalt	1.78890	1.79279	81.7
Magnesium	105	Iron	1.93597	1.93991	83.0

*Nominal values for the metals; the diffraction angles differ somewhat for various alloys and are modified by the magnitude of the strain.

Two general methods are employed in the recording of diffraction patterns:

The photographic or X-ray film method, as shown in Figure 22.

The X-ray diffractometer or counter-tube method, with electrical readout attachments, as shown in Figure 23.

Equipment shown in Figure 22 is portable and can be mounted in place on a large structure for field use. The diffractometer type shown in Figure 23 is a laboratory instrument, and the size of specimen that could be tested is limited by the geometry of the instrument.*

(2) X-Ray Film Method. The apparatus consists essentially of a film in a light-tight cassette mounted perpendicularly to the incoming X-ray beam, with a hole through which is inserted the pinhole system that collimates the beam, as shown in Figure 22(a). The film records the rays diffracted by the specimen, and shows, on development, almost circular rings. The diameter of a diffraction ring divided by the distance from the film to the specimen gives 2 tan (180 - 2θ) from which θ is obtained for insertion in Equation (20).

For best results it is advisable to oscillate the film using the metal tube containing the pinholes as the axis of oscillation. This removes much of the spottiness of the diffraction lines, as shown in Figure 24. If the grain size of the specimen is large, it may also be necessary to oscillate the specimen a few degrees, keeping the distance from the film to the irradiated spot on the specimen strictly constant. This distance can be measured by inside micrometers or can be adjusted to a predetermined distance by means of a special gage inserted between the cassette and the specimen. Another method frequently employed is to compute the distance from specimen to film by measuring the diameter of a calibrating ring of known θ on the film. In this method a strain-free powder is placed on the surface of the test object. The powder is chosen to yield a ring near θ = 90 degrees that does not interfere with measurements of the ring produced by the specimen. Silver powder is used for aluminum alloys.

---

*It would be possible to build a specially designed diffractometer-type equipment that can be used for the field measurement of residual stresses in large structural components of space rockets, although no such equipment is commercially available at the present time.

Specimen
Film
Reflected Beam
2θ
$180-2\theta$
Collimator
C
X-ray
Source
$180-2\theta$
Reflected Beam
Normals to
Reflecting Planes

(a) Schematic Diagram

Film holder

X-ray tube

Specimen
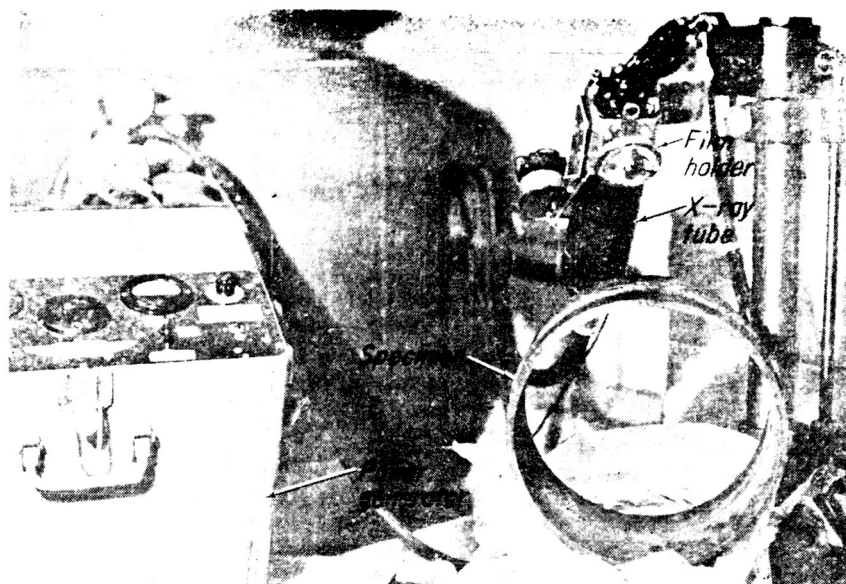
(b) Apparatus

Figure 22. Portable X-Ray Diffraction Equipment
Which Employs Film Method

(Vaughan and Crites)[55]
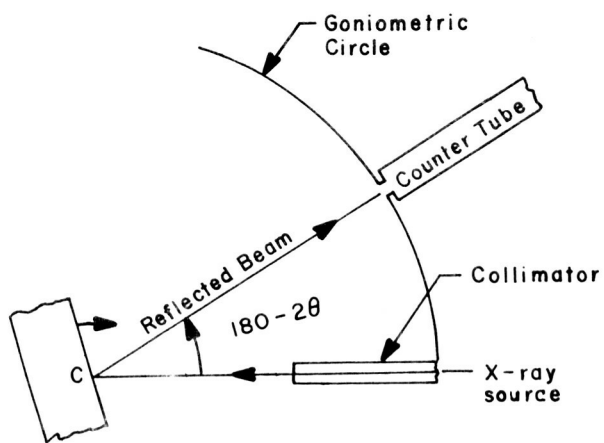
(b) Schematic Diagram
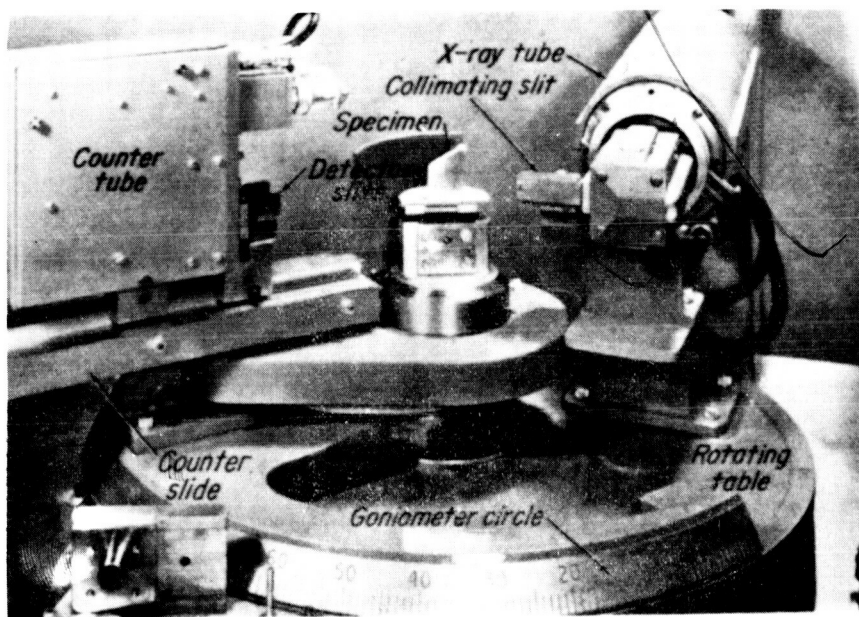
(b) Apparatus

Figure 23. X-Ray Diffractometer Setup
(Vaughan and Crites)[55]

(a) Stationary   (b) Oscillated
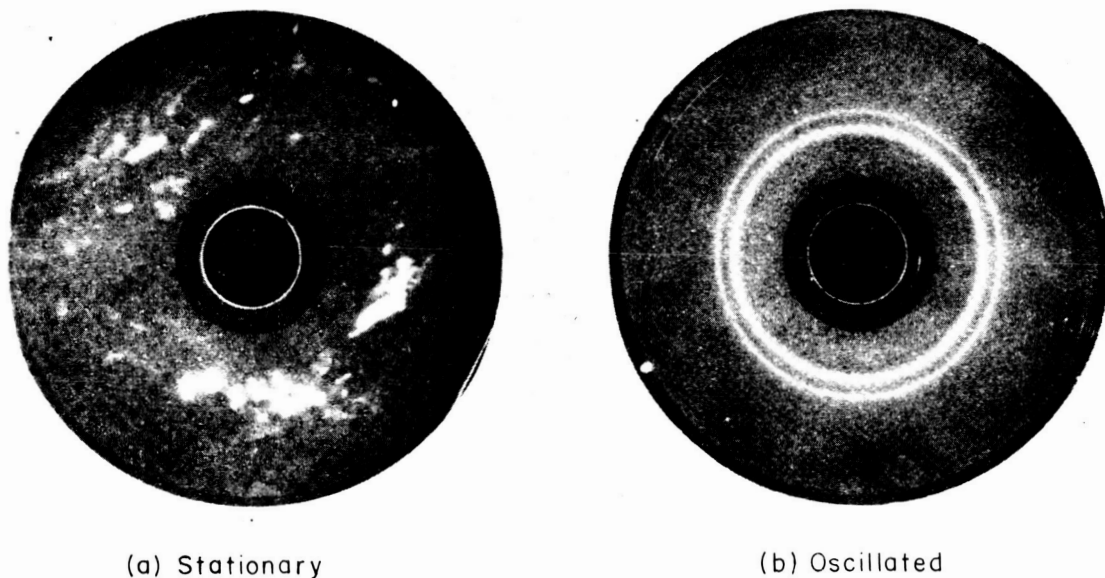
Figure 24.   Improvement of Diffraction Lines
by Oscillation

(Norton and Rosenthal)[50]

For maximum accuracy, the surface of the test object should be free from cold work introduced by machining. If the surface is not in suitable condition, electropolishing is probably the best way to condition it, but good results are also obtained by etching the surface, provided the etching does not leave etch pits so deep that they relieve the surface stresses.

Visual reading of the films can be made by removing a very fine cross hair or scratch over the film under good illumination. The reading also may be made using microphotometers.

(3) X-Ray Diffractometer Method. The X-ray diffraction method and the film method differ, in most cases, only in the detector and the angle made by the specimen with the X-ray beam. The angle between the X-ray beam and the specimen surface is 90 degrees in the film method but is an angle of θ degrees for the diffraction method.

A counter and a receiving slit are moved along a geometric circle to record the intensity of the reflected beam, as shown in Figure 25. . The diffraction angle is determined as the angle of the maximum intensity.

b.   Strain-Analysis Procedures

Although a complete stress analysis would require sufficient data to construct the ellipsoid defined by the loçi and interplaner distances about a specific area on the specimen (Figure 26), it is generally of interest to know the strain or stress in a given direction, ϕ. Thus, the ellipsoid reduces to an ellipse of which the major and minor axes, d_ϕ and d_3, would differ from a given stress σ_ϕ.
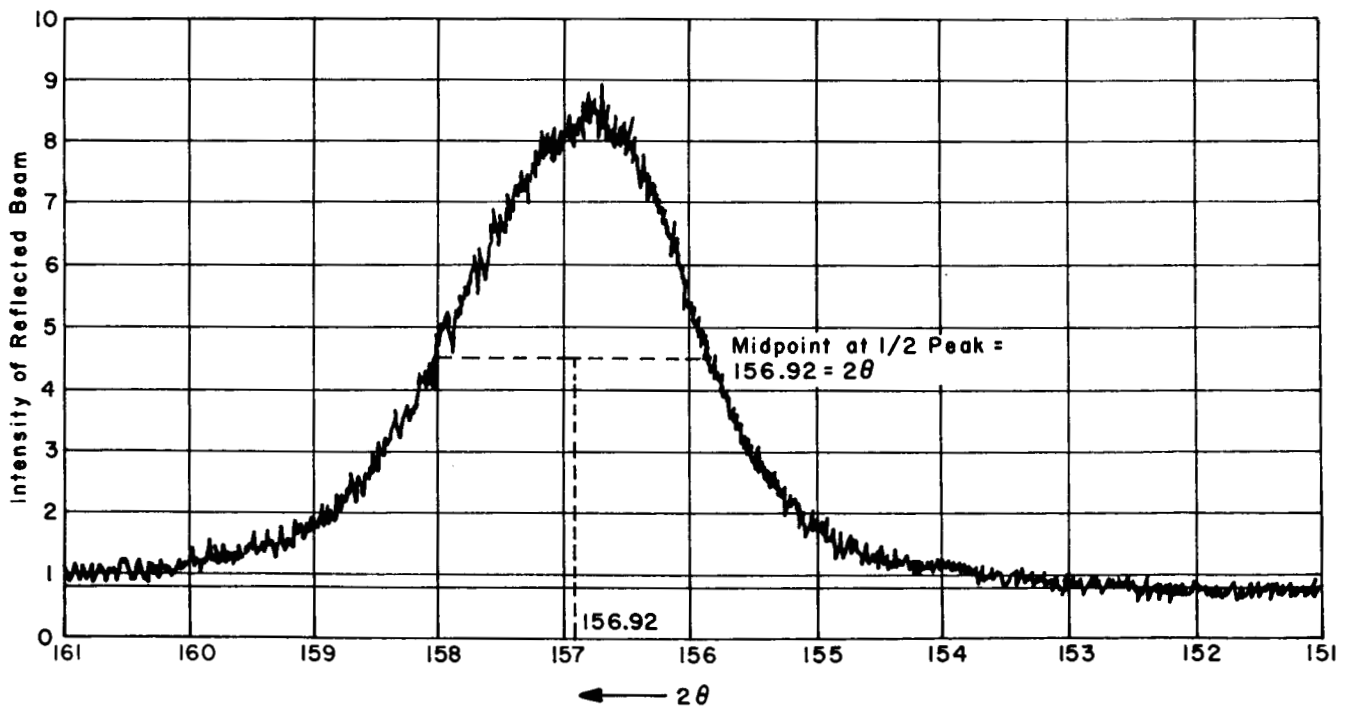
Figure 25.   An Example of Intensity Recording by a
Counter

(Vaughan and Crites)[55]

Because the value of E, ν, $\sin^2 \psi$, and $\cot \theta$ are constant for a given material, reflecting plane, X-ray, and angle ψ, the stress σ_ϕ is quickly computed by multiplication of $\Delta \theta$ by a predeterminable constant:

$$\sigma_\phi = K \, \Delta\theta \,. \tag{24}$$

c.   Values of the Elastic Constants

The preceding equations assume isotropic material.   In general, this assumption is not valid for the individual grains of a metal even when it is valid for the metal as a whole.   This fact, together with the fact that a diffracted beam comes from only those grains having certain orientations in the specimen, has given rise to much uncertainty concerning the correct values to use for Young's modulus and Poisson's ratio.[52]   Some investigators[53,57,58] believe that the effective values of the constants vary with the chemical composition of the specimens, their heat treatment, the radiation used, and the angle of incidence of the radiation on the surface, and recommend that the operator always calibrate his apparatus for the given set of conditions that he uses.   Certain other investigators, including Norton and his collaborators, have found that the ordinary values of the elastic constants are satisfactory to use in X-ray work.

5.   Determination of Residual Stresses by Measuring Stress-Sensitive Properties

When stresses exist in metals, some physical or mechanical properties, such as the propagation speed of shear waves and hardness, are changed.   It is theoretically possible to develop techniques for determining residual stress by measuring such stress-sensitive properties.   Stress-measuring techniques that have been developed or proposed include ultrasonic techniques and hardness-measuring techniques.   However, none of these techniques have been developed beyond the laboratory stage.

a.   Ultrasonic Techniques

It has been recognized for some time that velocity and attenuation of sound waves in a metal specimen often change when stresses are applied to the specimen.   Attempts have been made to use this phenomenon for determining stresses in metals.   Since shorter waves are able to penetrate more (or are absorbed less) in metals, the ultrasonic waves are more suitable than ordinary sound waves.

Firestone and Frederick[59] first reported that the velocity of Rayleigh waves was affected by surface stresses and Frederick[60] has

more recently reported on the utilization of this phenomenon to measure residual surface stresses. Hikata, et al.,[61] measured the stress-induced changes in the velocity and attenuation of compressional waves propagating through aluminum. A number of other investigators have reported experimental results that illustrate the stress dependence of ultrasonic velocity or attenuation.[62, 63, 64, 65, 66]

The velocity of an elastic wave, V, propagating through a homogeneous elastic medium is given by

$$V = \sqrt{\frac{C}{\zeta}} \, , \tag{25}$$

where C is the elastic modulus and ζ is the density. By taking the differential of the above equation, one finds that

$$\frac{\Delta V}{V} = \frac{1}{2} \left[\frac{\Delta C}{C} - \frac{\Delta \zeta}{\zeta} \right] . \tag{26}$$

Equation (26) shows that a fractional change in the elastic modulus or the density would affect the velocity. The density of a metal changes as a compressive or tensile stress is applied. One would expect that the speed would increase when compressive stresses are applied and the density increases. It has been found that stresses cause changes in $\frac{\Delta C}{C}$ and $\frac{\Delta \zeta}{\zeta}$ (shear stresses will cause no change in $\frac{\Delta \zeta}{\zeta}$). Among various techniques that have been proposed so far for determining residual stresses, the following two appear to be promising:

The technique which makes use of a stress-induced change in the angle of polarization of polarized ultrasonic waves

The technique which makes use of stress-induced change in the absorption of ultrasonic waves.

(1) Polarized Ultrasonic Wave Technique. This technique is based on the stress-acoustic effect similar to the familiar stress-optic effect on which the photoelastic technique is based. In the optical case, a stress inside an optically transparent object will change the index of refraction, thus, changing the velocity of light. When a polarized light beam is passed through that object, the different components of light traveling along the axes of principal stress will have different velocities and will cause a rotation of the angle of polarization of the light beam.

When polarized ultrasonic waves pass through a stressed metal, the angle of polarization changes proportionally to the stress level. Benson and Raelson[64] mentioned this phenomenon as the acoustoelastic phenomenon. Figure 28 shows an example of the acoustoelastic setup. Ultrasonic waves are generated by a radio-frequency pulse generator coupled to a Y-cut quartz crystal. The crystal is mounted against the test sample with wax, and another such crystal is mounted at the output end of the sample. Signals passing through the sample are then amplified and displayed on an oscilloscope
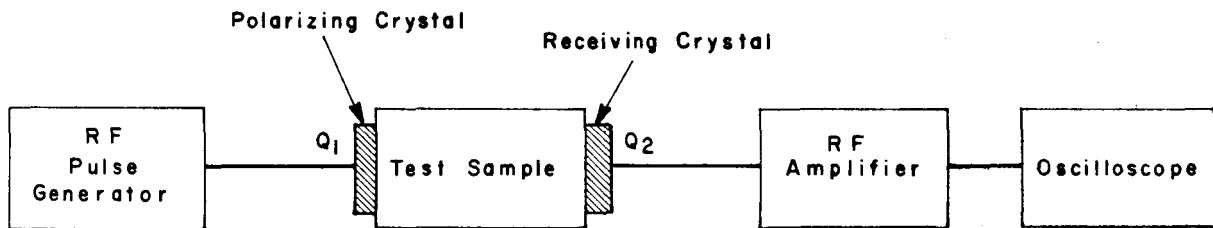
Figure 28. Acoustoelastic Setup

(Benson and Raelson)[64]

(2) Ultrasonic Attenuation Technique. It is well known that the absorption of mechanical vibrational energy (megacycle frequencies were used) depends on the mechanical properties of the metal. A residual stress would therefore manifest itself by the change in the absorption of vibrational energy. By opposing the effect of this stress on the ultrasonic attenuation by suitable means, such as the application of an opposite external stress, a measure of the respective residual stress (tension. compression) component might be obtained. In the case of ferromagnetic material, an external magnetic field might be employed.

The technique proposed by Bratina and Mills[64] involves the following procedures. By plotting the relative attenuation (db/μ sec) versus applied elastic stress (or magnetic field strength), a point is reached where the respective components of the residual and the external stresses are equal and opposite. This point corresponds to a maximum in attenuation.

b. Hardness-Measuring Techniques

Kokubo[67] performed experiments on a number of metals to show the effect of strain on hardness measurements. He applied a bending load sufficient to cause 0.3 percent strain on the outer fibers of the specimen and took Vickers hardness readings, using a 5-kg (11 lb) load, on the material in the strained state. A summary of his data is presented in Table IV. It can be seen that in all cases, except for the brass, aluminum, copper, and Armco iron, all in the annealed condition, the applied tensile stresses made the material appear 5 to 12 percent softer while the compressive stresses caused only 0 to 3 percent increase in apparent hardness.

Based on the information obtained by Kokubo, Sines and Carlson[68] suggested a nondestructive method for determining residual stresses in machine parts and structures. The method called for external loads of varying degrees be applied to a part while hardness measurements are taken. If the residual stress is compressive, an applied compressive stress will have little or no effect on the hardness measurements and a tensile stress also will show no effect as long as the sum of the applied stress and residual stress is compressive; but, if the tensile stress is great enough so that the sum becomes tensile, the material will appear softer as the applied compressive stress is increased. However, if the metal appears to increase in hardness as the applied compressive stress is increased, it is known that the sum of the applied and residual stress is still tensile; but when a compressive stress is reached that gives no further increase in the hardness measurements, the sum becomes compressive. The residual stress is equal and opposite to the applied stress that causes the transition in hardness measurements.

The state of surface residual stress influences the yield compressive strength obtained when a small hard ball is gently pressed on the smooth surface of the specimen to be studied. Pomey, et al.,[60] suggested a method of measuring residual stresses based on the above phenomenon. A small hard ball, 0.06 to 0.16 inch in diameter, is pressed with increasing load on the specimen surface, and a relationship between the load and the electric resistance of the contact point is obtained. A sudden fall in resistance occurs when portions of the specimen under the ball becomes plastic. The corresponding load gives in surface stresses of the specimen.

Table IV. Effect of Strain on Hardness Measurement (Kokubo)[67]

Material	Condition	0.3 Percent Applied Strain	Change in Vickers Hardness	Change in Hardness (percent)
Armco iron	Rolled	+	-12.5	-8.0
		-	2.5	2.5
	Annealed	+	1.0	1.0
		-	4.0	5.0
0.2 percent carbon steel	Rolled	+	-15.0	-11.0
		-	2.5	2.0
	Annealed	+	-8.0	-7.0
		-	1.0	1.0
0.7 percent carbon steel	Rolled	+	-22.0	-9.0
		-	2.0	1.0
	Annealed	+	-14.0	-6.5
		-	5.0	3.0
Brass	Rolled	+	-16.0	-12.0
		-	3.0	2.0
	Annealed	+	-2.0	-1.5
		-	2.0	3.0
Aluminum	Rolled	+	-2.0	-5.0
		-	1.0	2.0
	Annealed	+	0.7	4.0
		-	1.2	6.0
Copper	Rolled	+	-9.0	-10.0
		-	0.0	0.0
	Annealed	+	0.0	0.0
		-	4.0	8.0

6. Determination of Residual Stresses by Hydrogen-Induced and Stress-Corrosion Cracking Techniques

Techniques have been developed to determine residual stresses by observing cracks caused in the specimen due to the residual stresses. The cracks may be induced by hydrogen or stress corrosion.

a. Hydrogen-Induced Cracking Technique Applied to High-Strength Steel Specimens

Masubuchi and Martin[70] investigated the use of hydrogen-induced cracking to study residual stresses in welded joints, especially in complex weldments. Welded specimens were made with heat-treated SAE 4340 steel (approximate ultimate tensile strength was 260,000 psi). Specimens were then immersed in an electrolyte and charged with hydrogen by applying DC current, using the specimen as the cathode and a set of lead strips as the anode. The electrolyte was 4 percent sulfuric acid to which was added 5 drops per liter of poison; the poison was 2 grams of phosphorus dissolved in 40 milliliters of CS_2. The current density ranged between 0.35 and 0.8 ampere per square inch of exposed specimen surface. Various crack patterns that could be related to residual-stress distributions were obtained when different specimens were tested. Figure 29 shows the crack pattern obtained in a complex welded structure after hydrogen charging for $2\frac{1}{2}$ hours.

Hydrogen-induced-cracking tests were conducted on weldments in a heat-treated, low-alloy, high-strength steel (ultimate tensile strength was about 120,000 psi), the U. S. Navy HY-80 steel (a quenched-and-tempered high-strength steel with yield strength over 80,000 psi), and carbon steel. When steels of lower strength were used, longer charging times were required to produce cracks, and crack patterns were less pronounced. The hydrogen-induced-cracking techniques do not seem to work on a carbon-steel weldment.

b. Stress-Corrosion Cracking Technique Applied to Steel Specimens

Investigators including McKinsey,[71] Rädeker,[72] and Masubuchi and Martin[70] have used stress-corrosion cracking to study residual stresses in welded joints in carbon steel and in low-alloy high-strength steels. Figure 30 is a radiograph of a butt-welded specimen in a commercial heat-treated, low-alloy, high-strength steel after being immersed for 31 hours in a boiling aqueous solution of 60 percent $Ca(NO_3)_2$ and 4 percent NH_4NO_3. The crack pattern is quite similar to those obtained in SAE 4340 steel specimens tested by the hydrogen-induced cracking technique.
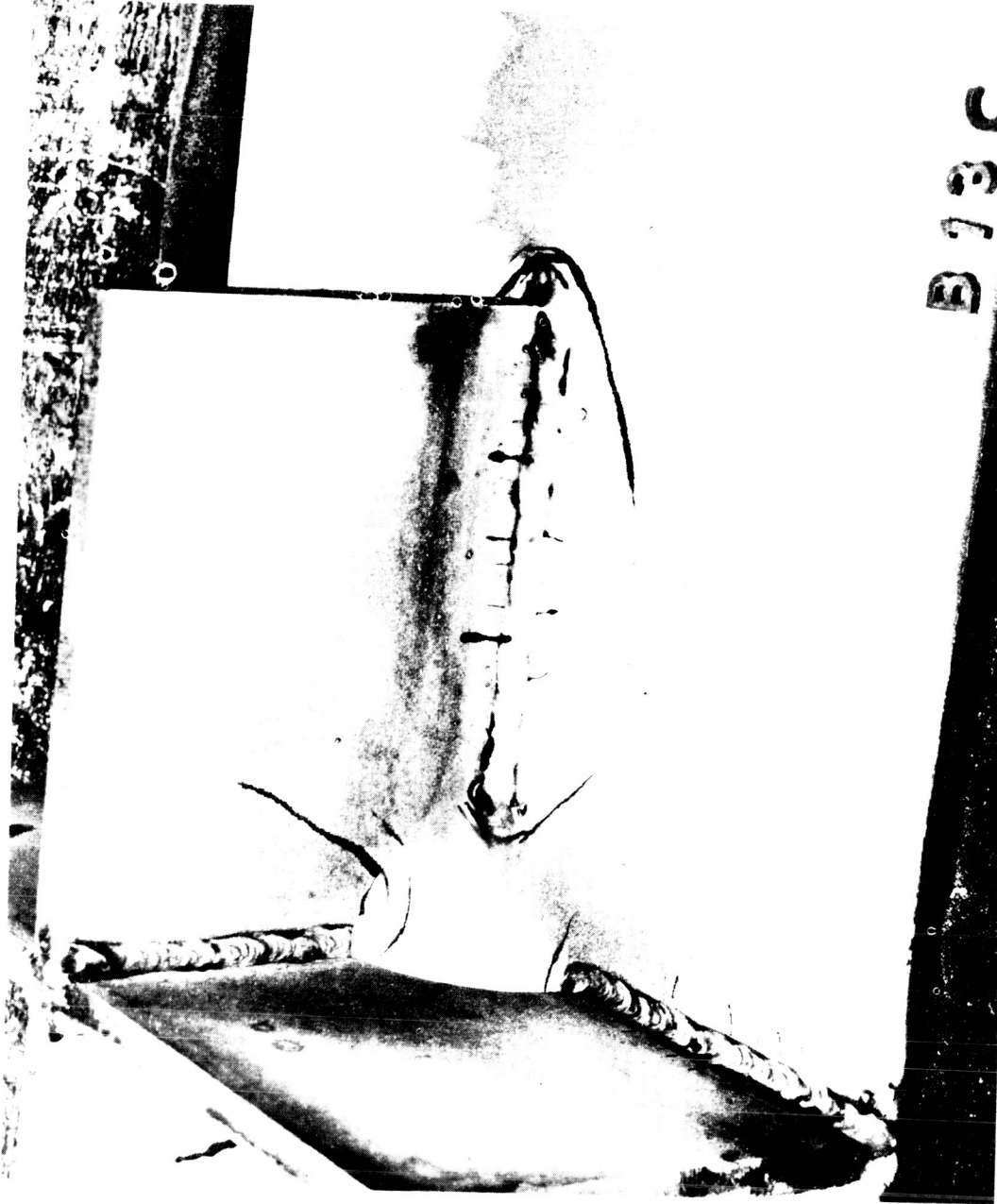
Figure 29. Crack Pattern Produced by Hydrogen-Induced Cracking Technique in
a Complex-Structure Specimen Made With Heat-Treated SAE 4340 Steel Plates

(Masubuchi and Martin)[70]
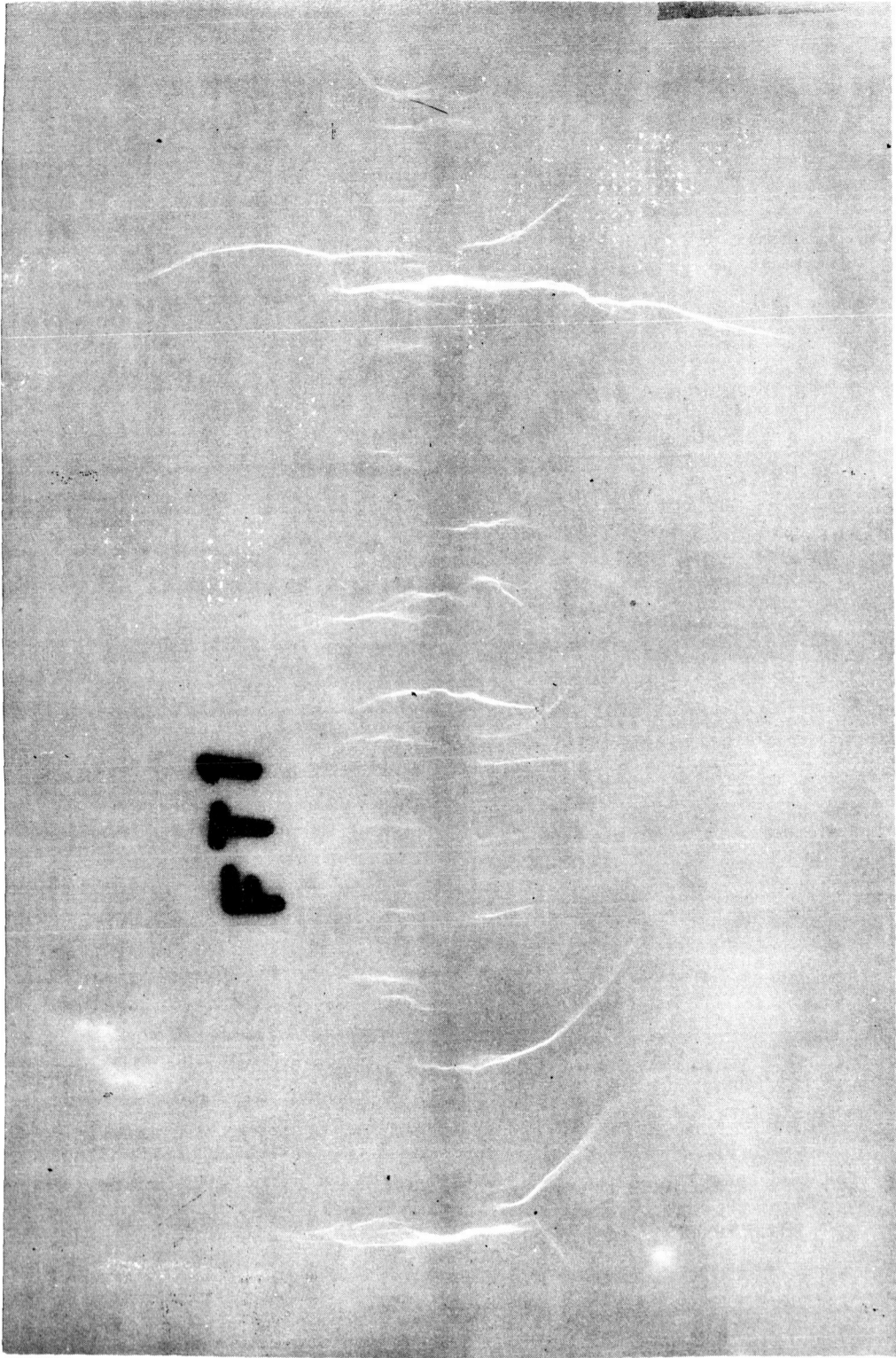
Figure 30. Radiograph of Butt-Welded Specimen Made with a Commercial Low-Alloy High-Strength Steel Plate After Stress-Corrosion Cracking Test for 31 Hours

(Masubuchi and Martin)[70]

c. Use of Cracking Technique in Studying Residual Stresses in Aluminum Alloys

No work has been reported on the use of cracking techniques in studying residual stresses in aluminum alloys. Stress-corrosion cracking, however, has been identified with certain aluminum alloys of the Al-Cu, Al-Mg, Al-Zn-Mg-Cu, and Al-Si-Mg types.[73,74] For example, failures developed in 2 days when a specimen of 7079-T6 alloy was stressed to 48,000 psi (75 percent of the yield strength) and exposed to the 3.5 percent NaCl alternative immersion test.

Section IV. MEASUREMENT OF RESIDUAL STRESSES DURING FABRICATION OF METAL STRUCTURES

This section describes measurement of residual stresses produced during quenching, machining, forming, and welding processes. For each of the above processes, methods of measuring residual stresses will be discussed along with typical data, especially data on high-strength aluminum alloys.

1. Residual Stresses Produced by Quenching

With the introduction of heat-treated aluminum alloys, the problem of quenching stresses in aluminum alloys has become important.

a. General Nature of Residual Stresses Produced by Quenching

When a round bar is quenched, for example, the outer layer cools more quickly than the core. Consequently, the outer layer shrinks on the core which has not yet begun to contract, i. e., the outer layer is submitted either to elastic strain or to over-straining. As a result of the subsequent cooling of the core, a state of equilibrium is next set up between the stretched outer zone and the compressed core. In time, cooling of the core continues, and the core is thereby subjected to tension. The outer layer will experience compressive residual stresses. The magnitude and distribution of residual stresses depend on various factors including the temperature history, the material properties (thermal conductivity, the coefficient of expansion, etc.), and geometry of the specimen.

b. Examples of Measurement of Quenching Stresses in Aluminum Alloys

Residual stresses produced in aluminum alloys during quenching have been studied by investigators including Wasserman,[75] Brick, et al.,[76] and Zeerleder.[77] Wasserman and Brick, et al., used X-ray diffraction techniques to measure residual stresses, while Zeerleder used a stress-relaxation technique.

Figure 31 shows longitudinal residual stresses determined by Zeerleder[77] in an extruded bar of Avional D (4 percent Cu, 0.2 percent Si, 0.6 percent Mg, 0.5 percent Mn) 1.97 inches in diameter.[33] The bar was water quenched from 970°F, and then aged for 24 hours at 120°F. The bar was cooled for 1 second before quenching. Residual stresses were determined by the Bauer-Heyn method (refer to Figures 9 and 10). Compressive stresses were produced in areas near the

surface, and tensile stresses were produced in the central areas. Increasing temperature of the quenching bath reduced residual stresses, as shown in Figure 31.
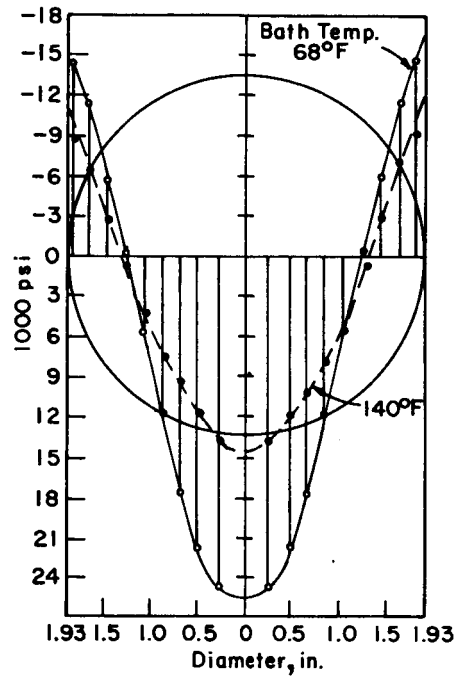
Note:
(1.97 in. in Diameter, Water Quenched
from 970°F; Aged 24 Hours at 120°F
With 1-Second Cooling Period Before
Quenching)

Figure 31.   Longitudinal Residual Stresses in a Vional D
Extruded Bar

(Zeerleder)[77]

2.   Residual Stresses Produced by Machining

It has been known that highly localized residual stresses exist in thin layers near the surface prepared by various machining, shot blasting, and grinding operations.[33] Because of the highly localized nature of these residual stresses, the X-ray diffraction techniques are the only techniques that have been used for measuring these stresses.[78, 79]

Frommer and Lloyd[78] made X-ray studies of residual stresses produced during machining of the aluminum alloys Y alloy and Hiduminium RR 56.* Table V summarizes the experimental results. High compressive stresses were produced in thin layers near the surface. The "thickness of compressive stress layer" quoted in the table indicates the depth of etching necessary to obtain practically zero surface stress. The approximate thickness of the compressive layer ranged from 0.025 inch for shot blasting to practically zero for surface milling.

3. Residual Stresses Produced by Forming

It has been known that stresses remain after a metal part is formed by bending or pressing and then freed.[80, 81, 82, 83, 84]

a. General Nature of Residual Stresses Produced by Forming

Curve BAOCD in Figure 32 represents the longitudinal stress distribution in a beam of rectangular section and unit width bent by pure bending moment.[80] When a beam is formed and is still under the bending load, the outer fibers of the beam have yielded plastically on both the tension and the compression faces, as indicated by BA and CD. When the beam is released from the bending moment, elastic springback occurs and the final stress distribution through the beam is a compressive stress on the tension face and a tensile stress on the compression face, having changed sign three times through the section, as shown by curve FEOGH in Figure 32. The value of these residual stresses depends largely on the mechanical properties of the material at the time of bending, by the degree of bend, and the geometry of the section.

b. Examples of Measurement of Residual Stresses in Aluminum Alloys

Yen[84] investigated residual stresses due to room-temperature forming of structural sections such as angles, tees, and channels. Figure 33(a) shows longitudinal residual stresses in an angle after it was formed to a final radius of 90 inches, which Figure 33(b) shows residual stresses in a channel formed to a final radius of $56\frac{1}{4}$ inches. Both sections were made of 7075 aluminum alloy.

---

*Y alloy: 3.5-4.5 Cu, 1.2-1.7 Mg, 1.8-2.3 Ni, 0-0.2 Ti.
Hiduminium RR 56: 2 cu, 1.25 Ni, 1.2 Fe, 0.8 Mg, 0.08 Ti, 0.6 Si.

Surface Stresses Brought on by Operation			
Measurement Obtained At	Stress Sum (Compressive), (tons/in.^{2})	Approximate Thickness of Compressive Stress Layer, (in.)	Alloy
Actual surface (unetched)	3.3	~0.002	RR 56
0.006 in. beneath original surface	7.2	~0.015	Y alloy
0.005 in. beneath original surface	20.7	~0.024	RR 56
Actual surface of base of recess (unetched)	6.9	>0.004 <0.015	RR 56
Actual surface (unetched)	Nil	Nil	RR 56
Actual surface (unetched)	Nil	Nil	RR 56
Actual surface of sidewall	14.7	~0.006	RR 56
Actual surface of sidewall	16.5	~0.011	Y alloy
0.006 in. beneath original surface	22.5	~0.025	RR 56

Table V. Survey of Magnitude of Compressive Surface-Layer Stresses Induced by Various Machining Operations and by Shot Blasting (Frommer & Lloyd)[78]

Operation		Machining Data		
Type of Operation	Description	Cutting Speed (rpm)	Feed (in./rev)	Depth of Cut (in.)
Turning	Flat surface faced off with fine finishing cut	-	~0.0015	~0.0005
	Cylindrical surface turned with rough cut	375	~0.012	~0.050
	Surface faced off under conditions producing chatter marks	-	-	-
Recessing	Recess made with flat-bottom drill ($\frac{1}{2}$ in. dia)	290	~0.005	-
Surface milling (cutter not enclosed by material of job)	Flat surface side-milled with end mill (2 in. long, $\frac{3}{8}$ in. dia)	220	~0.010	~0.125
	Flat surface milled with straddling mill (6 in. dia, $\frac{5}{8}$ in. wide)	220	~0.010	~0.125
Milling of slots and grooves (cutter enclosed by material of job)	Tapered groove ($\frac{7}{8}$ in. deep, $5\frac{1}{4}$ in. long) made with 7-degree angle cutter ($\frac{7}{16}$ in. dia)	220	~0.010	~$\frac{7}{32}$
	Arc-shaped groove sunk with formed, spiral-fluted milling cutter (tapered 4-degree, max. cutting dia 0.455 in.)	1700	Rough cut 0.05 Fine cut 0.01	0.010-0.020
Shot blasting	Flat surface faced off on lathe (fine finishing cut) and then shot-blasted	Diameter of steel shot = 0.040 in. Air pressure in mains ~30 psi Throttle at "half pressure"		

NOTES:

All data refer to specimens which were fully heat treated before the operation quoted.

When several similarly machined specimens were examined, the highest stress values obtained are quoted in the table.

The stress values quoted refer to the immediate surface when measurable X-ray patterns were obtainable from that surface; otherwise they refer to that stratum beneath the surface (exposed by etching) where first measurable patterns could be obtained.

The "thickness-of-compressive-stress layer" quoted indicates the depth of etching necessary to obtain practically "stress-free" patterns.
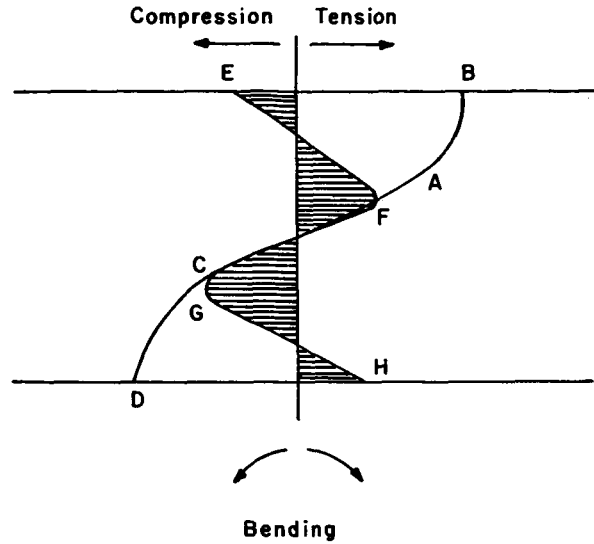
Figure 32.   Formation of Residual Stress by Bending a Beam

The residual stresses were determined by a sectioning technique.   The length of the section was marked into many parallel strips, and the length of each strip was measured after forming.   Then the section was slit along the parallel marks into thin strips, and the lengths were measured again.   The average longitudinal stress, σ_x, in each strip was determined

$$\sigma_x = E \cdot \frac{L_o - L}{L_o} \, ,$$

where

L_o = the length before slitting

L = the length after slitting

Yen also calculated residual-stress distributions based on the theory of plasticity.   Calculated values coincided well with the observed values.

Hawkes[83] used an X-ray back-reflection technique to measure the surface residual stresses in bars and sheets resulting from the cold and hot forming of high-strength aluminum alloys (British specifications, DTD 683, DTD 687, and B.S.S. L65).

Figure 33.   Residual Stresses Produced by Bending of an
Angle and Channel in 7075 T6

(Yen)[84]

4.   Residual Stresses Produced by Welding

Welding is one of the major fabrication processes that pro-
duce stresses in metal structures.

a.   General Nature of Residual Stresses Produced by Welding

The residual stresses in a welded joint are caused by the
contraction of the weld metal and the plastic deformation produced in
the base-metal region near the weld.   Residual stresses in a welded
joint are classified as "residual welding stress" which occurs in a joint
free from any external constraint, and "reaction stress" (or locked-in
stress") which is induced by an external constraint.

(1) Residual Stresses in Butt-Welded Joints. A typical distribution of residual stresses in a butt weld in shown in Figure 34. The stresses of concern are those parallel to the weld direction, designated σ_x, and those transverse to the weld, designated σ_y.

The distribution of the σ_x residual stress along a line transverse to the weld is shown in Figure 34(b). Tensile stresses of high magnitude are produced in the region of the weld; these taper off rapidly and become compressive after a distance of several times the width of the weld. The weld metal and heat-affected zone are trying to shrink to the direction of weld, and the adjacent plate material is preventing this shrinkage. The distribution of σ_y residual stress along the length of the weld is shown in Figure 34(c). As shown, tensile stresses of relatively low magnitude are produced in the middle of the joint, and compressive stresses are observed at the end of the joint.

If the contraction of the joint is restrained by an external constraint, the distribution of σ_y is as shown by the broken line in Figure 34(c). Tensile stresses approximately uniform along the weld are added as the reaction stress. An external constraint, however, has little influence on the distribution of σ_x residual stresses.

(2) Residual Stresses in Spot-Welded Joints. Distributions of residual stresses in spot-welded joints are very dependent on the weld pattern used. The simplest case to consider is the residual stress due to a single spot weld. The components of stress which are of most concern are those in the radial direction, σ_r, and those in the circumferential direction, σ_θ. Inside the weld zone, both σ_r and σ_θ stresses are tensile and are as high as the yield stress. Outside the weld zone, radial stresses are tensile and circumferential stresses are compressive, both approaching zero as the distance from the weld increases. Concentrated residual stresses often exist in areas close to the original interface of the sheets.

b. Residual Stresses and Shrinkage in Weldments in Aluminum Alloys

Only limited information is available on residual stresses and distortions in weldments in aluminum alloys.[85, 86, 87, 88]

Hill[86] investigated residual stresses in butt joints in Alloy 5456-H321 plates welded by the inert-gas-shielded arc welding using Alloy 5556 consumable electrodes. Figure 35 shows a typical distribution of longitudinal residual stresses in a $\frac{1}{2}$ x 36 x 48-inch panel by welding two $\frac{1}{2}$ x 18 x 48-inch plates. Variation in yield strength of the material
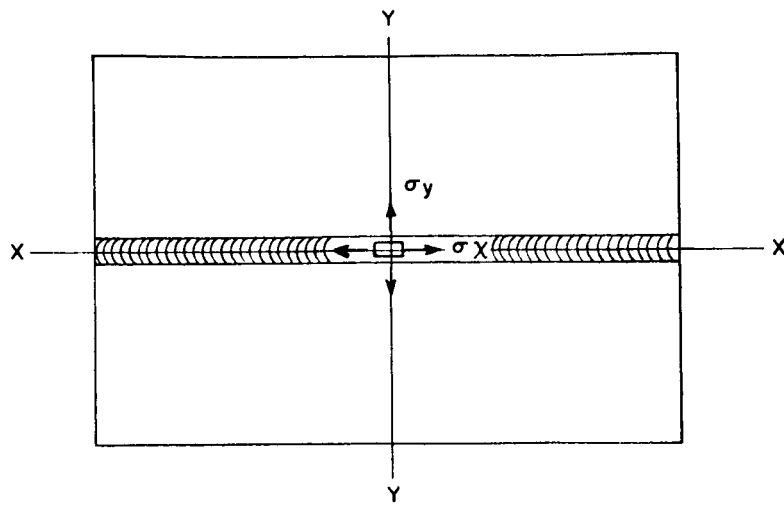
(a) Butt Weld
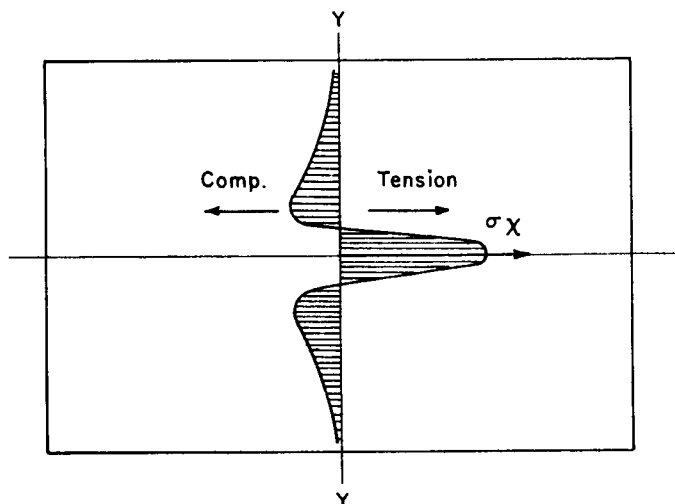
(b) Distribution of σ_x Along YY
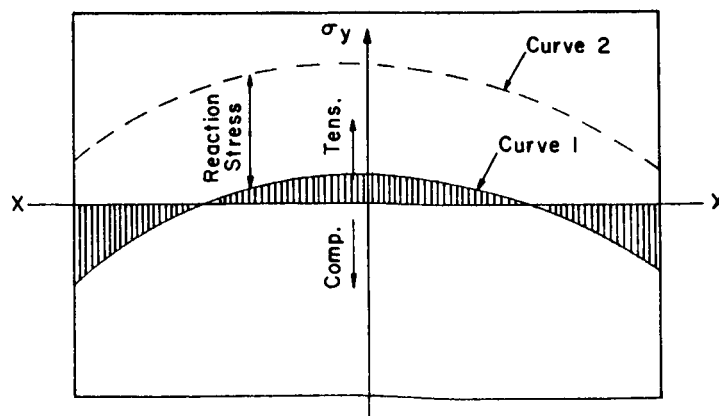
(c) Distribution of σ_y Along XX

Figure 34. Distribution of Residual Stresses in a Butt Weld

with distance from the centerline of weld is also shown. The residual tensile stresses in and adjacent to the weld approach the yield strength. These tensile stresses are confined to the region in which the heat of welding has lowered the yield strength of the material.
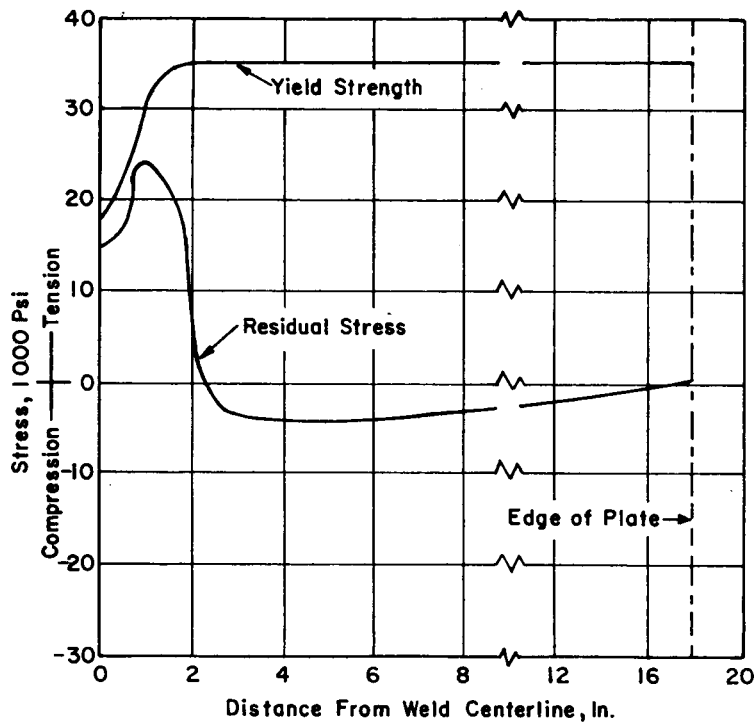
Figure 35. Distribution of Yield Strength and Residual Stresses in a Longitudinally Welded 5456-H321 Plate 36 Inches Wide and $\frac{1}{2}$ Inch Thick

(Hill)[86]

(1) Transverse Skrinkage. Capel[87] investigated shrinkage transverse to the weld which occurred during butt welding (60-degree vee, no root gap) two 0.24 x 6 x 20-inch plates in aluminum, stainless steel, and carbon steel. The aluminum plates were welded by the inert-gas tungsten-arc welding, whereas stainless steel and carbon-steel plates were welded with covered electrodes. The transverse shrinkage was given by the following formulas:

$$\Delta \ell \text{ (aluminum)} = \frac{20.4 \times W \times 10^3}{S \times U}$$

$$\Delta \ell \text{ (stainless steel)} = \frac{22.7 \times W \times 10^3}{S \times U}$$

$$\Delta \ell \text{ (carbon steel)} = \frac{17.4 \times W \times 10^3}{S \times U} , \qquad (27)$$

where

$\Delta \ell$ = transverse shrinkage, mm

W = V x I, V is arc voltage, volts, and I is arc current, amperes

S = thickness of layer of weld metal, mm

U = welding speed, cm/min.

Capel[87] mentioned that the large shrinkage of aluminum was caused mainly by the low welding speed in comparison with that of the covered electrodes.

c. Residual-Stress Measurements During Welding

Several attempts have been made to measure stress changes that take place during welding; such attempts include observation of strain changes using high-temperature electric-resistance strain gages mounted on the surface of plates being welded. However, these attempts have not yet provided useful information primarily because of difficulties in analyzing experimental data. The resistance change observed on an electric-resistance strain gage, ΔR, is composed of

$$\Delta R = \Delta R_1 (\epsilon') + \Delta R_2 (\epsilon'') + \Delta R_3 (\epsilon_T) + \Delta R_4 (T) , \qquad (28)$$

where

$\Delta R_1 (\epsilon')$ is the resistance change that corresponds to the elastic strain, ϵ', from which stresses can be computed

$\Delta R_2 (\epsilon'')$ is the resistance change that corresponds to the plastic strain, ϵ''

ΔR_3 (ϵ_T) is the resistance change that corresponds to the thermal strain caused by the temperature change

ΔR_4 (T) is the change in resistance caused by the change in temperature.

It is very difficult to determine ΔR_1 (ϵ') from the measured resistance change, ΔR.

Strain change during welding can be measured in some applications in which ΔR_2 (ϵ''), ΔR_3 (ϵ_T), and ΔR_4 (T) are negligible. Travis, et al.,[89] used constrained joints, as shown in Figure 36, to study cracking under hindered contraction. The change of reaction stresses produced in the constraining bar was measured by strain gages mounted on the bar. Two types of specimens as shown in Figures 36(b) and 36(c) were used, the latter being designed to cause a bending moment as well as a separating force to be imposed upon the test weld. According to the investigators, the 9-inch moment specimen was more suitable than the pure transverse loading-type specimen for studying weld cracking. Figure 37 shows examples of experimental results obtained on the moment-type specimens made in the U. S. Navy HY-80 steel. The separating force of the U-bar was calculated from the strain measured on the bar. The figure illustrates the effects of preheat on the magnitude of separating force and on cracking under the restrained condition. Occurrence of weld cracking is noticed by decrease in the separating force, since cracking reduces residual stresses. With sufficiently high preheat, there was no cracking. With no preheat, cracking took place in 15 minutes after the start of welding. With a 200°F preheat, cracking was delayed more than $1\frac{1}{2}$ hours.

d. Measurement of Elastic and Plastic Strains in Areas Near the Weld

Using the Gunnert strain indicator, as shown in Figure 13, Masubuchi[90, 91] made an investigation of the distribution of elastic and plastic strains in areas near the weld. The specimen was a slit-type weldment in carbon steel, as shown in Figure 38; a double-vee slit 10-inches long was made by machining in a plate $\frac{3}{4}$ x 31 x 43 inches, and the slit was welded with covered electrodes. Figure 38 also shows locations of strain-measuring points. For each of the measuring points, strain-measuring depressions, as shown in Figure 13, were prepared prior to welding on the specimen surface and distance between the depressions were measured. After the specimen was welded, the

(a) Pinned End V-Bar Apparatus

MATERIAL: 1" COLD ROLLED STEEL PLATE.
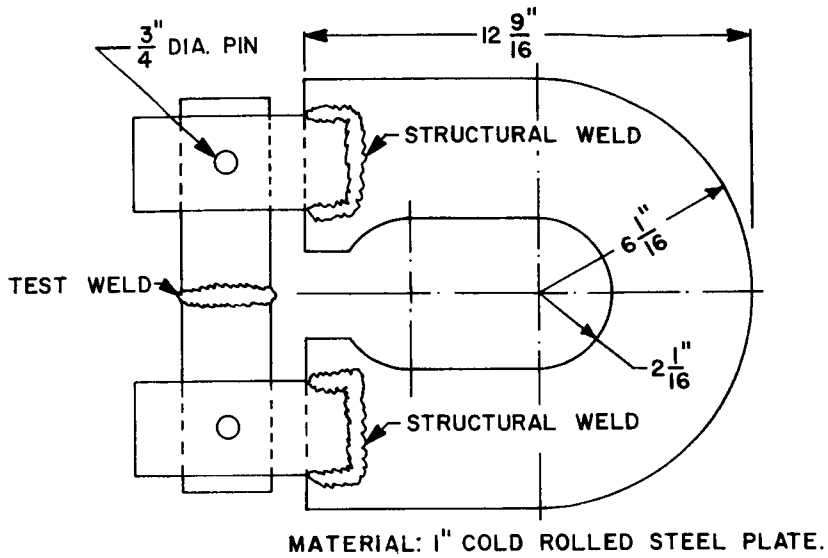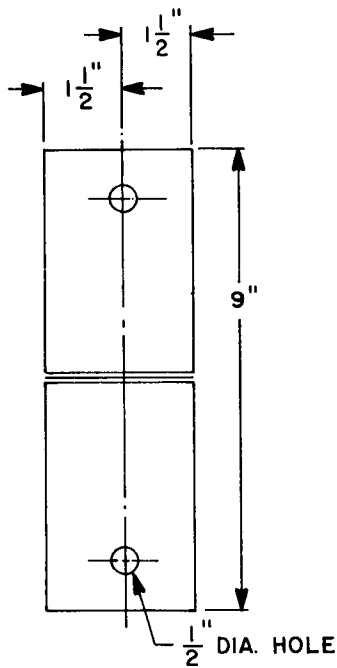
(b) Specimen Design
For Pure Transverse
Loading.
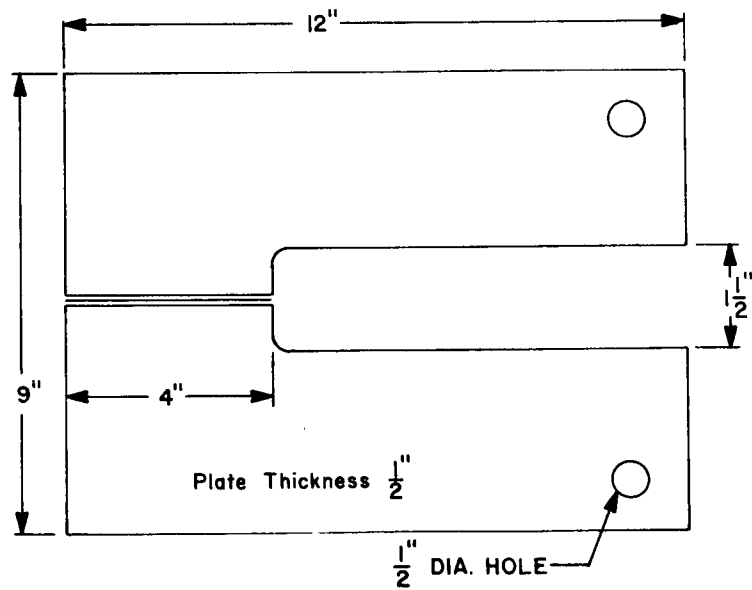
(c) Nine-Inch Moment Arm Specimen Design.

Note: Other apparatus designs including the horizontal lever arm apparatus
and the fixed-end V-bar apparatus also were used.

Figure 36.   Constrained Joint to Study Cracking Under
Hindered Contraction

(Travis, et al.)[89]
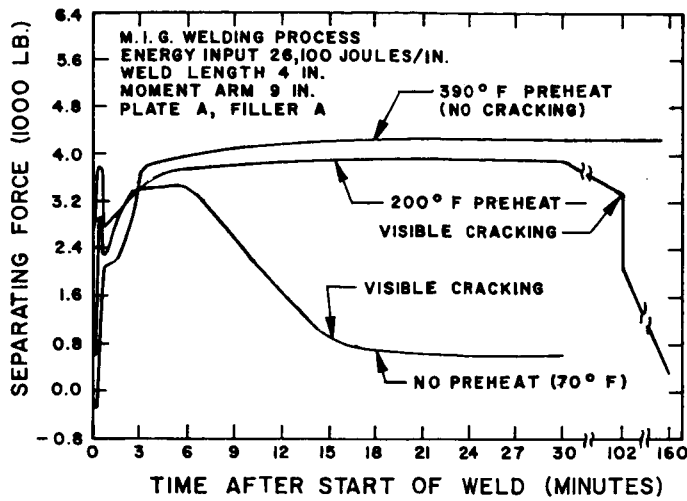
Chemical Comparison (percent) of the Base and the Filler Metal

	C	Mn	Si	S	P	Mo	Cr	V
Plate A	0.29	1.73	0.22	0.020	0.018	0.48	—	—
Filler Metal A	0.35	1.00	0.45	0.020	0.020	—	1.10	0.18

Figure 37. Change of Separating Force After Welding
in 9-Inch Arm Specimen in HY-80 Steel

(Travis, et al)[89]
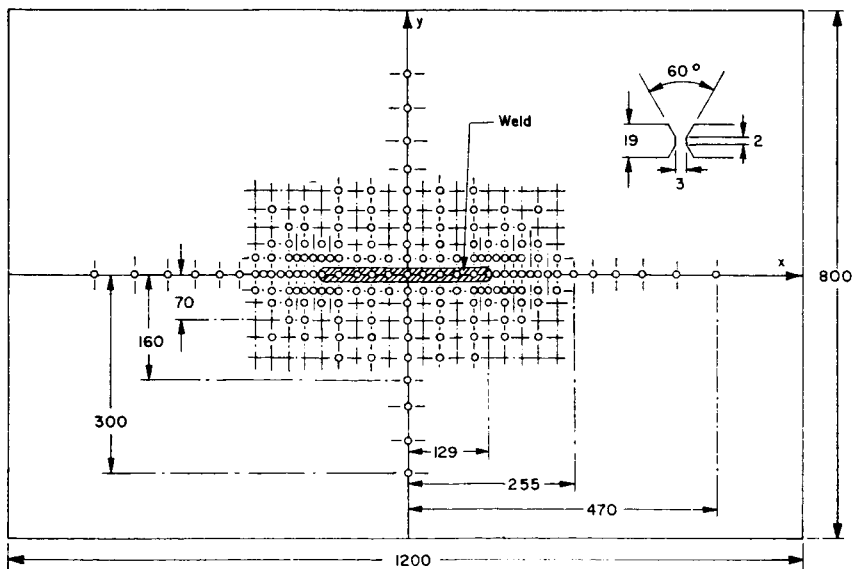
Figure 38. General View of Slit-Type Specimen and Location
of Residual-Stress Measuring Points
(Values are Shown in Millimeters)

(Masubuchi)[91]

distances between the depressions were measured to determine strains produced by welding. Since the strain produced by welding may contain both elastic and plastic strains, particularly in areas near the weld, the elastic part of the strain also was measured by the relaxation method using the Gunnert core drill.

Figure 39 shows distributions of strains produced by welding. In this figure, the values of I determined with strain components (ϵ_x, ϵ_y, and γ_{xy}) by the following equation are plotted:

$$I = \left[\sigma_x'^2 - \sigma_x'\sigma_y' + \sigma_y'^2 + 3\tau_{xy}'^2 \right]^{1/2} , \qquad (29)$$

where

$$\sigma_x' = \frac{E}{1 - \nu^2} (\epsilon_x + \nu\, \epsilon_y)$$

$$\sigma_y' = \frac{E}{1 - \nu^2} (\epsilon_y + \nu\, \epsilon_x)$$

$$\tau_{xy}' = G\, \gamma_{xy}.$$

As known from Equation (29), the values σ_x', σ_y', and τ_{xy}' are components of an apparent stress assuming that the strain (ϵ_x, ϵ_y, and γ_{xy}) is elastic. According to Mises, the yield condition in a plane-stress state is

$$I = \sigma_Y ,$$

where σ_Y is the yield stress of the material. Therefore, I can be used as a measure to determine whether or not the material at a specific position has undergone plastic deformation during welding. It is believed that the region has undergone plastic deformation when the value of I is larger than the value of σ_Y.

Figure 39 shows that the value of I was generally large in regions near the weld. Curves of equal I value (equi-I curves) also are shown in Figure 39(c). The half breadth of the plastic region that corresponds to the yield strength (21 kg/mm^2 or 30,000 psi) was about 55 mm ($2^5/_{32}$ in.), and the penetration of the plastic region beyond the end of the weld was about 50 mm (2 in.).

The values of I, due only to elastic-strain recovery (I_e), were obtained (broken lines in Figure 39) and compared with those determined with strain caused by welding. No difference between the values
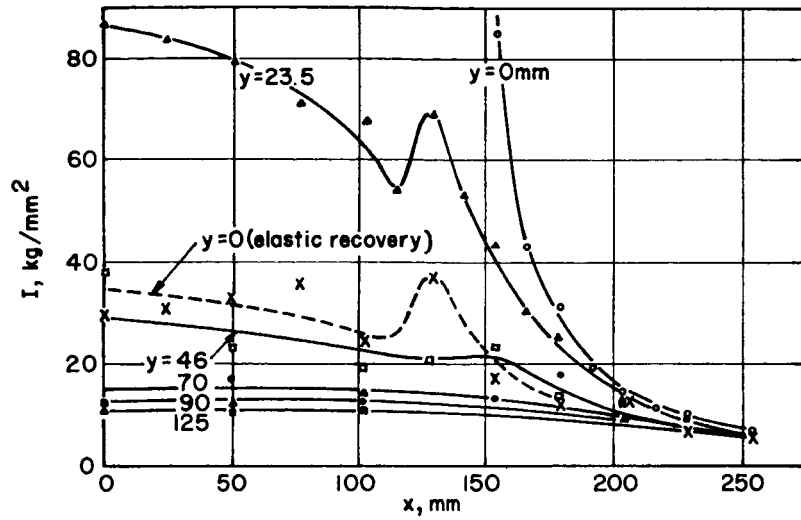
(a.) Distribution of I along x-direction
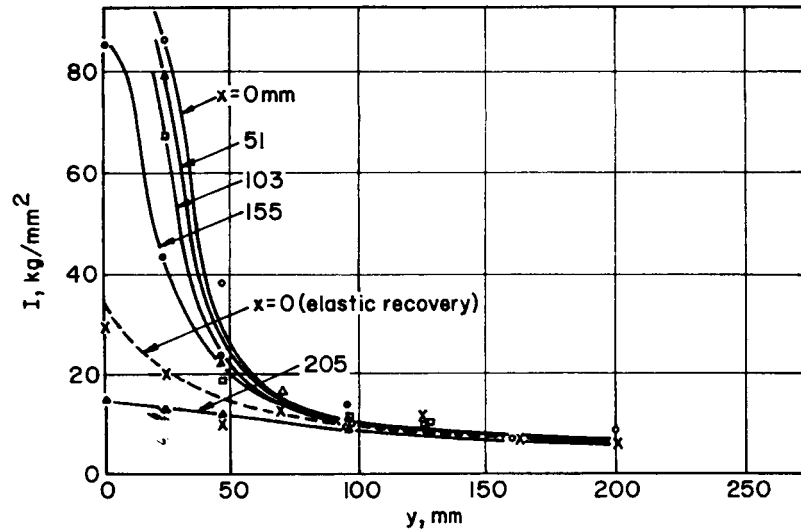
(b.) Distribution of I along y-direction
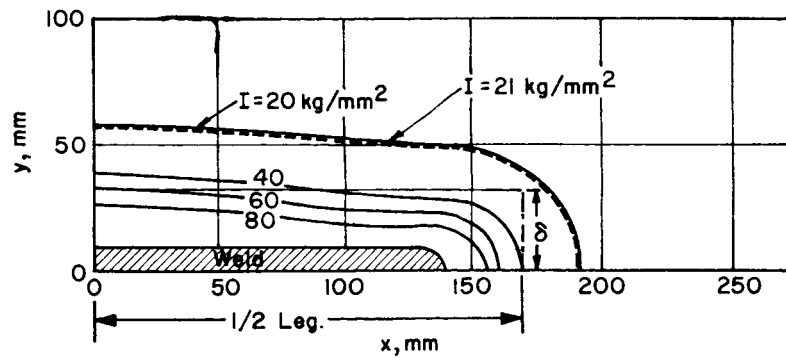
(c) Equi-I curves

Figure 39.   Distribution of I as Calculated from Strain
Produced by Welding. See Equation (29)

(Masubuchi)[91]

I and I_e was observed in the area outside the above-mentioned plastic region; however, the values of I_e were much lower than those of I in the plastic region. The values of I_e on the weld metal were about 35 kg/mm^2 (50,000 psi). Since the yield stress of the weld metal is between 38 and 43 kg/mm^2 (54,000 and 61,000 psi), the state of residual stress in the weld metal was probably near the yield condition.

e.   Measurement of Degree of Constraint of a Welded Joint

In the welding fabrication of metal structures, especially those made in high-strength materials that are usually susceptible to cracking, care must be taken so that joints are not constrained beyond a certain limit. During the fabrication of complex structures, however, some joints may have to be welded under a severe constraint. In such cases it is quite useful to determine the degree of constraint of the joint. Investigations have been made to determine the degree of constraint of various types of welded joints.

Figure 40 shows a simple butt joint (length: L) restrained by a set of springs. When tensile stress, σ_o, uniformly distributed along the weld, or total load, $P = \sigma_o L$, is needed to cause transverse shrinkage, δ, the degree of constraint (the spring constant of the constraint), K, can be defined as

$$K = \frac{\sigma_o}{\delta} = \frac{P}{L\delta} .$$

(30)

Masubuchi[91] applied the above idea to a slit-type specimen, as shown in Figure 41. When welding is done in a part of the slit between $x = x_1$ and x_2 (slit length, L; weld length, $\ell = x_1 \sim x_2$), the degree of constraint, K, can be given by [refer to Figure 41(a)]

$$K = \frac{\pi}{2} \frac{E}{L} \cdot \frac{\ell}{L} \cdot \frac{1}{F} ,$$

(31)

where

$$F = \sum_{n=1}^{\infty} \frac{1}{n} \left[\int_{\theta_1}^{\theta_2} \sin \theta \, \sin n\theta \, d\theta \right]^2$$

$$x_1 = \frac{L}{2} \cos \theta_1$$

$$x_2 = \frac{L}{2} \cos \theta_2 .$$
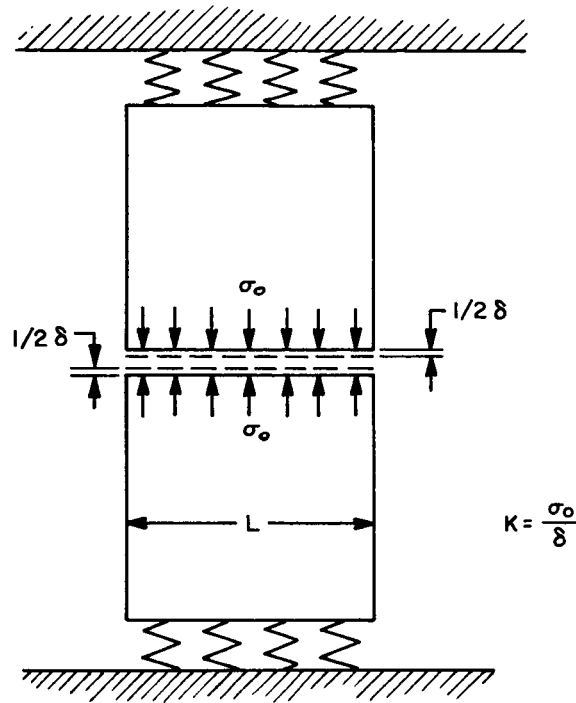
Figure 40. Definition of Degree of Constraint, K, of a Simple
Butt Joint Constrained by a Set of Springs

The physical measuring of K is as follows. When uniform stress, σ_O,
is applied along the part of the slit between $x = x_1$ and x_2, transverse
shrinkage, $[v]$, as shown in Figure 41, will occur along the slit. The
relationship between σ_O and the mean value of transverse shrinkage over
the portion of the slit where the load is applied, $[\bar{v}]$, is given by

$$\sigma_O = K [\bar{v}_\ell] \quad . \tag{32}$$

Figure 41(b) shows an experimental relationship between the
degree of constraint K and the transverse shrinkage obtained during
shielded metal-arc welding carbon-steel specimens $3/4$-inch thick.
The experiment was conducted on various combinations of slit length
L (3 to 20 inches) and weld length ℓ ($\ell/L = 0.3$ to 1.0). The transverse
shrinkage decreased as an increase in degree of constraint. Details
of experimental conditions are not described here.

The degree of constraint of a welded joint in a complex structure
can be determined experimentally.[92, 93, 94] Figure 42 shows a setup used
by Watanabe, et al.,[92] to measure the degree of constraint of a butt joint

(a) Slit-Type Specimen
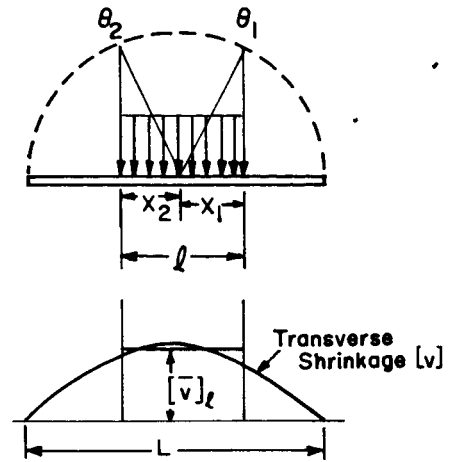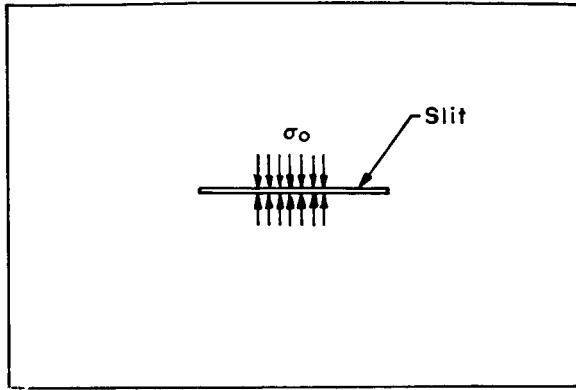
Degree of Constraint, K, kg/mm^2/mm
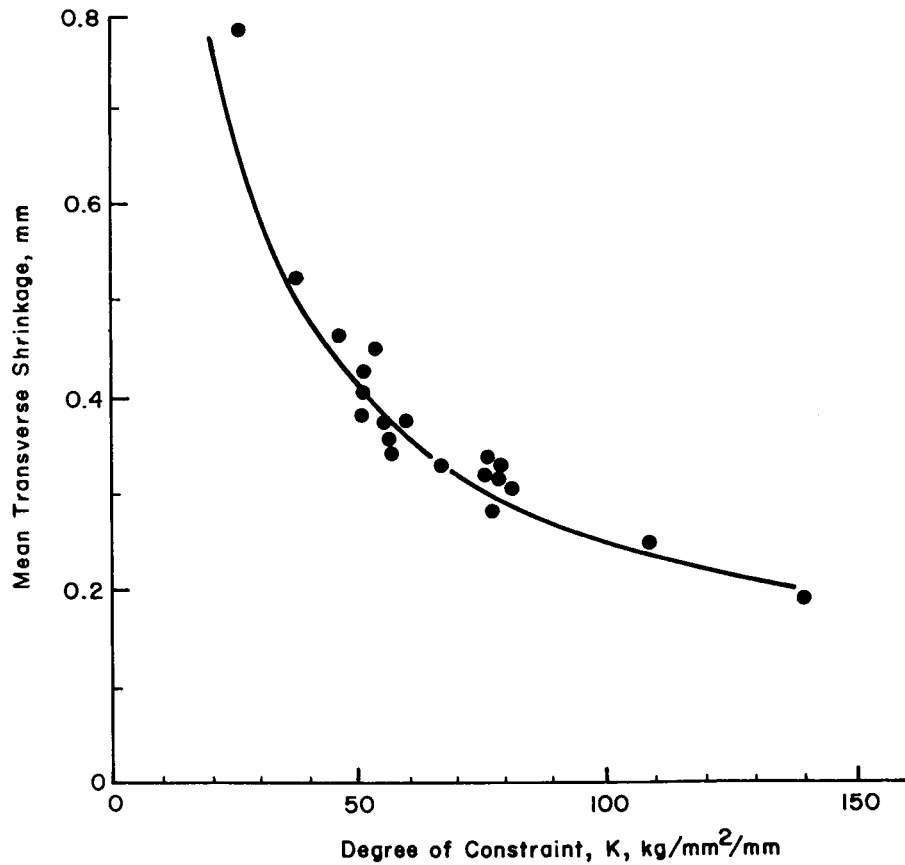
(b) Relationship Between Degree of Constraint and Transverse Shrinkage in Slit-Type Specimens, Arc Welding of Carbon-Steel Ship plates

Figure 41. Degree of Constraint of Slit-Type Specimens (Masubuchi)[91]

between two deck assemblies of an actual cargo ship. A and B are turnbuckles which were hooked to small steel pieces welded to the deck plate. Dial gages are numbered 1, 2, and 3. Changes in the gap between the deck plates were measured with the dial gages while the plates were pulled together by the turnbuckles. The tightening force was determined by strain gages mounted on the turnbuckles. The degree of constraint of the joint was then calculated by Equation (30). Attempts were made successfully to estimate from laboratory weld-shrinkage data the shrinkage that took place during joining the large assemblies.
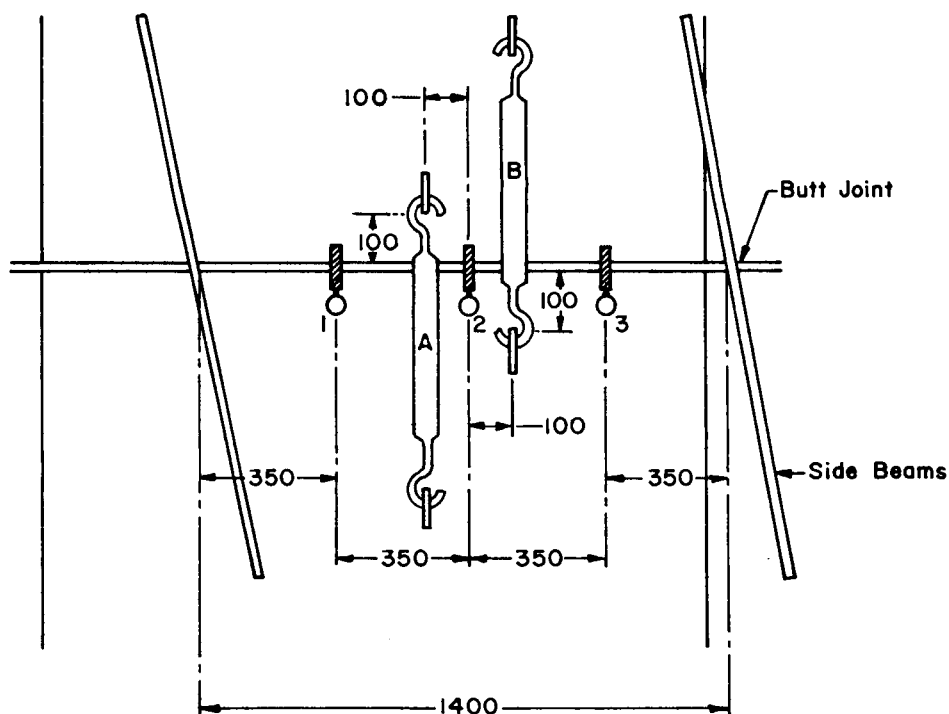
A,B
,2,3: Dial Gages
Unit, mm

Figure 42. Measurement of the Degree of Constraint of
a Butt Joint Between Deck Assemblies of an
Actual Cargo Ship

(Watanake, et al.)[12]

Section V. SELECTION AND USE OF APPROPRIATE MEASUREMENT TECHNIQUES AND EVALUATION OF RESULTS

This section contains information pertaining to the selection of appropriate measurement techniques, the use of mathematical analysis in the experimental studies of residual stresses, and the evaluation of experimental data on the basis of the effects of residual stresses on the behavior of structures.

1. Selection of Appropriate Measurement Techniques

In determining residual stresses in metals and metal structures it is important to select measurement techniques that are most appropriate for a particular job. Factors to be considered are[20]

permissible extent of damage to the structure (destructive or nondestructive testing)

required quality of measurement (accuracy of data, determination of stress components, etc.)

effects of variations in metal properties

applicability to field tests

cost and time.

Table VI shows the characteristics of typical methods for measuring residual stresses.

a. Permissible Extent of Damage to the Structure

Permissible extent of damage to the structure is an important factor in selecting appropriate methods for measuring residual stresses in metal structures. Stress-relaxation techniques are destructive; however, the extent of the damage to the structure can be limited (semi-nondestructive) in some cases. For example, the Gunnert technique requires making circular plugs 0.8 inch in diameter.

If absolutely no damage to the structure is allowed for measuring residual stresses, the only presently available technique is the X-ray diffraction technique. The ultrasonic technique is still in the development stage. The hardness technique and cracking techniques are not suitable to be applied to actual structures.

Table VI. Characteristics of Techniques for Measuring Residual Stresses

	Stress-Relaxation Techniques			
	Strain Gages	Extensometer	Grid System	Photoelastic Coating
(1) Extent of damage to the structure	←————————————————Destructive (extent varies)————————→			
(2) Quality of measurement				
Approximate strain sensitivity, microin./in.	5	(10 to 100)	50	10
Determine stress components	Yes	Yes	Yes	Yes
Usual gage length, in.	$1/64$ to 1	Varies	Varies	Very small
Applicability to uneven stress field	Yes	Yes	Yes	Yes
Surface or interior strains	←————————————Surface measurement————————→			
(3) Effects from variations in materials	←————————————Not affected————————→			
(4) Field application				
Field, F or laboratory, L	F, L	F, L	Primarily L	L, F
Remote indicating	Yes	No	No	No
Operating environment	A, W[b]	A	A	A
(5) Cost and time				
Complexity of equipment[c]	1, 2	1, 2	1, 2	3
Time required[d]	1	1	2	2
Required operator experience[e]	2	2	2	3

(a) Sensitivity in stress is given.
(b) A: air, W: water.
(c) 1 - 4: less expensive - expensive.
(d) 1 - 4: short - long.
(e) 1 - 4: less experienced - highly experienced.

| Brittle Coating | X-Ray Diffraction Technique | | Ultrasonic Techniques | Hardness Techniques | Cracking Techniques |
	Film Technique	Diffractometer			
←———————————————— Nondestructive ————————————————→					Destructive
500	400	300	10,000 psi[a]	500	Qualitative
Not appropriate	Yes	Yes	No	Not appropriate	Indirect
Very small	←—— Lattice spacing ——→		-	-	-
Yes	Yes	Yes	No	Yes	Yes
	←—— Surface strain ——→		Interior stress	Surface strain	-
←———————————————————— Affected ————————————————————→					
L, F	L, F	L	L, F	Primarily L	L
No	No	No	Yes	No	-
A, W	A	A	A	A	-
1	4	4	4	2	2
1	3	3	1	2	4
1	4	4	4	2	2

b. Required Quality of Measurement

In selecting measuring techniques and designing test programs, it is important to know whether they will provide data that meet the required quality, including accuracy of stress analysis, determination of stress components, etc.

(1) Accuracy of Strain Measurement. Some techniques provide accurate quantitative data while others provide only qualitative data. The accuracy of measured values in actual cases depends upon various factors including the strain sensitivity of gages used, methods of cutting in case of stress-relaxation techniques, surface condition of the specimen, condition of measuring devices and equipment, and the skill and experience of operators.

Table VI shows approximate values of maximum strain sensitivity of devices (or the lowest strains that can be detected by the devices) in microinches per inch. For aluminum alloys with Young's modulus of approximately 10×10^6 psi, 10 microinch-per-inch strain corresponds to 100 psi stress. Bonded strain gages provide the best strain sensitivity. However, it must be mentioned that the fluctuation of data in the actual measurement would be considerably greater than the maximum strain sensitivity of the gages unless extreme care is taken during the measurement.

(2) Determination of Stress Components. Some techniques provide information on stress components so that the directions and the magnitudes of principal stresses can be determined, while others do not provide enough information on stress components. Techniques that belong to the first group include bonded strain gages, extensometers, grid systems, photoelastic coatings, and the X-ray diffraction technique.

(3) Gage Length. Table VI shows usual gage lengths used in various techniques. The gage length must be short enough so that variations in stress can be detected; however, too short a gage length also is not favorable. For example, when the X-ray diffraction technique is used to determine residual stresses that are widely distributed in a large structure, such as those shown in Figure 6(a), extreme care must be taken to eliminate the effects of localized residual stresses such as those caused by grinding, as shown in Figure 6(c).

(4) Application to Uneven Stress Field. Most techniques are applicable to specimens that contain unevenly distributed residual stress, although some are not applicable to such cases. At the present stage of development the ultrasonic technique is not applicable to unevenly distributed residual stresses.

(5) Surface Strain or Strains in the Interior Determined.
Suppose that the curve ABCD in Figure 43 represents the thickness-
direction distribution of residual stresses parallel to the plate surface,
σ_x, having highly localized tensile stresses in a thin layer near the
surface. Stresses determined by different techniques may vary con-
siderably.

When the X-ray diffraction technique is used, only surface strains
to a depth of approximately 0.0001 inch are determined; the surface
stress OA is measured. In the stress-relaxation techniques using
bonded strain gages, extensometers, grid systems, photoelastic coat-
ings, and brittle coatings, strain measurements are made on the
surface. However, the measured values do not exactly represent
the stress on the very surface, OA. When a plug is cut as shown in
Figure 43, for example, the relaxation of the surface stress is restric-
ted by the metal in the central portion and residual stresses as shown
by a curve A'B'C'D' may still remain in the plug. Therefore, the
stress determined by strain release measured on the surface does
not represent OA but AA' which is somewhat between the localized
skin stress OA and the mean stress OM. OA' depends on various
factors including the stress distribution, ABCD, or sharpness of the
curve near the surface, the plate thickness, and the size of the plug.

In the ultrasonic technique, it is believed that stresses in the
interior of the material, e.g., around BC, are determined.
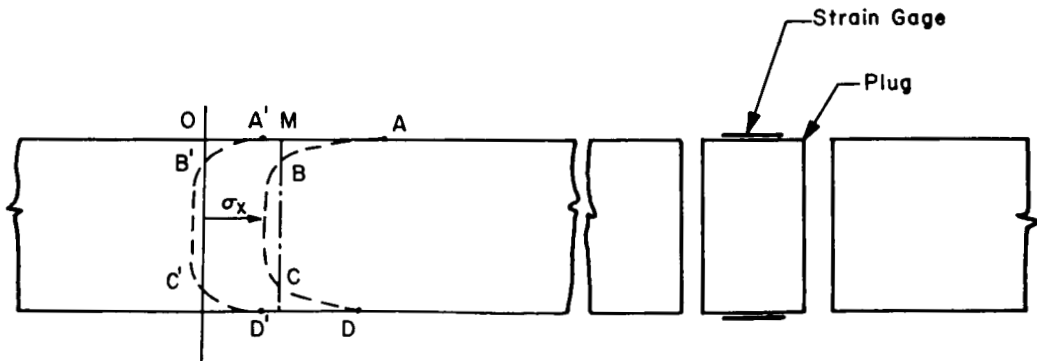
Figure 43.   Thickness-Direction Distribution
of Residual Stress

c. Effects of Variations in Material Properties

Large fabricated structures contain variations in metal properties: welded structures have the weld metal, the heat-affected zone, and the base metal, and heat treatments also change material properties. These variations in metal properties can cause serious problems when the X-ray diffraction technique and the ultrasonic technique are used.

It has been recognized that diffraction lines are broadened, resulting in lower accuracy in strain measurements when the X-ray diffraction technique is used on heat-treated materials.

d. Field Application

Some techniques are applicable to both laboratory and field tests, while others are applicable to laboratory tests only. Diffractometers commercially available at the present time are for the laboratory use; however, special equipment for a field test may be made.

Whether or not the remote reading can be made is an important factor in selecting techniques for field tests. Bonded strain gages have advantages over other techniques in this respect.

In some cases, the structures may be exposed to environments other than air, i.e., water or oil. Some techniques work under various environments.

e. Cost and Time

Cost and time for determining residual stresses depend on many factors including the shape and size of the specimen, number of measuring points, and the accuracy of measurement, etc. Table VI shows only in relative numbers the complexity of equipment, time required for measurement, and required operator experience.

Electric-resistance strain gages are relatively simple to operate and not expensive. However, cost and time for stress-relaxation procedures such as drilling and sectioning can be tremendous, depending upon the machining required.

The X-ray diffraction technique is a rather slow process. At each measuring point, the X-ray diffraction measurement must be made in two directions, each requiring 15 to 30 minutes exposure time for the film technique.

f. Use of Various Techniques in Studying Residual Stresses in Metal Structures

As shown in Table VI, there is no single residual-stress measuring technique which satisfies all requirements of nondestructiveness, high-strain sensitivity, applicability to field tests, low cost, and short measuring time. However, each technique has some advantages over other techniques and eventually have certain areas of application.

(1) Bonded Strain Gages. Bonded strain gages have been widely used in many residual-stress measurements, since strain gages have great advantages, on the basis of the quality of data and cost required, over other strain-measuring techniques. The following are examples in which strain gages may be used for measuring residual stresses produced during the fabrication of metal structures:

Strain gages may be mounted on portions of metal structures and strain changes which take place during fabrication be traced.

During the fabrication of structures, there may be a number of occasions in which metal parts are removed, such as drilling or cutting holes of various sizes. Measurements of residual stresses by the stress-relaxation technique may be made during these occasions.

(2) Extensometers, Grid Systems, Photoelastic Coatings, and Brittle Coatings. Extensometers, grid systems, photoelastic coatings, and brittle coatings have several unique features as stress-measuring devices and consequently unique areas of application; however, their use is rather limited.

The Gunnert method, which employes a mechanical extensometer with short gage length, has been used to measure residual stresses in welded plates. The Gunnert method also has been used to measure residual stresses in actual structures such as ships.[95]

(3) X-Ray Diffraction Techniques. The X-ray diffraction technique has been used fairly widely, although to a much less extent compared with bonded strain gages, for the measurement of residual stresses. The X-ray diffraction technique is the only technique that is applicable to measure such residual stresses as those in ball bearings, gear teeth, and surface residual stress after machining or griding.[96,97,98,99,100] The X-ray diffraction technique also has been used to measure residual stresses in structural components of airplanes.[101]

(4) <u>Ultrasonic Technique.</u> According to recent information, the ultrasonic technique is capable of determining the magnitude of stresses in a simple stress field, such as a bar under tensile loading. However, it has not been proved that this technique is useful for determining unevenly distributed residual stresses in metal structures. The usefulness of this technique lies somewhere in the future.

(5) <u>Hardness Techniques.</u> No actual application of the hardness techniques has been reported.

(6) <u>Cracking Techniques.</u> Cracking techniques will be useful for studying residual stresses in complex structural models, but they are not suitable to be applied to actual structures.

2.   Use of Mathematical Analysis in the Experimental Studies of Residual Stresses

The proper use of mathematical analysis based primarily on the theory of elasticity and plasticity is sometimes very useful in the study of residual stresses in metal structures. In some simple cases, the distribution of residual stresses can be calculated analytically. In most practical problems, the geometry of the specimen is so complicated that it is almost impossible to calculate residual-stress distributions. Nevertheless, mathematical analysis is still useful in studying residual stresses in practical problems, because mathematical analysis will promote a correct understanding of the problem, different sets of data such as residual stress and distortion can be related quantitatively by a mathematical analysis, and the number of experimental conditions necessary to obtain certain information can be reduced by proper use of a mathematical analysis.

a.   <u>Calculation of the Distribution of Residual Stresses</u>

Figure 33 shows calculated distributions for residual stresses produced by forming an angle and a channel. The calculation done by Yen[84] was based on the theory of plasticity. The stress-strain curve was assumed to be composed with two straight lines representing the elastic portion (with slope E) and the plastic portion (with slope a). Calculated values coincided well with the observed values.

Analytical studies of residual stresses due to welding have been made by a number of investigators.[102, 103, 104, 105, 106, 107] In order to calculate the change of stresses during welding, it is necessary to know the thermal history of the weldment and properties of the metal at various temperatures. Because of the difficult mathematical

analysis required, theoretical investigations have been limited to
simple models such as a simple butt weld. Kozimirov and Nedoseka[88]
calculated residual-stress distributions in butt welds in the AMg5V
alloy (aluminum alloy containing 5 percent manganese, and about 0.1
percent vanadium).

b. Use of Mathematical Analysis in Studying Practical Problems

Masubuchi[90, 91] made a systematic investigation in which
mathematical analysis was used extensively in studying various prac-
tical problems of residual stresses in welded joints. A few examples
are given in the following paragraphs.

(1) Distortion in Framed Structures. When frames are
fillet welded to a plate, angular changes take place. It the welded
structure is free from outer constraint, the plate will simply bend
to a polygonal form having a knuckle at the weld, as shown in Figure
44(a). However, when the structure is constrained by some means,
a different type of distortion is produced. For example, when the
movement of stiffeners welded to a plate is prevented, wavy distor-
tion of the plate, as shown in Figure 44(b), results.

Extensive investigations were made by Japanese investigators on
the wavy distortion of the bottom plate of welded ships.*[106, 108, 109, 110]
It was found that wavy distortion of a welded structure can be calculated
if the angular changes at the fillet joints are known. In the simplest
case of a symmetric distortion, as shown in Figure 44(b), the distor-
tion at Point P, δ, is given by[91]

$$\frac{\delta}{\ell} = \frac{1}{4} \phi - \left(\frac{x}{\ell} - \frac{1}{2}\right)^2 \phi , \tag{33}$$

where

δ = distortion at point P

x = distance between P and the center of the span

---

*It is believed that the initial distortion and residual stresses pro-
duced in the plate, as shown in Figure 44(b), decreases the buckling
strength of the plate. The major reason for the corrugation damage of
the bottom-shell plating which occurred in a number of all-welded
transversely framed cargo boats some time ago was attributed to exces-
sive wavy distortion.[109, 110, 111]

ℓ = length of span

ϕ = angular change at the fillet joint.

(a) Free Joint

(b) Constrained Joint
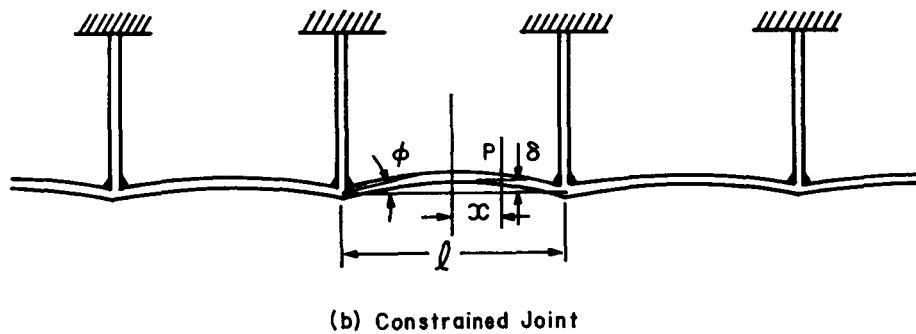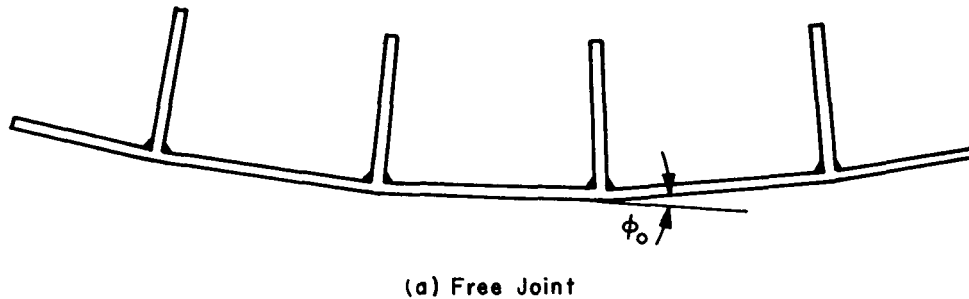
Figure 44.   Distortions Caused by Angular Changes in Free
and Constrained Fillet-Welded Structures

(Masubuchi, et al.)[108]

The distortion of the specimen after the constraining member was
removed was smaller than that which was produced in a free joint,
indicating that less angular change was produced during welding
because of the constraint.   The angular change, ϕ, also decreased
when the length of span decreased since the degree of constraint
increased.   Masubuchi, et al.,[108] presented the following formula
to express the influence of the length of span, ℓ, and the flexual
rigidity of the plate, D, on the amount of angular change:

$$\phi = \frac{\phi_0}{1 + \frac{2D}{\ell}\frac{1}{C}} \quad , \tag{34}$$

where

ϕ_0 = angular change in a free joint

ϕ = angular change in a constrained joint

C = coefficient.

Experimental investigations were made to determine the values of ϕ_0 and C for various conditions.[106, 112]

(2) Residual Stress and Longitudinal Distrotion of a Welded Beam. When a T-bar as shown in Figure 45(a) is manufactured by welding, longitudinal shrinkage of the weld metal induces longitudinal distortion of the beam unless the weld line coincides with the neutral axis of the beam. Longitudinal residual stress, σ_x, and curvature of longitudinal distortion, $1/R$, are given by the following equation (Figure 45):[91, 113]

$$\sigma_x = -E\epsilon_x'' + \frac{M_y^*}{I_y} Z + \frac{P_x^*}{A}$$

$$\frac{1}{R} = \frac{M_y^*}{EI_y} = \frac{P_x^* \ell^*}{EI_y} \quad , \tag{35}$$

where

ϵ_x'' = nonelastic strain in the x-direction

A = sectional area of the joint

I_y = moment of inertia of the joint around the neutral axis

P_x^* = apparent shrinkage force, $P_x^* = \iint E\epsilon_x'' dydz$

M_y^* = apparent shrinkage moment, $M_y^* = \iint E\epsilon_x'' zdydz = P_x^* \ell^*$

ℓ^* = distance between the neutral axis and the acting axis of apparent shrinkage force.

Equation (35) shows that it is necessary to know the distribution of nonelastic strain, ϵ_x'', in order to know that distribution of residual stress, σ_x; however, information about the moment, M_y^*, only is sufficient to determine the amount of distortion, $1/R$. The moment, M_y^*, is determined when the magnitude of the apparent shrinkage force, P_x^*, and the location of its acting axis are known.

a. General view

b. Nonelastic strain ϵ_x''

c. Residual stress σ_x
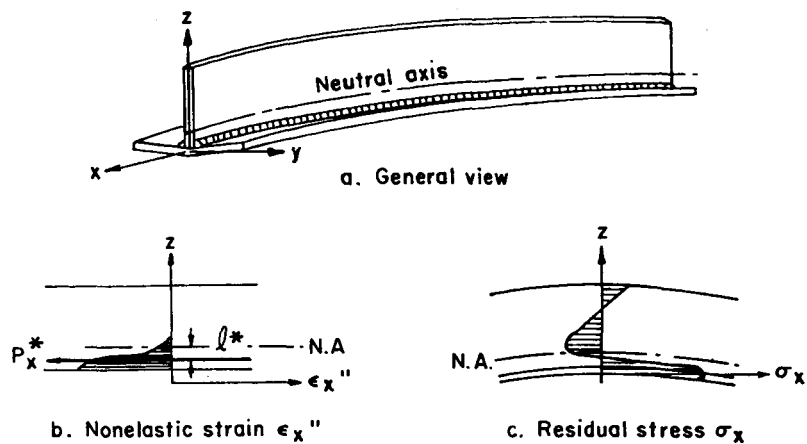
Figure 45.   Analysis of Longitudinal Distortion in Fillet Joint

(a) Typical Distortion

(b) Eight Stable Distortions Obtained in a Thin Plate Welded by Submerged-Arc Process
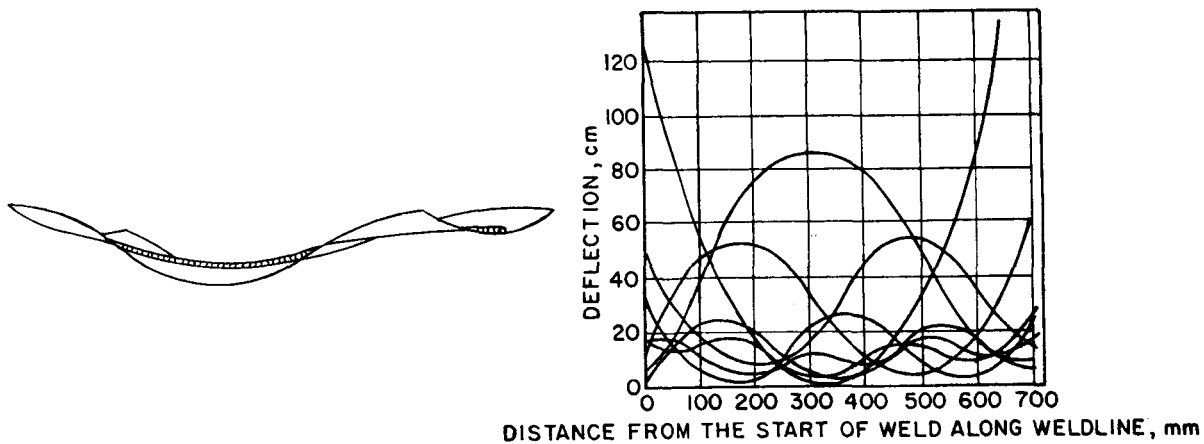
Figure 46.   Buckling Distortion Due to Welding of a Thin Plate

(Masubuchi)[114]

Sasayama, et al.,[113] investigated experimentally the effects of welding conditions and the dimensions of beams on the amount of P_x^*. It was found that the acting axis of P_x^* usually is located in the weld metal.

(3) Buckling Distortion in Welded Thin Plates. When a thin plate is welded, the plate will buckle because of compressive residual stresses produced in areas outside the weld. Figure 46 shows longitudinal distortions of a long strip, 0.09 x 0.16 x 283 inches in size, after a weld bead was laid by the submerged-arc process along the centerline of the plate.[106, 114] The specimen showed eight stable wavy distortions, as shown in Figure 46(b). The amplitude of distortion decreased with the increase in the wavelength or with the decrease in the number of waves. A mathematical analysis based on the theory of elastic stability suggested the following relationship:[115]

$$A = C \left(\frac{\overline{\ell}}{2b}\right)^n , \tag{36}$$

where

A = amplitude

$\overline{\ell}$ = mean wavelength

2b = width of the plate

C and n = constants.

By analyzing experimental data, it was found that the value of n was approximately 2; in other words, the amplitude increased almost proportionally to the square of the wavelength.

The above results indicate important characteristics of the buckling-type distortion caused by welding:

In the buckling-type distortion, more than one stable distortion can exist. A complicated thing is that in some cases only a few distortion instead of all possible distortions may really appear, and a few other distortions may occur in other specimens, giving quite confusing data.

Nevertheless, some regular relationships exist among seemingly quite different distortions, as shown in Equation (36).

3. Evaluation of Experimental Data on the Basis of the Effects of Residual Stresses on the Behavior of Stresses

An important problem related to the measurement of residual stresses is the difficulty of evaluating experimental data on the basis of potential effects of residual stresses on the behavior of the metal structure. Since this report is primarily concerned with the measurement of residual stresses, thorough discussions of the effects of residual stresses on the behavior of metal structures is not given here. Brief discussions are given on the effects of residual stresses on ductile fracture, brittle fracture, fatigue fracture, buckling, and dimensional stability.

a. Ductile Fracture

It has been established that the effects of residual stress on fracture properties, including the fracture strength, elongation, and the energy absorption of a metal structure are negligible when the fracture occurs in a ductile manner after the structure has exhibited considerable plastic deformation.

b. Brittle Fracture

During the last several years, considerable information has been developed on the influence of residual stresses on brittle fracture, especially in welded structures. It has been noticed by investigators that there is a difference between the evidence obtained from brittle failures in actual structures and the experimental results obtained with notched specimens. Actual fractures occurred at stresses far below the yield stress of the material, while the nominal fracture stress of a notch specimen is as high as the yield stress, even when the specimen contains very sharp cracks. A number of research programs have been carried out on low-stress fracture of weldments.[116, 117, 118, 119, 120, 121, 122, 123, 124, 125, 126] Although these still are disagreements among researchers in the interpretation of experimental findings,[125, 126] it has been established that low-stress brittle fracture occurs in a weldment when certain conditions are satisfied. The following is a mechanism suggested by Kihara and Masubuchi[119] on the effect of residual stress on brittle fracture.

Figure 47 shows, schematically, general tendencies of fracture strength of welded specimens at various temperatures and the effects of sharp notches and residual stress on fracture strength. When a specimen does not contain a sharp notch, fracture will occur at the ultimate strength of the material at temperatures concerned, as

shown by curve PQR. When a specimen contains a sharp notch (but no residual stress), fracture will occur at stresses shown by curve PQST. When the temperature is higher than the fracture transition temperature, T_f, a shear-type fracture occurs at a high stress. When the temperature is below T_f, the fracture appearance changes to a cleavage type, and the stress at fracture decreases to the value near the yield stress. When a notch is located in areas where high residual tensile stresses exist, various types of fracture can occur, as follows:

When the temperatue is higher than T_f, the fracture stress is as high as curve PQ. Residual stress has no effect on fracture stress.

When the temperature is lower than T_f but higher than the crack-arresting temperature, T_a, a crack may occur at a low stress but it will be arrested.

When the temperature is lower than T_a, the following two phenomena can occur, depending upon the stress level at fracture initiation:

1)   When a crack initiates at a stress below the critical stress VW, the crack will be arrested after running a certain distance. The complete fracture will occur at the yield stress (ST).

2)   When a crack initiates at a stress higher than VW, complete fracture occurs.

Analytical investigations of brittle fracture also have been made. The fracture mechanics theory developed by Griffith,[127] Irwin,[128,129] and other investigators has been widely applied to unstable brittle fractures of high-strength materials, especially ultrahigh-strength materials for aerospace applications.[130,131,132] When uniform tensile stress is applied to a plate containing a sharp transverse crack, the fracture strength, σ, decreases with increasing crack length, $\ell = 2a$ (provided that ℓ is greater than a certain critical length ℓ_c):

$$K = \sigma\sqrt{\pi a} = K_c. \tag{37}$$

In other words, fracture occurs when the stress-intensity factor, K, reaches a certain value, K_c, which is characteristic for the material.

K_c is called the critical stress-intensity factor or the fracture toughness of a material.*
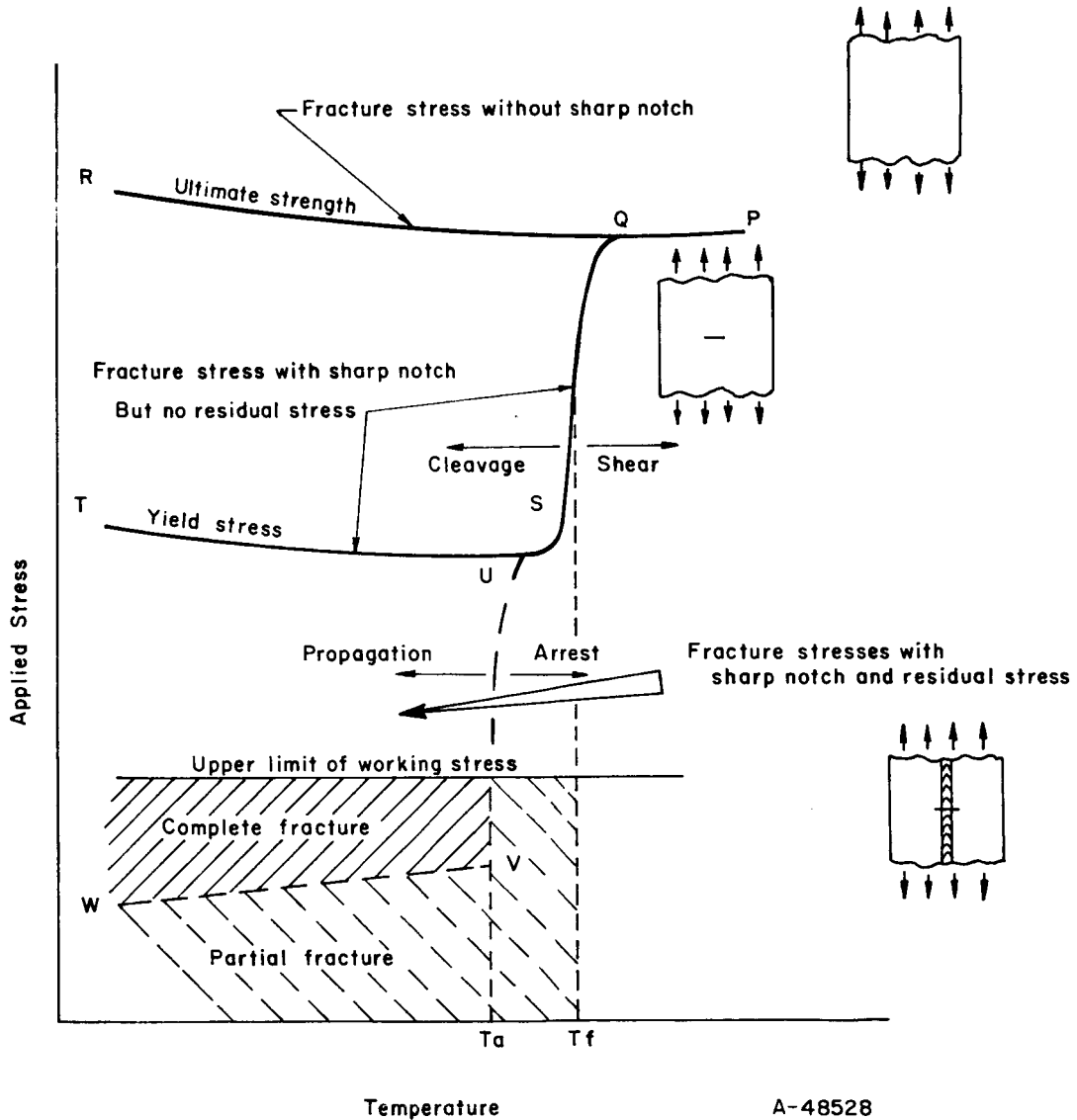
Figure 47. Effects of Sharp Notch and Residual Stress
on Fracture Strength

(Kihara and Masubuchi)[119]

*The ASTM Committee on Fracture Testing of High-Strength Sheet Materials[133] has described methods of measuring fracture toughness of high-strength sheet materials (ferrous and nonferrous materials having a strength-to-density ratio of more than 700,000 psi/lb/in.^{3}).

Kammer, et al.,[134] proposed the mechanism shown schematically in Figure 48 to explain analytically the effects of residual stress on brittle fracture. When a material does not contain residual stress, the relationship between crack length, ℓ, and the strain-energy release rate with crack extension $G = K^2/E$ (E is Young's modulus) is expressed by a straight line, OA, as expected by Equation (37). Fracture will extend when the G value is greater than $G_c = K_c^2/E$; in other words, an initial crack has to be longer than ℓ_c for unstable fracture to occur. However, when uniform tensile stress, σ, is applied to a plate that contains residual stresses, the relationship between the crack length and the strain-energy-release rate may be as shown schematically by curve ORB. If an initial crack is located in an area which contains high tensile residual stresses, the G value, while the crack is still short, is increased significantly and unstable fracture can occur from a crack as short as ℓ_{rc} (the G value is greater than G_c for any crack longer than ℓ_{rc}).

Figure 48 explains why low-applied-stress fractures as shown in Figure 47 take place when a sharp notch is located in areas containing high tensile residual stresses. This type of approach can be used for evaluating residual-stress distributions on the basis of their potential effects on brittle fracture of the metal structure. When the residual-stress distribution is known, the G value when a crack extends to a certain length can be calculated and compared with the material property G_c. Methods of calculating the G value for a given stress distribution have been proposed by several investigators including Masubuchi[135] and Barenblatt.[136]

c.   Fatigue Fracture

Much research has been done on the effects of residual stresses on the fatigue fracture of metals and metal structures.[137, 138, 139] The problem, however, is still under debate. A number of investigators have reported that the fatigue strength (the number of cycles at fracture under a given load, or the endurance limit) increased when specimens had compressive residual stresses, especially on the specimen surfaces. On the other hand, a number of investigators have believed that the effect of residual stress would be wiped out after certain numbers of stress cycles are applied to specimens.

It has been established that the fatigue strength is strongly dependent on the condition of the surface of a specimen. Many investigators have observed that notches on the specimen, even when they were very shallow, decreased drastically the fatigue strength of the specimen. Consequently, it is reasonable to assume that high tensile residual stresses in areas near the surface may decrease the fatigue strength of a structure.
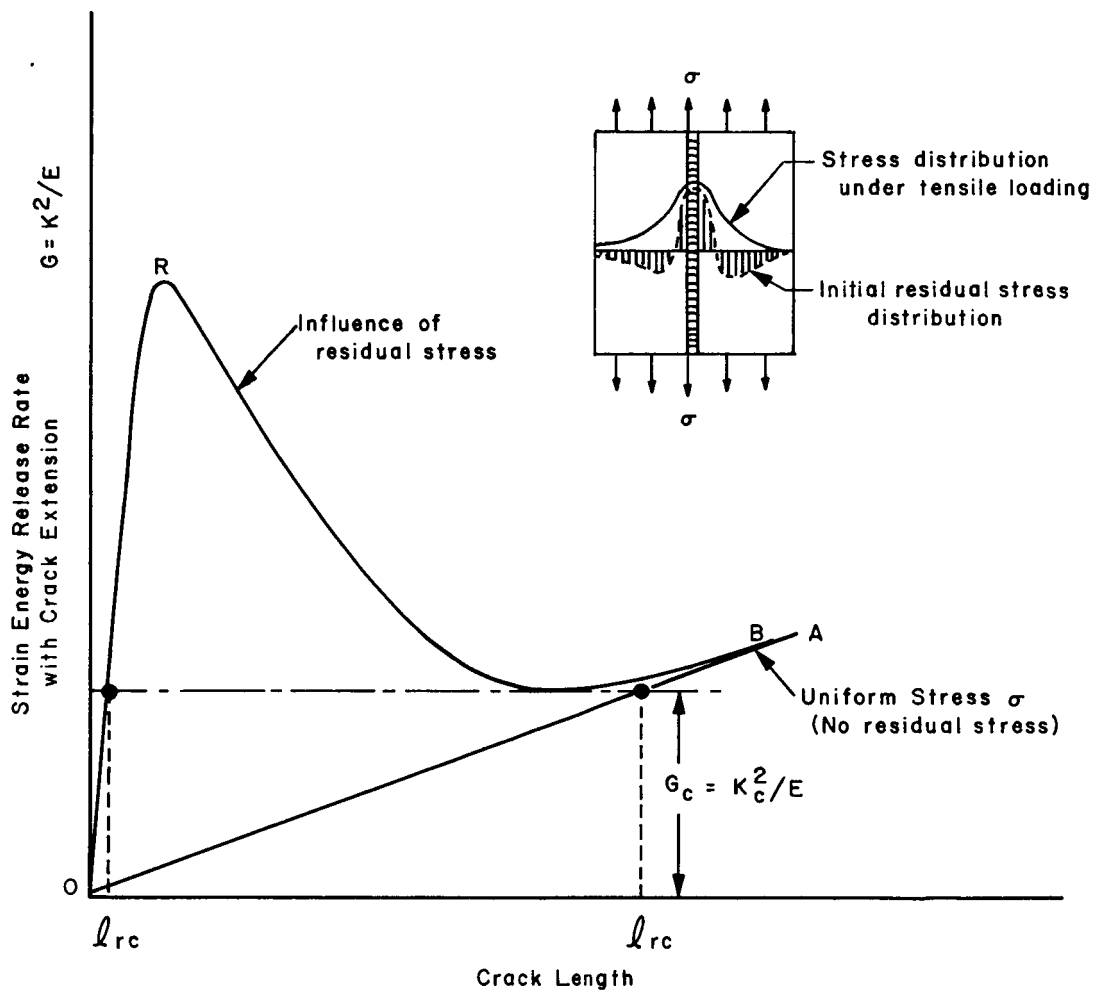
Figure 48. Mechanisms of Effects of Residual Stresses
on Brittle Fracture

(Kammer, et al.)[134]

d. Buckling

Failures due to instability, or buckling, sometimes occur
in metal structures composed of slender beams or thin plates. Buckling
occurs under compressive axial loading, and it also occurs under bend-
ing and torsional loading. It has been known that residual compressive
stresses decrease the buckling strength of a metal structure.[140, 141]
Distortion caused by residual stresses also decreases the buckling

strength, as described in relation to Figure 44. Commission X of the International Institute of Welding recently prepared a report based on the information given at a colloquium to the study of the effects of residual stresses on instability phenomena in metallic structures.[141] Residual stresses reduce significantly the stability of metal structures under certain conditions. For example, the critical load of an axially loaded I-beam fabricated by welding may only be about 50 percent of that of a beam without residual stresses.

With regard to the effect of buckling strength, residual stresses with the following nature are important:

Widely distributed compressive residual stresses

Distortion caused by residual stresses.

e. Dimensional Stability

When a metal part which contains residual stresses is machined, distortion may take place because of redistribution of residual stresses. With regard to the dimensional stability, residual-stress distributions which cause bending or torsional distortion by the removal of metal portions are most detrimental. Localized stresses usually are not important from the viewpoint of dimensional stability.

Section VI. RECOMMENDATIONS FOR FURTHER RESEARCH

One of the most important observations made during this state-of-the-art survey has been that there is no nondestructive method that can be used to measure, with satisfactory accuracy and reasonable cost and time, residual stresses produced in such metal structures as structural components of space boosters. It was also observed that little has been done to measure residual stresses and distortions during various stages of fabrication so that the structure will have minimum residual stresses and distortions after it is completed.

1. Development of Nondestructive Methods of Measuring Residual Stresses

At present, the destructive and semidestructive methods, in which the elastic strain release produced by drilling or machining is measured, are most widely used. However, they are not only damaging but also expensive and time consuming. It is, therefore, urgent to develop nondestructive methods for measuring residual stresses. The most promising techniques, on the basis of the presently available information, are the X-ray diffraction technique and the ultrasonic technique.

The X-ray diffraction technique has been used to some extent for determining residual stresses in metals. However, the accuracy of data must be improved and the time required for testing needs to be shortened before the technique can be used extensively. It has been recognized that the diffractometer technique has various advantages over the film technique, however, the diffractometer technique is applicable only to small specimens. Limited applications may be one of major reasons why no portable diffractometer unit is commercially available. It is recommended that efforts be made to build portable diffractometer units so that residual-stress measurements can be made with greater accuracy and less time.

At the present stage, the ultrasonic technique is a laboratory technique that works only on simple stress fields. Efforts must be made to develop the technique so that it can be used on metal structures containing complex residual stresses.

2. Measurement and Control of Residual Stresses During Fabrication

In most fabrication jobs it is too late to find that the structures have high residual stresses after they are completed. It is more advantageous to measure residual stresses at various stages of fabrication and to control the residual stresses and distortions to a minimum.

To do this thoroughly requires simple and reliable nondestructive methods of residual stresses which are not available at the present time. Nevertheless, there are ways to obtain some information about residual stresses produced during various stages of fabrication. Since there is no single technique which can be applied to all cases, a combination of various techniques will be most appropriate for a specific job. For controlling residual stresses and distortions produced during welding fabrication of structures, for example, the following can be done:

When a hole is drilled or cut, residual-stress measurements based on the stress-relaxation technique may be made.

Strain gages may be mounted on some portions of a structure somewhat away from the weld and the strain changes produced by welding can be measured. This technique will be useful to study reaction stresses produced in constrained joints, such as patch welds.

Measurements can be made on transverse shrinkage across the weld, longitudinal shrinkage along the weld, and distortion of a welded structure. Rough estimation of residual stresses may be made from these observations.

Measurements can be made on the degree of constraint of a joint (Figure 42). These measurements will help prevent cracking due to excessive constraint of a weld joint.

Measurement of the above-mentioned values plus appropriate mathematical analysis based on the measured data would provide, in most cases, information which is useful in controlling residual stresses and distortions and in preventing troubles such as weld cracking.

3. Effects of Variations in Procedures on the Magnitude and Distribution of Residual Stresses

It has been known that the magnitude and distribution of residual stresses will be changed when variations in procedures are made. For example, residual stresses and distortions may be different when different welding procedures are used. Information on these subjects is quite useful in predicting how much residual stress will be produced after the fabrication and in selecting proper manufacturing procedures. More research is needed on the effects of variations in procedures on the magnitude and distribution of residual stresses, especially residual stresses and distortions due to welding aluminum alloys. Extensive research has been made on residual stresses and distortions produced during welding steel, but only limited information is available on aluminum alloys.

LITERATURE CITED

1. S. P. Timoshenko, FUNDAMENTALS OF THE THEORY OF ELASTICITY, Appendix I of Handbook of Experimental Stress Analysis, edited by M. Hetenyi, New York, John Wiley and Sons, Inc., 1950, pp. 1013-1034.

2. METALS HANDBOOK, 8th Edition, Volume 1, American Society for Metals, 1961.

3. P. Nemenyi, SELPSTSPANNUNGEN ELASTISCHER GEBILDE, Handbuch der Physikalischen und Technischen Michanik, Leipzig, Germany, Band IV-1 Halfte, Verlang von Johann Ambrosius, 1931, pp. 199-212.

4. Transportation Technical Research Institute. THEORETICAL STUDIES ON THE RESIDUAL WELDING STRESS, H. Kihara and K. Masubuchi, June 1963, Report No. 6.

5. W. M. Wilson and C. C. Hao, RESIDUAL STRESSES IN WELDED STRUCTURES, The Welding Journal, 26(5), Research Supplement, 1947, pp. 295-s to 320-s.

6. von H Reissner, EIGENSPANNUNGEN UND EIGENSPANNUNG-SQUELLEN, Zeitschrift für Angewandte Mathematik und Mechanik, 11 (1), pp. 1-8, February 1931.

7. S. Moriguchi, FUNDAMENTAL THEORY OF DISLOCATION IN AN ELASTIC BODY, Oyo Sugaku Rikigaku, 1, pp. 29-36, 87-90, 1948.

8. E. Kroner, DISLOCATIONS AND CONTINUUM MECHANICS, Applied Mechanics Reviews, 15 (8), pp. 599-606, 1962.

9. E. Orowan, CLASSIFICATION AND NOMENCLATURE OF INTERNAL STRESSES, Symposium on Internal Stresses in Metals and Alloys, The Institute of Metals, pp. 47-59, 1948.

10. M. Hetényi, editor, HANDBOOK OF EXPERIMENTAL STRESS ANALYSIS, New York, John Wiley & Sons, Inc., 1950.

11. R. G. Trueting, J. J. Lynch, H. B. Wishart, and D. G. Richards, RESIDUAL STRESS MEASUREMENTS, American Society for Metals, 1952.

LITERATURE CITED (Continued)

12. K. Heindlhoffer, EVALUATION OF RESIDUAL STRESS, New York, McGraw-Hill Book Company, Inc. 1948.

13. W. R. Osgood, RESIDUAL STRESSES IN METALS AND METAL CONSTRUCTION, New York, Reinhold Publishing Corporation, 1954.

14. J. Mathar, DETERMINATION OF METAL STRESS BY MEASURING THE DEFORMATION AROUND DRILL HOLES, Transactions of the American Society of Mechanical Engineers, 86, pp. 249-254, 1934.

15. W. Soete, MEASUREMENT AND RELAXATION OF RESIDUAL STRESSES, The Welding Journal, 28 (8), Research Supplement, pp. 354-s to 364-s, 1949.

16. E. W. Suppiger, C. Riparbelli, and E. R. Ward, THE DETERMINATION OF INITIAL STRESSES AND RESULTS OF TESTS ON STEEL PLATES, The Welding Journal, 30 (2), Research Supplement, pp. 91s-104s, 1951.

17. H. Kihara, WELDING DATA BOOK, The Japan Welding Engineering Society, Tokyo, 1954.

18. E. Heyn and O. Bauer, ON STRESSES IN COLD DRAWN METALS, Internationale Zeitschrift für Metallographic, 1, pp. 16-50, 1911.

19. E. Heyn, INTERNAL STRAINS IN COLD WROUGHT METALS, AND SOME TROUBLES CAUSED THEREBY, Journal of the Institute of Metals, 12, pp. 1-37, 1914.

20. N. A. Crites, WHICH TYPE OF STRESS-ANALYSIS METHOD, Product Engineering, 32 (39), pp. 90-96.

21. N. A. Crites, FOR STRESS ANALYSIS BRITTLE-COATING METHODS PRODUCT ENGINEERING, 32 (42), pp. 63-72, 27 November 1961.

22. A. A. Crites, YOUR GUIDE TO TODAY'S STRAIN GAGES, Product Engineering, 33 (4), pp. 69-81, 19 February 1962.

23. N. A. Crites, EQUIPMENT AND APPLICATION-TODAY'S STRAIN GAGES, Product Engineering, 33 (6), pp. 85-93, 19 March 1962.

24. C. C. Perry and H. R. Lissner, THE STRAIN GAGE PRIMER, New York, McGraw-Hill Book Company, Inc., 1955.

25. R. Gunnert, RESIDUAL WELDING STRESSES, METHOD FOR MEASURING RESIDUAL STRESS AND ITS APPLICATION TO A STUDY OF RESIDUAL WELDING STRESSES, Stockholm, Almqvist E. Wicksell, 1955.

26. N. A. Crites, H. Grover, A. R. Hunter, EXPERIMENTAL STRESS ANALYSIS BY PHOTOELASTIC TECHNIQUES, Product Engineering, 33 (18), pp. 57-69, 3 September 1962.

27. G. S. Holister, THE PHOTOELASTIC METHOD APPLIED TO MATERIALS RESEARCH, Applied Materials Research, 1 (3), pp. 149-159, October 1962.

28. F. Zandman and M. R. Wood, PHOTO STRESS, Product Engineering, 27 (9), pp. 167-178, September 1956.

29. F. Zandman, PHOTO STRESS ANALYSIS, Product Engineering, 30 (9), pp. 43-46, 2 March 1959.

30. F. Zandman, PHOTOELASTIC-COATING TECHNIQUE FOR DETERMINING STRESS DISTRIBUTION IN WELD STRUCTURES, The Welding Journal, 39 (5), Research Supplement, pp. 191-s to 198-s, 1960.

31. G. S. Holister, PHOTOELASTIC STRAIN GAGES, Applied Materials Research, 2 (1), pp. 20-30, January 1963.

32. Commission X of the International Institute of Welding, MEASURING OF RESIDUAL STRESSES AND STRAINS, R. Gunnest, 1962, Document No. X-286-62-OE.

33. O. J. Horges, RESIDUAL STRESSES, Chapter 11 of Handbook of Experimental Stress Analysis, edited by M. Hetenyi, New York, John Wiley and Sons, Inc., 1950, pp. 459-578.

34. C. S. Barrett, A CRITICAL REVIEW OF VARIOUS METHODS OF RESIDUAL STRESS MEASUREMENT, Proceedings of the Society of Experimental Stress Analysis, 2 (1), pp. 147-156, 1944.

LITERATURE CITED (Continued)

35. J. L. Meriam, E. P. De Garmo, and F. Jonassen, A METHOD FOR THE MEASUREMENT OF RESIDUAL WELDING STRESSES, The Welding Journal, 25 (6), Research Supplement, pp. 340-s to 343-s, 1946.

36. H. Kihara and K. Masubuchi, RESIDUAL STRESSES AND DISTORTIONS IN WELDMENTS, Tokyo, Sampo Co., 1957, Written in Japanese.

37. Commission X of the International Institute, STRAIN MEASURING BY MEANS OF THE SETZDEHNUNGSMESSER, A. Vinckier, 1956, Document No. X-145-56.

38. C. W. Gadd, RESIDUAL STRESS INDICATIONS IN BRITTLE LAOUER, Proceedings of the Society for Experimental Stress Analysis, 4 (1), pp. 74-77, 1946.

39. A. A. Kazimirov and A. Ya. Nedoseka, RESIDUAL WELDING STRESSES INVESTIGATED BY MEANS OF PHOTOELASTIC TRANSDUCERS, Avtomaticheskaya Svarka, 15 (1), 1962, pp. 37-45.

40. E. Stäblein, STRESS MEASUREMENTS ON BILLETS QUENCHED FROM ONE SIDE, Stahl und Eisen, 52, pp. 15-17, 1932.

41. M. Mesnager, METHODS DE DETERMINATION DES TENSIONS EXISTANT DANS UN CYLINDRE CIRCULAIVE, Comptes Rendus hebedaires des Seances de l'Academie des Sciences, 169, pp. 1391-1393, 1927.

42. G. Sachs, EVIDENCE OF RESIDUAL STRESSES IN RODS AND TUBES, Zeitschrift für Metallkunde, 19, pp. 352-357, 1927.

43. American Institute of Mining and Metallurgical Engineers, Metals Technology, A NEW METHOD FOR DETERMINATION OF STRESS DISTRIBUTION IN THIN WALLED TUBING, G. Sachs and G. Espey, October 1941, Technical Publication 1384.

44. W. Soete and R. Vancrombrugge, HET METEN VAN EIGENSPANNINGEN IN DIEPTE, Lastijidschrift, No. 1, 1948.

LITERATURE CITED (Continued)

45. Commission X of the International Institute of Welding and Welding Research Abroad, METHOD FOR MEASURING TRI-AXIAL RESIDUAL STRESSES, R. Gunnert, 1957, 1958, Document No. X-184-57-OE.

46. Commission X of the International Institute of Welding, Welding Research Abroad, METHOD FOR MEASURING RESIDUAL STRESSES IN THE INTERIOR OF A MATERIAL, R. Gunnert, 1957, 1960, Document No. X-162-57.

47. D. Rosenthal and T. Norton, A METHOD OF MEASURING TRIAXIAL RESIDUAL STRESS IN PLATES, The Welding Journal, 24 (5), Research Supplement, pp. 295-s to 307-s, 1945.

48. J. H. Norton and D. Rosenthal, STRESS MEASUREMENT BY X-RAY DIFFRACTION, Proceedings of the Society for Experimental Stress Analysis, 1 (2), pp. 73-76, 1944.

49. J. H. Norton and D. Rosenthal, APPLICATIONS OF THE X-RAY DIFFRACTION METHOD OF STRESS MEASUREMENT TO PROBLEMS INVOLVING RESIDUAL STRESSES IN METALS, Proceedings of the Society for Experimental Stress Analysis, 1 (2), pp. 77-81, 1944.

50. J. T. Norton and D. Rosenthal, RECENT CONTRIBUTIONS TO THE X-RAY METHOD IN THE FIELD OF STRESS ANALYSIS, Proceedings of the Society for Experimental Stress Analysis, 5 (1), pp. 71-77, 1947.

51. St. John X-Ray Laboratory, Califon, New Jersey, BIBLIOGRAPHY ON X-RAY STRESS ANALYSIS, H. R. Isenberger, 1949.

52. C. S. Barrett, X-RAY ANALYSIS, Handbook of Experimental Stress Analysis, Chapter 18, edited by M. Hetenyi, New York, John Wiley and Sons, Inc., 1950, pp. 977-1012.

53. W. S. Hyler and L. R. Jackson, PRECAUTIONS TO BE USED IN THE MEASUREMENT AND INTERPRETATION OF RESIDUAL STRESSES BY X-RAY TECHNIQUE, Residual Stresses in Metals and Metal Construction, New York, Reinhold Publishing Company, 1954, pp. 297-303.

LITERATURE CITED (Continued)

54. D. P. Koistinen and R. E. Marburges, A SIMPLIFIED PRO-
    CEEDURE FOR CALCULATING PEAK POSITION IN X-RAY
    RESIDUAL STRESS MEASUREMENTS ON HARDENED STEEL,
    Transactions ASM, 51, pp. 537-555, 1959.

55. D. A. Vaughan and N. A. Crites, MEASUREMENT OF STRESS
    BY X-RAY DIFFRACTION, Product Engineering, 34 (20),
    30 September 1963.

56. E. V. Condon and H. Odishaw, editors, HANDBOOK OF
    PHYSICS, PART 8, THE SOLID STATE, New York, McGraw-
    Hill Book Company, 1958.

57. F. Bollenrath, V. Hauk, and E. Osswald, RONTGENOGRAPHISCHE
    SPANNUNGSMESSUNGEN BEI UBERSCHREITEN DER FLIESS-
    GRENZE AN ZUGSTABEN AUS UNLEGIERTEM STAHL, Zeit-
    schrift des Vereines Deutscher Ingenieure, 83, pp. 129-132,
    1939.

58. R. B. McCauley and R. P. Hudec, Private Communication.

59. F. A. Firestone and J. R. Frederick, REFINEMENTS IN
    SUPERSONIC REFLECTOSCOPY, POLARIZED SOUND, Journal
    of the Acoustical Society of America, 18, pp. 200-211, 1946.

60. J. R. Frederick, USE OF ULTRASONIC SURFACE WAVES IN
    THE DETERMINATION OF RESIDUAL STRESS IN METALS,
    Journal of Acoustical Society of America, 32, p. 1499,
    November 1960.

61. A. Hikata, R. Truell, A. Granato, B. Chick, and K. Lucke,
    SENSITIVITY OF ULTRASONIC ATTENUATION AND VELOCITY
    CHANGES TO PLASTIC DEFORMATION AND RECOVERY IN
    ALUMINUM, Journal of Applied Physics, 27 (4), pp. 396-404,
    1956.

62. R. H. Bergman and R. A. Shahbender, EFFECT OF A STATI-
    CALLY APPLIED STRESSES ON THE VELOCITY OF PROPAGA-
    TION OF ULTRASONIC WAVES, Journal of Applied Physics,
    29 (12), pp. 1736-1738, 1958.

LITERATURE CITED (Continued)

63. R. W. Benson and V. T. Raelson, ACOUSTOELASTICITY, Product Engineering, 30 (29), pp. 56-59, 20 July 1959.

64. W. J. Bratina and D. Mills, INVESTIGATION OF RESIDUAL STRESS IN FERROMAGNETICS USING ULTRASONICS, Nondestructive Testing, 18 (1), pp. 110-112, 1960.

65. Midwest Research Institute, ULTRASONIC METHODS FOR NON-DESTRUCTIVE MEASUREMENT OF RESIDUAL STRESS, F. Rollins, May 1961, WADD Technical Report 61-42, Part I.

66. R. W. Rumke, Private Communication.

67. S. Kokubo, CHANGES IN HARDNESS OF A PLATE CAUSED BY BENDING, Science Reports of the Tohoku Imperial University, Japan, Series 1, Vol. 21, pp. 256-267, 1932.

68. G. Sines and R. Carlson, HARDNESS MEASUREMENTS FOR DETERMINATION OF RESIDUAL STRESSES, ASTM Bulletin, No. 180, pp. 35-37, February 1952.

69. J. Pomey, F. Goutel, and L. Abel, DETERMINATION DES CONTRAINTES RESIDUELLES DAN LES PIÉCES CEMENTÉES, Publications scientifiques et Techniques du Ministére de l'air, No. 263, 1950.

70. Battelle Memorial Institute, INVESTIGATION OF RESIDUAL STRESSES BY USE OF HYDROGEN CRACKING, The Welding Journal, 40 (12) Research Supplement and RESIDUAL STRESSES IN STEEL WELDMENTS, K. Masubuchi and D. C. Martin, 31 August 1962, a summary report to Bureau of Ships, Department of the Navy, Contract No. NObs-84738.

71. C. R. McKinsey, EFFECT OF LOW-TEMPERATURE STRESS RELIEVING ON STRESS-CORROSION CRACKING, The Welding Journal, 33 (4), Research Supplement, pp. 161-s to 166-s, 1954.

72. W. Rädeker, A NEW METHOD FOR PROVING THE EXISTENCE OF INTERNAL STRESS CAUSED BY WELDING, Schweissen und Schneiden, 10 (9), pp. 351-358, 1958.

LITERATURE CITED (Continued)

73. Aluminum Company of America, AVOIDING STRESS-CORROSION CRACKING IN HIGH STRENGTH ALUMINUM ALLOY STRUCTURES, E. H. Spuhler and C. L. Burton, 1 August 1962.

74. H. C. Rutemiller and D. O. Sprowls, STRESS CORROSION OF ALUMINUM--WHERE TO LOOK FOR IT, HOW TO PREVENT IT, paper prepared for presentation at the Missile Industry Symposium of the 18th Conference and Corrosion Show of N. A. C. E., 19-23 March 1962.

75. G. Wasserman, ÜBER ABSCHRECKSPANNUNGEN (Quenching Stresses), Mitteillungen Kaiser-Wilhelm-Institut für Eisenforschung, 17, pp. 167-174, 1935.

76. R. M. Brick, A. Phillips, and A. J. Smith, QUENCHING STRESSES AND PRECIPITATION REACTION IN ALUMINUM-MAGNESIUM ALLOYS, Trans. Amer, Inst. Min. Met. Eng., 117, pp. 102-118, 1935.

77. A. von Zeerleder, QUENCHING STRESSES IN ALUMINUM ALLOYS, Journal of Institute of Metals, 67, pp. 87-99, 1941.

78. L. Frommer and E. H. Lloyd, THE MEASUREMENTS OF RESIDUAL STRESSES IN METALS BY THE X-RAY BACK REFLECTION METHOD, WITH SPECIAL REFERENCE TO INDUSTRIAL COMPONENTS IN ALUMINUM ALLOYS, Journal of the Institute of Metals (London), 70, pp. 91-124, 1944.

79. M. J. Donachie, Jr. and J. T. Norton, RESIDUAL STRESSES IN SHOT-PEENED ALUMINUM BARS, Proceedings of the Society for Experimental Stress Analysis, 19 (2), pp. 222-224, 1962.

80. G. Forrest, RESIDUAL STRESSES IN BEAMS AFTER BENDING, Symposium on Internal Stresses in Metals and Alloys, The Institute of Metals, pp. 153-168, 1947.

81. W. Betteridge, THE RELIEF OF INTERNAL STRESSES IN ALUMINUM ALLOYS BY COLD WORKING, Symposium on Internal Stresses in Metals and Alloys, The Institute of Metals, pp. 171-177, 1947.

LITERATURE CITED (Continued)

82. J. Soja, REDUCTION OF WARPAGE BY CREEP FORMING AND DIE QUENCHING OF NONFERROUS ALLOYS, Metal Progress, 76 (2), pp. 77-80, August 1959.

83. G. A. Hawkes, RESIDUAL STRESSES RESULTING FROM THE FORMING OF HIGH STRENGTH ALUMINUM ALLOYS, Journal of the Royal Aeronautical Society, 63, pp. 90-94, February 1959.

84. C. S. Yen, CALCULATING RESIDUAL STRESSES IN SOME FORMED PARTS, The American Society of Mechanical Engineers Paper Number 61-AV-38, pp. 1-7, 1961.

85. I. N. Artem'eva, STRESSES AND STRAINS AS INFLUENCED BY THE WELDING OF DURALUMIN D16T, Svarchnoe Proizvodatvo, 6 (2), pp. 15-19, 1960.

86. H. N. Hill, RESIDUAL WELDING STRESSES IN ALUMINUM ALLOYS, Metal Progress, 80 (2), pp. 92-96, 1961.

87. L. Capel, ALUMINUM WELDING PRACTICE, British Welding Journal, 8 (5), pp. 245-257, 1961.

88. A. A. Kazimirov and A. Ya. Nedoseka, THE RESIDUAL STRESSES AND DISTORTION WHICH DEVELOP WHEN THE AMg5V ALLOY IS WELDED, Avtomaticheskaya Svarka, 15 (10), pp. 16-21, 1962.

89. R. E. Travis, J. M. Barry, W. G. Moffatt, and C. M. Adams, Jr., WELD CRACKING UNDER HINDERED CONTRACTION: COMPARISON OF WELDING PROCESS, The Welding Journal, 43 (11), Research Supplement, pp. 504-s to 513-s, 1964.

90. K. Masubuchi, NEW APPROACH TO THE PROBLEMS ON RESIDUAL STRESS AND DEFORMATION DUE TO WELDING, Monthly Report of Transportation Technical Research Institute, Tokyo, Japan, 8 (12), pp. 247-364, 1959.

91. K. Masubuchi, ANALYTICAL INVESTIGATION OF RESIDUAL STRESSES AND DISTORTIONS DUE TO WELDING, The Welding Journal, 39 (12), Research Supplement, pp. 525-s to 537-s, 1960.

92. M. Watanabe, O. Takagi, K. Satoh, and F. Aso, EXTERNAL CONSTRAINT AND SHRINKAGE OF BUTT-WELDED JOINTS, Journal of the Society of Naval Architects of Japan, 104, pp. 153-162, 1958.

93. M. Watanabe and K. Satoh, EVALUATION OF RESTRAINT INTENSITY AND REACTION FORCE FOR SOME WELD CRACKING TEST SPECIMENS, Journal of the Japan Welding Society, 33 (7), pp. 513-523, 1964.

94. K. Satoh, FACTORS AFFECTING SHRINKAGE STRESSES OF WELDS UNDER RESTRAINT, Journal of the Japan Welding Society, 33 (6), pp. 439-445, 1964.

95. Commission X of the International Institute of Welding, CHANGES OF THE RESIDUAL STRESSES IN THE INTERIOR OF WELDS AND PLATES IN THE MAIN DECKS OF SHIPS DURING SERVICE, R. Gunnert, 1959, Document No. X-228-59-OE.

96. A. L. Christenson and E. S. Rowland, X-RAY MEASUREMENT OF RESIDUAL STRESS IN HARDENED HIGH CARBON STEEL, Transactions ASM, 45, pp. 638-676, 1953.

97. E. H. Kinelski and J. A. Berger, X-RAY DIFFRACTION FOR RESIDUAL STRESS MEASUREMENTS OF RESTRAINED WELDMENTS, The Welding Journal, 36 (12), Research Supplement, pp. 513-s to 517-s, 1957.

98. J. G. Roberts, X-RAY FIND RESIDUAL STRESS IN HARDEST STEELS, SAE Journal, 70 (3), pp. 50-51, 1962.

99. Battelle Memorial Institute, DETERMINATION OF RESIDUAL STRESS IN BEARINGIZED BOLT HOLES IN 2014-T6 ALUMINUM, D. A. Vaughan and C. M. Schwartz, 15 September 1964, Final Report to Ogden Air Materials Area, Hill Air Force Base.

100. T. Yoshida and K. Hirano, MEASUREMENT OF RESIDUAL STRESS IN WELDMENTS BY X-RAY DIFFRACTION METHOD, PART 1 AND PART 2, Journal of the Japan Welding Society, 33 (7), pp. 533-537, 538-543, 1964.

LITERATURE CITED (Continued)

101. D. A. Bolstad, R. A. Davis, W. E. Quist, and E. G. Roberts, MEASURING STRESS IN STEEL PARTS BY X-RAY DIFFRACTION, Metal Progress, 84 (1), pp. 88-124, 1963.

102. N. S. Boulton and H. E. Lance Martin, RESIDUAL STRESSES IN ARC WELDED PLATES, Proc. Institution of Mechanical Engineers, pp. 133, 295-a 339, 1936.

103. O. E. Rodgers and J. R. Fetcher, THE DETERMINATION OF INTERNAL STRESSES FROM THE TEMPERATURE HISTORY OF A BUTT-WELDED PLATE, The Welding Journal, 17 (11), Research Supplement, pp. 4s-7s, 1938.

104. M. Watanabe and Satoh, PLASTIC STUDY ON RESIDUAL STRESSES DUE TO WELDING, Technology Reports of the Osaka University, 1 (13), pp. 179-190, October 1951.

105. N. O. Okerblom, FLANGE DEFORMATION IN THE WELDING OF T-SECTIONS, British Welding Journal, 6 (4), pp. 145-154, 1959.

106. H. Kihara, M. Watanake, K. Masubuchi, and K. Satch, RESEARCHES ON WELDING STRESS AND SHRINKAGE DISTORTION IN JAPAN, Vol. 4 of the 60th Anniversary Series of the Society of Naval Architects of Japan, Tokyo, Japan, 1959.

107. K. Masubuchi, CALCULATION AND MEASUREMENT OF RESIDUAL STRESSES DUE TO SPOT HEATING, Welding in the World, 1 (1), pp. 18-27, 1963.

108. K. Masubuchi, Y. Ogura, Y. Ishihara, and J. Hoshino, STUDIES ON THE MECHANISM OF THE ORIGIN AND THE METHOD OF REDUCING THE DEFORMATION OF SHELL PLATING IN WELDED SHIPS, International Shipbuilding Progress, 3 (19), pp. 123-133, 1956.

109. Shipbuilding Research Association of Japan, INVESTIGATION ON THE CORRUGATION FAILURE OF BOTTOM PLATING OF SHIP, June 1957, Report of the 16th Research Committee, Report No. 19.

110. Nippon Kaiji Kyokai (Japanese Maritime Corp.), REPORT OF SHIP'S HULL FAILURES INVESTIGATION COMMITTEE, 1954.

111. J. M. Murray, CORRUGATION OF BOTTOM SHELL PLATIC, Trans. Inst. Naval Architects, London, Volume 94, pp. 229-250, 1954.

112. S. Hirai and Y. Nakamura, STUDIES OF EFFECTS OF WELDING PROCEDURES ON INITIAL CORRUGATION OF SHIP-BOTTOM PLATE, Ishikawajima Engineering Review, 12 (37), pp. 59-68, April 1955.

113. Commission X of the International Institute of Welding, LONGI-TUDINAL DEFORMATION OF LONG BEAM DUE TO FILLET WELDING, T. Sasayama, K. Masubuchi, and S. Mariguchi, 1955, Document No. X-38-55 (1955), Abstract was published in The Welding Journal.

114. K. Masubuchi, BUCKLING TYPE DEFORMATION OF THIN PLATE DUE TO WELDING, Proceedings of the 3rd Japanese National Congress for Applied Mechanics, pp. 107-111 (E), 1955.

115. T. Mura, ON THE BUCKLING DEFORMATION OF THIN PLATE DUE TO WELDING, Processing of the 3rd Japanese National Congress for Applied Mechanics, pp. 103-106 (E), 1955.

116. T. W. Greene, EVALUATION OF EFFECT OF RESIDUAL STRESSES, The Welding Journal, 28 (5), Research Supplement, pp. 193-s to 204-s, 1949.

117. A. A. Wells, THE BRITTLE FRACTURE STRENGTH OF WELDED STEEL PLATES, Quarterly Trans. Inst. Naval Arch., 48 (3), pp. 296-326, 1956.

118. D. C. Martin, R. S. Ryan, and P. J. Rieppel, EVALUATION OF WELD-JOINT FLAWS AS INITIATING POINTS OF BRITTLE FRACTURE, The Welding Journal, 37 (5), Research Supplement, pp. 244-s to 251-s, 1957.

119. H. Kihara and K. Masubuchi, EFFECT OF RESIDUAL STRESS ON BRITTLE FRACTURE, The Welding Journal, 38 (4), Research Supplement, pp. 159-s to 168-s, 1959.

LITERATURE CITED (Continued)

120. R. P. Sopher, A. L. Lowe, Jr., D. C. Martin, and P. J. Rieppel, EVALUATION OF WELD-JOINT FLAWS AS INITIATING POINTS OF BRITTLE FRACTURE--PART II, The Welding Journal, 38 (11), Research Supplement, pp. 441-s to 450-s, 1959.

121. A. A. Wells, INFLUENCE OF RESIDUAL STRESSES AND METALLURGICAL CHANGES ON LOW-STRESS BRITTLE FRACTURE IN WELDED STEEL PLATES, Welding Journal, 40 (4), pp. 182-s to 192-s, April 1961.

122. Commission X of International Institute of Welding, RECENT STUDIES IN JAPAN ON BRITTLE FRACTURE OF WELDED STEEL STRUCTURES UNDER LOW APPLIED STRESS, H. Kihara, 1962, Document No. X-291-62.

123. L. J. McGeady, THE EFFECT OF PREHEAT ON BRITTLE FRACTURE OF CARBON STEEL FOR PRESSURE VESSELS, Welding Journal, 41 (8), pp. 355-s to 367-s, August 1962.

124. W. J. Hall, W. J. Nordell, and W. H. Munse, STUDIES OF WELDING PROCEDURES, Welding Journal, 41 (11), pp. 505-s to 518-s, November 1962.

125. G. M. Boyd, THE CONDITIONS FOR UNSTABLE RUPTURING OF A WIDE PLATE, Trans. Inst. Naval Arch., 99 (3), Part II, pp. 349-366, July 1957.

126. C. Mylonas, PRESTRAIN, SIZE AND RESIDUAL STRESSES IN STATIC BRITTLE-FRACTURE INITIATION, The Welding Journal, 38 (10), Research Supplement, pp. 414-s to 424-s, 1959.

127. A. A. Griffith, THE PHENOMENA OF RUPTURE AND FLOW IN SOLIDS, Phil. Trans. Roy. Soc., 221, pp. 163-198, 1921, and THE THEORY OF RUPTURE, Proc. First Internat. Cong. Appl. Mech., pp. 55-63, 1924.

128. G. R. Irwin and J. A. Kies, FRACTURING AND FRACTURE DYNAMICS, The Welding Journal, 31 (2), Research Supplement, pp. 95-s to 100-s, 1952.

129. G. R. Irwin, FRACTURE, Encyclopedia of Physics, Volume VI, Elasticity and Plasticity, Berlin, Goettingen, Heidelberg, Springer-Verlag, 1958, pp. 551-590.

130. E. Orawan, FUNDAMENTALS OF BRITTLE BEHAVIOR IN METALS, Fatigue and Fracture of Metals, New York, John Wiley and Sons, Inc., 1952, p. 139.

131. D. K. Felbeck and E. Orowan, EXPERIMENTS ON BRITTLE FRACTURE OF STEEL PLATES, The Welding Journal, 34 (11), Research Supplement, pp. 570-s to 575-s, 1955.

132. Universal Technology Corporation, Dayton, Ohio, text used for Workshop in Fracture Mechanics held at Denver Research Institute, the text includes papers prepared by W. F. Payne, P. C. Paris, G. R. Irwin, C. D. Beachem, and C. F. Tiffany, 16-28 August 1964.

133. FRACTURE TESTING OF HIGH STRENGTH SHEET MATERIALS: A REPORT OF A SPECIAL ASTM COMMITTEE, ASTM Bulletin, No. 243, pp. 29-40, June 1960, No. 244, pp. 18-28, February 1960, and MATERIALS RESEARCH AND STANDARDS, 1 (11), pp. 877-885, November 1961.

134. Defense Metals Information Center, Battelle Memorial Institute, CRACKING IN HIGH-STRENGTH STEEL WELDMENTS, P. A. Kammer, K. Masubuchi, and R. E. Monroe, 7 February 1964, DMIC Report 197.

135. K. Masubuchi, DISLOCATION AND STRAIN ENERGY RELEASE DURING CRACK PROPAGATION IN RESIDUAL STRESS FIELD, Report of Trans. Tech. Res. Inst. Japan, No. 29, 1958.

136. G. I. Barenblatt, ON SOME BASIC IDEAS OF THE THEORY OF EQUILIBRIUM CRACKS, FORMING DURING BRITTLE FRACTURE, Problems of Continuum Mechanics published by the Society for Industrial and Applied Mathematics, 1961, pp. 21-38.

137. F. M. Rassweiler and W. L. Grube, INTERNAL STRESSES AND FATIGUE IN METALS, Proceedings of the Symposium on Internal Stresses and Fatigue in Metals, Detroit and Warren, Michigan, Elsevier Publishing Company, 1958, 1959.

138. SYMPOSIUM ON FATIGUE OF WELDED STRUCTURES, British Welding Journal, 7 (3), pp. 161-216, 1960.

LITERATURE CITED (Concluded)

139. DISCUSSIONS AT THE SYMPOSIUM ON FATIGUE OF WELDED STRUCTURES, British Welding Journal, 7 (7), pp. 472-481, 1960.

140. L. S. Beedle and L. Tall, BASIC COLUMN STRENGTH, The Journal of the Structural Division, Proceedings of the American Society of Civil Engineers, Proc. Paper 2555, Vol. 86, ST7, July 1960.

141. THE EFFECTS OF RESIDUAL STRESSES ON INSTABILITY PHENOMENA IN METALLIC STRUCTURES, Welding Research Abroad, 10 (10), pp. 63-67, 1964.

APPENDIX
STRESS CALCULATIONS

1. Stresses Acting on an Inclined Plane

To simplify the discussion, an analysis for the two-dimensional plane stress ($\sigma_z = \tau_{xz} = \tau_{yz} = 0$) is given here. Stress components on plane BC are (Figure 49)

$$\sigma_n = \sigma_x \cos^2 \phi + \sigma_y \sin^2 \phi + 2 \tau_{xy} \sin \phi \cdot \cos \phi$$

$$\tau = \tau_{xy} (\cos^2 \phi - \sin^2 \phi) + (\sigma_y - \sigma_x) \sin \phi \cos \phi , \tag{38}$$

where

σ_n is the normal stress on plane BC

τ is the shearing stress on plane BC

ϕ is the angle between the normal to the plane, N, and the n-axis.

$\tau = 0$ at the following angles ϕ and $\phi + \dfrac{\pi}{2}$:

$$\frac{1}{2} \tan \phi = \frac{\sin \phi \cdot \cos \phi}{\cos^2 \phi - \sin^2 \phi} = \frac{\tau_{xy}}{\sigma_x - \sigma_y} . \tag{39}$$

These two directions are called the principal directions.

2. Calculation of Thermal Stresses in a Three-Bar Frame

Strains in the middle and the side bars must be the same:

$$\frac{\sigma_m}{E_m} + a \cdot \Delta T = \frac{\sigma_s}{E_s} , \tag{40}$$

where

σ_m and σ_s = stresses in the middle and side bars, respectively

E_m and E_s = Young's modulus of the middle and side bars, respectively

125

$$\alpha = \text{coefficient of linear thermal expansion}$$

$$\Delta T = \text{the temperature change.}$$

Forces in the bars must be in equilibrium:

$$\sigma_m A_m + \sigma_s A_s = 0 \ , \tag{41}$$

where A_m and A_s = sectional area of the middle and side bars, respectively. In this case, $A_s = 2 A_m$.
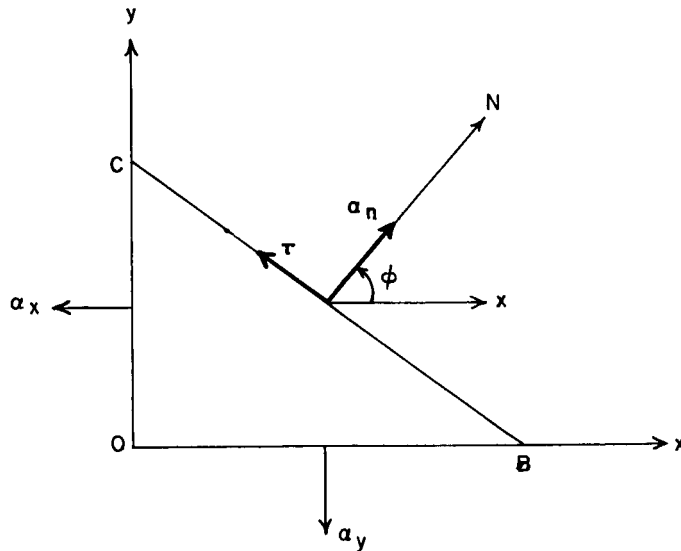

Figure 49. Stress Components on Inclined Plane BC

By solving the above equation, σ_m is given as follows:

$$\sigma_m = -2\alpha \cdot \Delta T \cdot E_s \times \cfrac{1}{2 \cfrac{E_s}{E_m} - 1} \ . \tag{42}$$

Since changes in properties in the temperature range between room temperature and approximately 300°F are not great, they are assumed to be constant as follows:

$$E_m = E_s = 10.8 \times 10^6 \text{ psi}$$

$$\alpha = 13.3 \times 10^{-6}/\text{F}.$$

The magnitude of thermal stress when the middle bar is heated is

$$\sigma_m = -2 \times 13.3 \times 10.8 \times \Delta T = -287 \times \Delta T.$$

Thus, the line AB is determined. Curves PBCQ and EDR represent the yield stress at various temperatures (Table I).

3. Stress Components Expressed in the Polar Coordinates
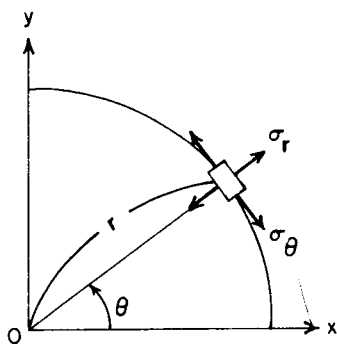
$$x = r \cos \theta, \qquad y = r \sin \theta$$

$$\text{or} \quad x + iy = re^{i\theta}$$

$$i = \sqrt{-1}$$

$$\frac{1}{2}(\sigma_\theta + \sigma_r) = \frac{1}{2}(\sigma_y + \sigma_x)$$

$$\frac{1}{2}(\sigma_\theta - \sigma_r) + i\tau_{r\theta} = \left\{ \frac{1}{2}(\sigma_y - \sigma_x) + i\tau_{xy} \right\} e^{2i\theta}.$$

*N. I. Muskhelishvili, SOME BASIC PROBLEMS OF MECH-ANICAL THEORY OF ELASTICITY, Croningen, Holland, P. Noordhott Ltd., 1953.

DISTRIBUTION

	Number of Copies
U. S. Army Missile Command Distribution List A	179
Defense Documentation Center Cameron Station Alexandria, Virginia - 22314	20
RSIC Supplemental Distribution List A	69
Battelle Memorial Institute 505 King Avenue Columbus 1, Ohio	25
Director, Scientific and Technical Information Headquarters, National Aeronautics and Space Administration Attn: A&S 1925 Florida Avenue Washington, D. C.	1
Mr. Howard G. Allaway Assistant Director for Operations Scientific and Technical Information Division Washington, D. C. - 20546	1

National Aeronautics and Space Administration
George C. Marshall Space Flight Center
Redstone Arsenal, Alabama

Attn: MS-T, Mr. Wiggins	5
R-ME-DF	1
R-ME-MM, Mr. Wilson	5
R-P&VE-S	1
R-QUAL-AT	1
R-TEST-CT	1
Attn: AMSMI-SME	1
AMSMI-XE, Mr. Lowers	1
-XS, Dr. Carter	1
AMSMI-IE	1
AMSMI-R, Mr. McDaniel	1
-RBR	50
-RBLD	10
-RFE, Mr. Kobler	1
-RSM	1
-RSS	1
-RST	1
-RTR	1
-RAP	1

DOCUMENT CONTROL DATA - R&D

(Security classification of title, body of abstract and indexing annotation must be entered when the overall report is classified)

1. ORIGINATING ACTIVITY (Corporate author)	2a. REPORT SECURITY CLASSIFICATION
Battelle Memorial Institute Columbus, Ohio	UNCLASSIFIED
	2b. GROUP N/A

3. REPORT TITLE

NONDESTRUCTIVE MEASUREMENT OF RESIDUAL STRESSES IN METALS
AND METAL STRUCTURES

4. DESCRIPTIVE NOTES (Type of report and inclusive dates)

Progress Report

5. AUTHOR(S) (Last name, first name, initial)

Masubuchi, Koichi

6. REPORT DATE	7a. TOTAL NO. OF PAGES	7b. NO. OF REFS
30 April 1965	128	141

8a. CONTRACT OR GRANT NO.	9a. ORIGINATOR'S REPORT NUMBER(S)
DA-01-021-AMC-11706(Z)	
b. PROJECT NO.	RSIC-410
c.	9b. OTHER REPORT NO(S) (Any other numbers that may be assigned this report)
d.	AD _____

10. AVAILABILITY/LIMITATION NOTICES

Qualified requesters may obtain copies of this report from DDC.

11. SUPPLEMENTARY NOTES	12. SPONSORING MILITARY ACTIVITY Redstone Scientific Information Center Directorate of Research and Development U. S. Army Missile Command Redstone Arsenal, Alabama

13. ABSTRACT

This report presents a state-of-the-art survey of the nondestructive measurement and evaluation of residual stresses produced in metals and metal structures. The report is concerned primarily with residual stresses produced during the fabrication of structures made of high-strength aluminum alloys.

Discussions are presented in four sections which provide the following:

fundamental information on residual stresses that is needed to understand measurement techniques

review of methods of measuring residual stresses, including stress-relaxation techniques, X-ray diffraction technique, the ultrasonic technique, the hardness technique, and cracking technique

measurement of residual stresses during fabrication of metal structures (methods of measuring residual stresses and typical experimental data are described)

selection and use of appropriate measurement techniques and evaluation of results.

DD $^{FORM}_{1\ JAN\ 64}$ **1473**

14. KEY WORDS	LINK A		LINK B		LINK C	
	ROLE	WT	ROLE	WT	ROLE	WT
Aluminum alloys Residual stresses Stress-relaxation technique X-ray diffraction technique Ultrasonic technique Hardness technique Cracking technique						

INSTRUCTIONS

1. ORIGINATING ACTIVITY: Enter the name and address of the contractor, subcontractor, grantee, Department of Defense activity or other organization *(corporate author)* issuing the report.

2a. REPORT SECURITY CLASSIFICATION: Enter the overall security classification of the report. Indicate whether "Restricted Data" is included. Marking is to be in accordance with appropriate security regulations.

2b. GROUP: Automatic downgrading is specified in DoD Directive 5200.10 and Armed Forces Industrial Manual. Enter the group number. Also, when applicable, show that optional markings have been used for Group 3 and Group 4 as authorized.

3. REPORT TITLE: Enter the complete report title in all capital letters. Titles in all cases should be unclassified. If a meaningful title cannot be selected without classification, show title classification in all capitals in parenthesis immediately following the title.

4. DESCRIPTIVE NOTES: If appropriate, enter the type of report, e.g., interim, progress, summary, annual, or final. Give the inclusive dates when a specific reporting period is covered.

5. AUTHOR(S): Enter the name(s) of author(s) as shown on or in the report. Enter last name, first name, middle initial. If military, show rank and branch of service. The name of the principal author is an absolute minimum requirement.

6. REPORT DATE: Enter the date of the report as day, month, year; or month, year. If more than one date appears on the report, use date of publication.

7a. TOTAL NUMBER OF PAGES: The total page count should follow normal pagination procedures, i.e., enter the number of pages containing information.

7b. NUMBER OF REFERENCES: Enter the total number of references cited in the report.

8a. CONTRACT OR GRANT NUMBER: If appropriate, enter the applicable number of the contract or grant under which the report was written.

8b, 8c, & 8d. PROJECT NUMBER: Enter the appropriate military department identification, such as project number, subproject number, system numbers, task number, etc.

9a. ORIGINATOR'S REPORT NUMBER(S): Enter the official report number by which the document will be identified and controlled by the originating activity. This number must be unique to this report.

9b. OTHER REPORT NUMBER(S): If the report has been assigned any other report numbers *(either by the originator or by the sponsor)*, also enter this number(s).

10. AVAILABILITY/LIMITATION NOTICES: Enter any limitations on further dissemination of the report, other than those imposed by security classification, using standard statements such as:

  (1) "Qualified requesters may obtain copies of this report from DDC."

  (2) "Foreign announcement and dissemination of this report by DDC is not authorized."

  (3) "U. S. Government agencies may obtain copies of this report directly from DDC. Other qualified DDC users shall request through

                               ."

  (4) "U. S. military agencies may obtain copies of this report directly from DDC. Other qualified users shall request through

                               ."

  (5) "All distribution of this report is controlled. Qualified DDC users shall request through

                               ."

If the report has been furnished to the Office of Technical Services, Department of Commerce, for sale to the public, indicate this fact and enter the price, if known.

11. SUPPLEMENTARY NOTES: Use for additional explanatory notes.

12. SPONSORING MILITARY ACTIVITY: Enter the name of the departmental project office or laboratory sponsoring *(paying for)* the research and development. Include address.

13. ABSTRACT: Enter an abstract giving a brief and factual summary of the document indicative of the report, even though it may also appear elsewhere in the body of the technical report. If additional space is required, a continuation sheet shall be attached.

It is highly desirable that the abstract of classified reports be unclassified. Each paragraph of the abstract shall end with an indication of the military security classification of the information in the paragraph, represented as *(TS)*, *(S)*, *(C)*, or *(U)*.

There is no limitation on the length of the abstract. However, the suggested length is from 150 to 225 words.

14. KEY WORDS: Key words are technically meaningful terms or short phrases that characterize a report and may be used as index entries for cataloging the report. Key words must be selected so that no security classification is required. Idenfiers, such as equipment model designation, trade name, military project code name, geographic location, may be used as key words but will be followed by an indication of technical context. The assignment of links, rules, and weights is optional.

13. Abstract (Concluded)

On the basis of findings obtained during this survey, recommendations are given for future research on nondestructive measurement of residual stresses produced during fabrication of metal structures.